

# Role of scaling dimensions in generalized noises in fractional quantum Hall tunneling due to a temperature bias

Matteo Acciai<sup>1,2\*</sup>, Gu Zhang<sup>3‡</sup>, and Christian Spånslätt<sup>1,4†</sup>

<sup>1</sup> Department of Microtechnology and Nanoscience (MC2), Chalmers University of Technology, S-412 96 Göteborg, Sweden

<sup>2</sup> Scuola Internazionale Superiore di Studi Avanzati, Via Bonomea 265, 34136, Trieste, Italy

<sup>3</sup> Beijing Academy of Quantum Information Sciences, Beijing 100193, China

<sup>4</sup> Department of Engineering and Physics, Karlstad University, Karlstad, Sweden

\* [macciai@sissa.it](mailto:macciai@sissa.it)

† [christian.spanslatt@kau.se](mailto:christian.spanslatt@kau.se)

‡ [zhanggu@baqis.ac.cn](mailto:zhanggu@baqis.ac.cn)

## Abstract

Continued improvement of heat control in mesoscopic conductors brings novel tools for probing strongly correlated electron phenomena. Motivated by these advances, we comprehensively study transport due to a temperature bias in a quantum point contact device in the fractional quantum Hall regime. We compute the charge-current noise (so-called  $\delta T$  noise), heat-current noise, and mixed noise and elucidate how these observables can be used to infer strongly correlated properties of the device. Our main focus is the extraction of so-called scaling dimensions of the tunneling anyonic quasiparticles, of critical importance to correctly infer their anyonic exchange statistics.

Copyright attribution to authors.

This work is a submission to SciPost Physics.

License information to appear upon publication.

Publication information to appear upon publication.

Received Date

Accepted Date

Published Date

1

## 2 Contents

3	<b>1 Introduction</b>	<b>2</b>
4	<b>2 Setup, conservation laws, and formalism</b>	<b>5</b>
5	2.1 Setup and conservation laws	5
6	2.2 Chiral Luttinger liquid formalism	7
7	<b>3 Charge currents and <math>\delta T</math> noise</b>	<b>8</b>
8	3.1 General expressions and scaling dimension	8
9	3.2 $\delta T$ noise for a small temperature bias	10
10	3.3 $\delta T$ noise for a large temperature bias	13
11	3.4 Full $\delta T$ noise and comparison to asymptotic limits	14
12	<b>4 Heat currents and heat-current noise</b>	<b>16</b>
13	4.1 Heat-current noise for small temperature bias	17
14	4.2 Heat-current noise for large temperature bias	19

15	4.3	Full heat-current noise and comparison to asymptotic limits	20
16	4.4	Generalized heat Fano factors	22
17	<b>5</b>	<b>Effective single-particle picture</b>	<b>25</b>
18	<b>6</b>	<b>Mixed noise</b>	<b>27</b>
19	<b>7</b>	<b>Summary and Outlook</b>	<b>29</b>
20	<b>A</b>	<b>Derivations of charge currents and delta-T noise</b>	<b>31</b>
21	A.1	Currents	31
22	A.2	Zeroth order (or equilibrium) charge-current noise	32
23	A.3	First order, or tunneling, charge-current noise	33
24	A.4	Crossed charge-current noise terms $S_{\alpha\beta}^{(02)} + S_{\alpha\beta}^{(20)}$	33
25	A.5	Summary of charge current fluctuations	35
26	<b>B</b>	<b>Derivations of heat currents and heat-current noise</b>	<b>36</b>
27	B.1	Currents	36
28	B.2	Zeroth order, or equilibrium, heat-current noise	37
29	B.3	First order or tunneling, heat-current noise	38
30	B.4	Crossed heat-current noise terms $\Sigma_{\alpha\beta}^{(02)} + \Sigma_{\alpha\beta}^{(20)}$	39
31	B.5	Summary of heat-current noises	42
32	<b>C</b>	<b>Derivation of mixed noise components</b>	<b>42</b>
33	C.1	General expressions	42
34	C.2	Relation with the thermoelectric response	43
35	<b>D</b>	<b>Scaling dimension modification by inter-channel interaction</b>	<b>45</b>
36	D.1	Charge transport	45
37	D.2	Heat transport	46
38	D.3	Unequal scaling dimensions on the two edges	47
39	<b>E</b>	<b>Some useful integral identities</b>	<b>48</b>
40	<b>F</b>	<b>Fourier transforms of the Green's function</b>	<b>48</b>
41	<b>G</b>	<b>Scattering theory for non-interacting electrons</b>	<b>49</b>
42	G.1	Delta-T noise	50
43	G.2	Heat-current noise	51
44		<b>References</b>	<b>52</b>
45	<hr/>		
46			

## 47 1 Introduction

48 Advancements in nanotechnology in the recent decade have paved the way towards detailed  
 49 control of heat flows in small-scale electronic devices. This development permits experimental  
 50 explorations of the quantum nature of heat [1], and in particular it introduces novel tools for  
 51 probing quantum systems where strong electron correlations play an important role. A fun-

52 fundamental example is the quantum Hall effect [2, 3], where in recent years it has been exper-  
53 imentally established that the heat conductance of the quantum Hall edge is quantized. This  
54 quantization holds both for the simpler integer [4] and for the strongly correlated fractional  
55 quantum Hall (FQH) edges [5–10], including those expected to host the elusive non-Abelian  
56 Majorana modes [11, 12]. Measurements of the heat conductance provides crucial information  
57 about the edge structure, such as the number of edge channels and their chiralities: properties  
58 that are often obscured in charge conductance measurements due to strong charge equilibra-  
59 tion. This is particularly relevant in the case of composite edges, such as the  $2/3$  and  $5/2$  FQH  
60 states. Here, the interplay of charge and thermal equilibration lengths can lead to different  
61 values of the charge conductance [13–18]. Via the bulk-boundary correspondence, access to  
62 the edge structure gives further insights into the corresponding bulk topological order [19],  
63 thereby demonstrating quantum heat transport as a powerful tool to pin-point the topological  
64 order of FQH states.

65 In this paper, we analyze another possibility to probe nanoscale electronic devices with  
66 heat, namely with novel noise spectroscopy tools. We study three types of such noise tools  
67 with focus on the situation with temperature-biased contacts. The first is non-equilibrium  
68 charge-current noise in the absence of a voltage bias but instead due to a pure tempera-  
69 ture bias. Such noise has been termed “thermally activated shot noise” or “delta- $T$  noise”.  
70 While it bears some similarity to conventional voltage-bias-induced shot noise [20–22], delta-  
71  $T$  noise has the additional and quite peculiar feature of being a non-equilibrium noise arising  
72 when no net charge current flows. Delta- $T$  noise was first theoretically analyzed in diffusive  
73 conductors [23], while the first experimental observation was achieved in an atomic break  
74 junction [24], showing good agreement with the scattering theory of non-interacting elec-  
75 trons [20]. Since then, delta- $T$  noise has been analyzed for a broad range of systems and  
76 setups [25–45]. A second type of novel noise drawing increasing attention is heat-current  
77 noise, i.e., fluctuations in the heat current [46–57]. Such fluctuations emerge due to, e.g.,  
78 thermal agitation, coupling to an electromagnetic environment, or from partitioning of heat  
79 currents due to scattering [1]. Finally, the third type of novel noise is the cross-correlation  
80 between charge and heat current fluctuations, known as “mixed noise”. Mixed noise has been  
81 studied so far only theoretically for weakly interacting systems or in the presence of a voltage  
82 bias only [52, 58, 59].

83 In the context of the strongly correlated FQH effect, delta- $T$  noise was theoretically shown  
84 to disclose important properties of quasiparticles with anyonic statistics [32, 37, 38]. In particu-  
85 lar, delta- $T$  noise was proposed as an experimental tool to extract the anyons’ so-called scaling  
86 dimensions [60], which are important, observable parameters characterizing, e.g., the tempo-  
87 ral decay of quasiparticle correlations. Under certain circumstances, the scaling dimensions  
88 can be further related to the FQH quasiparticle anyonic exchange statistics (a detailed discus-  
89 sion can be found, e.g., in Ref. [38]). As such, delta- $T$  noise holds promise as an important  
90 tool in the ongoing quest to detect and classify anyons [61–64], where an accurate identifica-  
91 tion of scaling dimensions is paramount to correctly infer anyonic exchange statistics. Also the  
92 heat-current noise due to a pure temperature bias was recently proposed to disclose scaling  
93 dimensions of FQH quasiparticles [55], an approach that does not require knowledge about  
94 the quasiparticle charges.

95 Making available a broad range of experimental tools to extract scaling dimensions of  
96 FQH quasiparticles is highly desirable for probing strong correlations, particularly as the origi-  
97 nally proposed method to extract scaling dimensions from exponents of the temperature and  
98 voltage dependence of QPC tunneling conductances is highly challenging [65] (however, see  
99 Refs. [63, 66] for recent developments). As such, pushing the utility delta- $T$ , heat-current,  
100 and mixed noises in the FQH effect is both important and pressing in order to disclose various  
101 phenomena related to strong electronic correlations. However, there are several missing in-

102 gradients in order to use these noises to confidently extract scaling dimensions in experiments:  
103 First, multi-terminal calculations explicitly connecting auto-correlated noise, cross-correlated  
104 noise and tunneling noise enforced by charge and energy conservation remain to be presented.  
105 Second, the similarities and differences between temperature- and voltage-biased noise have  
106 not been satisfactorily clarified. Third, the utility of mixed noise to probe FQH scaling di-  
107 mensions remains unexplored. Finally, an in-depth analysis of the differences and similarities  
108 between noise in strongly correlated systems and non-interacting systems, where the latter  
109 typically treated with a scattering approach, is absent.

110 In this work, we fill these gaps in the theory of temperature-biased noise and provide a  
111 comprehensive demonstration of how scaling dimensions in the FQH effect enter in novel,  
112 temperature-biased noise observables and thus how the scaling dimensions can be experi-  
113 mentally extracted. To this end, we provide a systematic study of temperature-biased noises  
114 generated in a quantum point contact (QPC) device in the FQH regime at Laughlin fillings  
115  $\nu = 1/(2n + 1)$  (with  $n$  a positive integer). Our main achievements are:

- 116 i) We perform a comprehensive calculation of the charge and heat-current noise (given in  
117 Eqs. (25) and (41), respectively) in the QPC device. Our findings not only recover previous  
118 results on auto-correlation and tunneling noise but describe also cross-correlation  $\delta T$   
119 and heat-current noise. We further provide fully analytical expressions for the small  
120 [Eqs. (27), (29), (42), (45)] and large [Eqs. (32), (36), (48)] temperature-bias limits.  
121 To the best of our knowledge, expressions for the cross-correlated noise have not been  
122 reported so far. However, an important advantage of considering cross-, rather than,  
123 auto-correlation noise is that the former vanishes in equilibrium, and therefore requires no  
124 subtraction of the thermal background noise. Moreover, our derived expressions manifest  
125 charge and energy conservation and can be used to accurately fit experimental data from  
126 both auto- and cross-correlation noise.
- 127 ii) We introduce a set of heat Fano factors (of which a single instance was previously intro-  
128 duced in Ref. [55]) and analyze how these quantities, given in Eq. (52), may be used  
129 to infer the scaling dimension of the tunneling particles. The heat Fano factors act as  
130 charge neutral analogues of the conventional Fano factor, used, e.g., to detect fractional  
131 charges [67–69]. The key utility of the heat Fano factors is to experimentally extract scal-  
132 ing dimensions without any reference to the tunneling charge, which is especially relevant  
133 for edges involving neutral modes [70–73].
- 134 iii) We introduce an effective density of states (EDOS), given in Sec. 5, for the QPC region, and  
135 thereby put strongly correlated tunneling on a similar footing as non-interacting tunneling  
136 analyzed within the scattering formalism. With this single-particle approach, we explic-  
137 itly elucidate how  $\delta T$  and heat-current noise in fact probe properties of the EDOS  
138 and, due to the device’s temperature bias, scaling dimensions of the tunneling particles  
139 naturally enter in both  $\delta T$  and heat current noise. A major benefit of this approach  
140 is that it can be straightforwardly adapted to analyze noise in related, strongly correlated  
141 systems.
- 142 iv) We provide general expressions, given in Eq. (74), for mixed charge and heat current noise  
143 and show that, close to equilibrium, the mixed noise is linked to thermoelectric conver-  
144 sion via the Seebeck coefficient. Our results thereby extend the utility of mixed noise  
145 in the presence of a temperature bias, previously considered only for weakly interacting  
146 electrons [58], to interacting, strongly correlated electrons. This connection provides not  
147 only a clear, physical interpretation of the mixed noise, but suggests a strategy for its  
148 experimental detection.

149 Together, these achievements significantly expand the scope and utility of temperature-biased  
 150 noise as a novel tool to experimentally probe FQH edge physics and collective electron be-  
 151 havior. Moreover, our detailed calculations establish a natural starting point for modeling  
 152 temperature-biased noise in related strongly correlated one-dimensional systems, such as dis-  
 153 ordered FQH line junctions [41, 74–77], disordered quantum wires [78], and quantum spin  
 154 Hall edges [79].

155 We have organized this paper as follows: In Sec. 2, we introduce the FQH setup of interest  
 156 and our theoretical formalism. In Sec. 3, we present expressions for delta- $T$  noise in the small  
 157 and large bias regimes. The analogous analysis for the heat-current noise is given in Sec. 4,  
 158 which includes the evaluation of the heat Fano factors. In Sec. 5, we exploit the effective  
 159 density of states to elucidate the properties of noise generated by a temperature bias. After  
 160 that, we derive and analyze expressions of mixed noise in Sec. 6.

161 For improved readability, in-depth details of our charge, heat, and mixed noise calcula-  
 162 tions are delegated to Appendix A, B, and C respectively. In Appendix D we provide a simple  
 163 toy-model to highlight how scaling dimensions are modified by local interactions. We fur-  
 164 ther include some useful integral identities in Appendix E and Fourier transforms of Green’s  
 165 functions in Appendix F. Finally, we provide a comprehensive analysis of charge- and heat-  
 166 current noise for non-interacting electrons in Appendix G by using the scattering approach,  
 167 calculations that we repeatedly refer to throughout the main text. As our unit convention, we  
 168 generally set  $\hbar = k_B = 1$  throughout our calculations, but restore these quantities for major  
 169 results.

## 170 2 Setup, conservation laws, and formalism

### 171 2.1 Setup and conservation laws

172 We study the setup in Fig. 1, consisting of two chiral quantum Hall edges bridged by a quantum  
 173 point contact (QPC, indicated by the dashed line). The QPC brings the two edges in proxim-

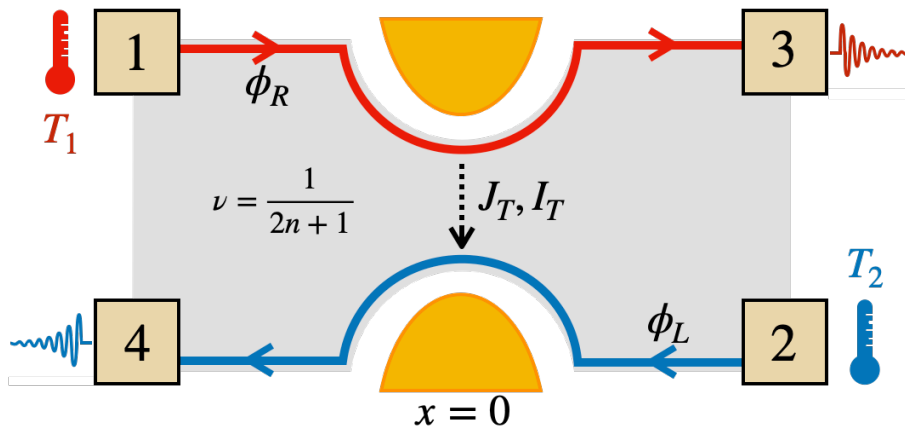


Figure 1: A quantum point contact device in the fractional quantum Hall regime at Laughlin filling  $\nu = (2n + 1)^{-1}$ , with  $n$  a positive integer. The source contacts 1 and 2 have temperatures  $T_1$  and  $T_2$ , respectively, and inject one right ( $\hat{\phi}_R$ ) and left ( $\hat{\phi}_L$ ) moving edge mode at these temperatures, respectively. Tunneling of charge and heat ( $I_T$  and  $J_T$  respectively) between the edge modes occur at  $x = 0$ . In this work, we analyze the resulting charge and heat currents and their fluctuations in drain contacts 3 and 4.

174 ity and causes inter-edge charge and energy exchange. Given a temperature difference  $\Delta T$   
 175 between the two source contacts, labelled by  $\alpha = 1, 2$ , our goal in this paper is to compute  
 176 the resulting noise correlations in the two drain contacts,  $\alpha = 3, 4$ . We define the correlations  
 177 between currents in contacts  $\alpha$  and  $\beta$  in terms of the symmetrized noise powers

$$S_{\alpha\beta}^{XX}(\omega) \equiv \int_{-\infty}^{+\infty} dt \langle \{ \delta \hat{X}_\alpha(t), \delta \hat{X}_\beta(0) \} \rangle e^{i\omega t}, \quad (1)$$

178 where  $\{ \dots, \dots \}$  denotes the anticommutator,  $\omega$  is the frequency, and  $\delta \hat{X}_\alpha(t) = \hat{X}_\alpha(t) - \langle \hat{X}_\alpha(t) \rangle$   
 179 is the operator describing the charge ( $X = I$ ) or heat ( $X = J$ ) fluctuations at drain  $\alpha$ . The  
 180 operators evolve in the Heisenberg picture (see next section), and the bracket  $\langle \dots \rangle$  denotes  
 181 a statistical average with respect to the local equilibrium states in the two source contacts at  
 182  $t \rightarrow -\infty$ . From Eq. (1), it follows that the noise powers satisfy the symmetry relation

$$S_{\alpha\beta}^{XX}(\omega) = S_{\beta\alpha}^{XX}(-\omega). \quad (2)$$

183 By using conservation of charge, we relate the incoming ( $\alpha = 1, 2$ ) and outgoing ( $\alpha = 3, 4$ )  
 184 charge currents,  $\hat{X} = \hat{I}$  in the device. Likewise, in the absence of a voltage bias in the device,  
 185  $V = 0$ , we can relate the incoming and outgoing heat currents by energy conservation. We  
 186 thus have

$$\hat{X}_3(t) = \hat{X}_1(t) - \hat{X}_T(t), \quad (3a)$$

$$\hat{X}_4(t) = \hat{X}_2(t) + \hat{X}_T(t). \quad (3b)$$

187 These relations define  $\hat{X}_T(t)$  as the charge ( $\hat{X} = \hat{I}$ ) and heat ( $\hat{X} = \hat{J}$ ) tunneling current, namely  
 188 the currents leaving the upper edge and entering the lower one. By inserting Eqs. (3) into  
 189 Eq. (1), we further express the noise measured in the drains in terms of the noises from the  
 190 source, or at the tunneling bridge, as

$$S_{33}^{XX}(\omega) = S_{11}^{XX}(\omega) - S_{1T}^{XX}(\omega) - S_{T1}^{XX}(\omega) + S_{TT}^{XX}(\omega), \quad (4a)$$

$$S_{44}^{XX}(\omega) = S_{22}^{XX}(\omega) + S_{2T}^{XX}(\omega) + S_{T2}^{XX}(\omega) + S_{TT}^{XX}(\omega), \quad (4b)$$

$$S_{34}^{XX}(\omega) = S_{12}^{XX}(\omega) + S_{1T}^{XX}(\omega) - S_{T2}^{XX}(\omega) - S_{TT}^{XX}(\omega), \quad (4c)$$

$$S_{43}^{XX}(\omega) = S_{21}^{XX}(\omega) + S_{T1}^{XX}(\omega) - S_{2T}^{XX}(\omega) - S_{TT}^{XX}(\omega), \quad (4d)$$

191 in which

$$S_{TT}^{XX}(\omega) \equiv \int_{-\infty}^{+\infty} dt \langle \{ \delta \hat{X}_T(t), \delta \hat{X}_T(0) \} \rangle e^{i\omega t}, \quad (5a)$$

$$S_{\alpha T}^{XX}(\omega) \equiv \int_{-\infty}^{+\infty} dt \langle \{ \delta \hat{X}_T(t), \delta \hat{X}_\alpha(0) \} \rangle e^{i\omega t}, \quad (5b)$$

$$S_{T\alpha}^{XX}(\omega) \equiv \int_{-\infty}^{+\infty} dt \langle \{ \delta \hat{X}_\alpha(t), \delta \hat{X}_T(0) \} \rangle e^{i\omega t}. \quad (5c)$$

192 At zero frequency,  $\omega = 0$ , the charge and heat (i.e., energy) conservation (4) becomes manifest  
 193 via the sum rule

$$\sum_{\alpha, \beta=3,4} S_{\alpha\beta}^{XX}(0) = S_{11}^{XX}(0) + S_{22}^{XX}(0), \quad (6)$$

194 where we used Eq. (2) together with  $S_{12}^{XX}(\omega) = S_{21}^{XX}(\omega) = 0$ , which follows since the two  
 195 source current fluctuations are uncorrelated. Note that in our description, we have omitted  
 196 currents and fluctuations propagating from contact 4 to contact 1 as well as from contact 3  
 197 to contact 2. In the following sections, we compute the average currents  $\langle X_\alpha(t) \rangle$  and noise  
 198 contributions  $S_{\alpha\beta}^{XX}(\omega)$  in the FQH regime.

## 199 2.2 Chiral Luttinger liquid formalism

200 At low energies, the FQH edge dynamics is described by the chiral Luttinger model [65, 80, 81].  
 201 Within this model, the combined Hamiltonian of the top and bottom edge segments is given  
 202 as

$$\hat{H}_0 = \frac{v_F}{4\pi} \int_{-\infty}^{+\infty} dx [ :(\partial_x \hat{\phi}_R)^2 : + :(\partial_x \hat{\phi}_L)^2 : ], \quad (7)$$

203 in which  $\hat{\phi}_{R/L}$  are bosonic field operators describing low-energy excitations propagating to  
 204 the right ( $R$ , on the top edge) or left ( $L$ , on the bottom edge) with speed  $v_F$ . The notation  
 205 “: ... :” indicates the usual normal ordering in the bosonization formalism. For notational  
 206 convenience, we will omit the normal ordering symbols from now on. The bosons obey the  
 207 equal-time commutation relations

$$[\hat{\phi}_{R/L}(x), \hat{\phi}_{R/L}(x')] = \mp i\pi \text{sgn}(x - x'). \quad (8)$$

208 By using Eq. (8) and the Heisenberg equation of motion with  $\hat{H}_0$ , we obtain the time evolution  
 209 of the free bosonic modes  $\hat{\phi}_{L,R}$  as

$$\hat{\phi}_{R/L}(x, t) = \hat{\phi}_{R/L}(x \mp v_F t), \quad (9)$$

210 and we see that the  $R$  ( $L$ ) boson indeed propagates to the right (left). From this chiral evolu-  
 211 tion, it follows that the time derivative reads  $\partial_t = \mp v_F \partial_x$  when acting on  $\hat{\phi}_{R/L}(x, t)$ .

212 We model the QPC region, taken at  $x = 0$ , by the tunneling Hamiltonian

$$\hat{H}_\Lambda = \Lambda e^{ie\nu V t} \hat{\psi}_R^\dagger(0) \hat{\psi}_L(0) + \text{H.c.} \quad (10)$$

213 This Hamiltonian describes weak tunneling of quasiparticles with fractional charge  $q^* = -\nu e$   
 214 (where  $-e$  is the electron charge) and includes, for the moment, also a voltage bias  $V \equiv V_1 - V_2$   
 215 between the two source contacts<sup>1</sup>. The operators  $\hat{\psi}_{R/L}$  are quasiparticle annihilation operators  
 216 related to the bosonic fields via the well-known bosonization identity

$$\hat{\psi}_{R/L}(x) = \frac{F_{R/L}}{\sqrt{2\pi a}} e^{\pm i k_F x} e^{-i\sqrt{\nu} \hat{\phi}_{R/L}(x)}. \quad (11)$$

217 Moreover,  $\Lambda$  in (10) is the tunneling amplitude, assumed as energy-independent within all  
 218 relevant energy scales. In Eq. (11),  $a$  is a short-distance cutoff,  $F_{R/L}$  are Klein factors,  $k_F$   
 219 is the electronic Fermi momentum, and  $\nu$  is the FQH filling factor. In this work, we limit  
 220 our calculations to the Laughlin states (see, e.g., Refs. [13, 14, 37, 82, 83] for details on noise  
 221 generation in QPCs for other FQH states) for which

$$\nu = \frac{1}{2n+1}, \quad n \in \mathbb{N}^+. \quad (12)$$

222 In the bosonized language, the charge and heat current operators along the edges read

$$\hat{I}_{R/L} \equiv \frac{ev_F \sqrt{\nu}}{2\pi} \partial_x \hat{\phi}_{R/L}, \quad (13a)$$

$$\hat{J}_{R/L} \equiv \pm \frac{v_F^2}{4\pi} (\partial_x \hat{\phi}_{R/L})^2 - V_{1,2} \hat{I}_{R/L}, \quad (13b)$$

<sup>1</sup>Although our focus in this work is the situation of only a temperature bias, we consider here the more general case with finite voltage bias  $V \neq 0$ , which is necessary in order to introduce the charge tunneling conductance (see Sec. 3.1) and to have a nonvanishing mixed noise (see Sec. 6).

223 where  $V_{1,2}$  are the voltages applied at the source contacts 1 and 2, respectively. Having defined  
 224  $\hat{H}_0$  and  $\hat{H}_\Lambda$ , we next compute the charge and heat tunneling currents at the generic position  
 225  $x_0$  along the device. To do so, we compute the time evolution of the charge and heat current  
 226 operators perturbatively in  $\Lambda$  up to order  $|\Lambda|^2$  (amounting to the weak tunneling limit). We  
 227 thus write

$$\hat{X}_{R/L}(x_0, t) = \hat{X}_{R/L}^{(0)}(x_0, t) + \hat{X}_{R/L}^{(1)}(x_0, t) + \hat{X}_{R/L}^{(2)}(x_0, t), \quad (14)$$

228 where the superscript (0) denotes time evolution with respect to the free Hamiltonian  $\hat{H}_0$  and  
 229

$$\hat{X}_{R/L}^{(1)}(x_0, t) = -i \int_{-\infty}^t dt' [\hat{X}_{R/L}^{(0)}(x_0, t'), \hat{H}_\Lambda^{(0)}(t')], \quad (15a)$$

$$\hat{X}_{R/L}^{(2)}(x_0, t) = - \int_{-\infty}^t dt' \int_{-\infty}^{t'} dt'' [\hat{H}_\Lambda^{(0)}(t''), [\hat{H}_\Lambda^{(0)}(t'), \hat{X}_{R/L}^{(0)}(x_0, t)']], \quad (15b)$$

230 for  $\hat{X} = \hat{I}, \hat{J}$ . The currents  $\hat{X}_{R/L}$  are related to the currents flowing *into* the drain contacts as

$$\hat{X}_3(t) = \hat{X}_R(x_3, t), \quad (16)$$

$$\hat{X}_4(t) = -\hat{X}_L(x_4, t), \quad (17)$$

231 where  $x_3$  and  $x_4$  are the locations of the drains and we adopted a convention where currents  
 232 are positive when they enter the associated contact. In Secs. 3 and 4 below, we give the results  
 233 for the charge and the heat transport, respectively.

### 234 3 Charge currents and delta-T noise

235 In this section, we present our results for the charge-current noise to leading order in the  
 236 tunneling (10), based on Eqs. (14) and (15). Full details of our calculations are presented in  
 237 Appendix A. The general expressions (25) below agree with several well-known results, see  
 238 e.g., Refs. [37, 84, 85], and we have included them to make the paper self-contained. Our  
 239 new results in this work are mainly the analysis of the cross-correlations, both in the small  
 240 temperature bias regime —especially the explicit expressions (30)—, and in the large-bias  
 241 regime (Sec. 3.3).

#### 242 3.1 General expressions and scaling dimension

243 We start with the average charge tunneling current through the QPC, located at  $x = 0$ , which  
 244 we obtain as (see Appendix A for details)

$$I_T \equiv \langle \hat{I}_T \rangle = 2ie\nu|\Lambda|^2 \int_{-\infty}^{+\infty} d\tau \sin(e\nu V\tau) G_R(\tau) G_L(\tau), \quad (18)$$

245 where  $V = V_1 - V_2$  is the voltage difference between the source contacts and

$$G_{R/L}(\tau) \equiv G_{R/L}(x=0, \tau) = \frac{1}{2\pi a} e^{\lambda \mathcal{G}_{R/L}(\tau)}, \quad (19)$$

246 are the quasiparticle Green's functions evaluated at the location of the QPC. In Eq. (19), the  
 247 exponents are given in terms of equilibrium bosonic Green's functions

$$\mathcal{G}_{R/L}(\tau) = \langle \hat{\phi}_{R/L}(0, \tau) \hat{\phi}_{R/L}(0, 0) \rangle - \langle \hat{\phi}_{R/L}^2(0, 0) \rangle = \ln \left[ \frac{\sinh(i\pi T_{1/2} \tau_0)}{\sinh(\pi T_{1/2} (i\tau_0 - \tau))} \right], \quad (20)$$



248 with  $\tau_0 \equiv a/v_F$  being the short-time cutoff. The Green's functions for the chiral right and left  
 249 movers depend on  $T_1$  and  $T_2$ , respectively (the temperatures of the two source contacts), and  
 250 manifest that the edge states injected from the sources are in equilibrium with their respective  
 251 contact until they reach  $x = 0$ .

252 The exponent in Eq. (19) contains also  $\lambda$ , which is the so-called scaling dimension of the  
 253 tunneling operator [60]. This parameter can be thought of as a dynamical exponent governing  
 254 the decay of the time correlation of the tunneling particles. Generally,  $\lambda$  is affected by non-  
 255 universal effects, e.g., inter-channel interactions [86–89], coupling to phonon modes [87],  
 256 disorder [70], neutral modes [70–73], and  $1/f$  noise [90, 91]. For completeness, we present  
 257 in Appendix D a simple toy model that showcases how scaling dimensions are modified by lo-  
 258 cal density-density interactions near the QPC. We thus stress that for the Laughlin states (12),  
 259 it is only in the very ideal case where such effects are absent that  $\lambda$  equals the filling factor  $\nu$   
 260 (in the weak backscattering regime). We further emphasize that universal, topological prop-  
 261 erties like the charge of the tunneling quasiparticles are not affected by any scaling dimension  
 262 modification. In the present work, the fractional charge  $q^*$  of the tunneling quasiparticles is  
 263 always set by the filling factor  $\nu$  via the relation  $q^* = -\nu e$ . Due to a well-known duality (see  
 264 e.g., Ref. [32]), our calculations in the ideal weak backscattering regime can be mapped onto  
 265 the ideal strong backscattering regime by taking  $\lambda = 1/\nu$  and  $q^* = -\nu e \rightarrow q^* = -e$ .

266 By inspecting Eq. (18), we see that  $I_T$  vanishes for  $V = 0$ , as expected, independently  
 267 of the temperatures  $T_1$  and  $T_2$ . This feature is a consequence of the particle-hole symmetry  
 268 of the linear spectrum of the edge modes, in combination with the assumption of an energy-  
 269 independent tunneling amplitude  $\Lambda$ . Based on the tunneling current (18), we next define the  
 270 associated *differential* charge tunneling conductance as

$$\frac{\partial I_T}{\partial V} = 2i(e\nu)^2 |\Lambda|^2 \int_{-\infty}^{+\infty} d\tau \tau \cos(e\nu V \tau) G_R(\tau) G_L(\tau). \quad (21)$$

271 Close to equilibrium, i.e., for  $T_1 = T_2 = \bar{T}$  and  $V = 0$ , we have the conductance

$$g_T(\bar{T}) \equiv \left. \frac{\partial I_T}{\partial V} \right|_{V=0, T_1=T_2=\bar{T}} = \frac{e^2 \nu^2}{2\pi} \left( \frac{|\Lambda|}{v_F} \right)^2 (2\pi \bar{T} \tau_0)^{2\lambda-2} \frac{\Gamma^2(\lambda)}{\Gamma(2\lambda)}, \quad (22)$$

272 which displays the well-known characteristic power-law scaling  $\bar{T}^{2\lambda-2}$  of the edge channels  
 273 (see, e.g., Ref. [65]). In Eq. (22),  $\Gamma(z)$  denotes Euler's Gamma function. In the non-interacting,  
 274 integer case  $\lambda = \nu = 1$ , the conductance becomes

$$g_T(\bar{T})|_{\lambda \rightarrow 1} = \frac{e^2}{2\pi} \left( \frac{|\Lambda|}{v_F} \right)^2 = \frac{e^2}{2\pi} D, \quad (23)$$

275 where we defined

$$D \equiv \frac{|\Lambda|^2}{v_F^2}. \quad (24)$$

276 A comparison to the scattering approach for tunneling of non-interacting electrons (see Ap-  
 277 pendix G) shows that  $D$  is the QPC reflection probability for this setup.

278 Considering next the charge-current noise, we obtain the following results for the zero  
 279 frequency charge-current noise components (finite-frequency expressions are given in Ap-

280 pendix A)

$$S_{11}^{II} = 2 \frac{\nu e^2}{h} k_B T_1, \quad (25a)$$

$$S_{22}^{II} = 2 \frac{\nu e^2}{h} k_B T_2, \quad (25b)$$

$$S_{TT}^{II} = 4(e\nu)^2 |\Lambda|^2 \int_{-\infty}^{+\infty} d\tau \cos\left(\frac{e\nu V \tau}{\hbar}\right) G_R(\tau) G_L(\tau), \quad (25c)$$

$$S_{33}^{II} = 2 \frac{\nu e^2}{h} k_B T_1 + S_{TT}^{II} - 4 \frac{\partial I_T}{\partial V} k_B T_1, \quad (25d)$$

$$S_{44}^{II} = 2 \frac{\nu e^2}{h} k_B T_2 + S_{TT}^{II} - 4 \frac{\partial I_T}{\partial V} k_B T_2, \quad (25e)$$

$$S_{34}^{II} = 2 \frac{\partial I_T}{\partial V} k_B (T_1 + T_2) - S_{TT}^{II}, \quad (25f)$$

$$S_{43}^{II} = S_{34}^{II}. \quad (25g)$$

281 As a first check of the validity of these expressions, we see that indeed they fulfill the conser-  
 282 vation equation (6). We also check the equilibrium case situation  $T_1 = T_2 = \bar{T}$  and  $V = 0$   
 283 which produces  $S_{11}^{II} = S_{22}^{II} = S_{33}^{II} = S_{44}^{II} = 2\nu e^2 k_B \bar{T}/h$  and  $S_{34}^{II} = S_{43}^{II} = 0$ . These are indeed the  
 284 expected equilibrium (Johnson-Nyquist) noises. The equilibrium form of  $S_{TT}^{II}$  is given below  
 285 in Eq. (27) and (28a).

286 We now move on to the main focus in this work, i.e., the non-equilibrium noise under  
 287 the condition where there is no voltage bias,  $V = 0$ , but instead a finite temperature bias  
 288  $T_1 - T_2 \neq 0$ . In this case, the integrals in Eq. (25) are analytically intractable, and we therefore  
 289 resort to asymptotic expansions to obtain analytical expressions for two special cases of the  
 290 temperature bias. To this end, we choose a symmetric parametrization

$$T_{1,2} = \bar{T} \pm \frac{\Delta T}{2}, \quad (26)$$

291 and focus on two important regimes. In the small bias limit, we have  $|\Delta T| \ll \bar{T}$  and we can  
 292 expand all integrals in powers of the small parameter  $\Delta T/(2\bar{T})$ . In the opposite regime of  
 293 a large temperature bias, one temperature is negligible compared to the other. This limit is  
 294 reached for  $|\Delta T| \rightarrow 2\bar{T}$ . For positive  $\Delta T$  we then have  $T_1 \rightarrow 2\bar{T} \equiv T_{\text{hot}}$  and  $T_2 \rightarrow 0$ . When  
 295  $\Delta T$  is negative,  $T_1 \rightarrow 0$  and  $T_2 \rightarrow 2\bar{T} \equiv T_{\text{hot}}$ . We present results for the small and large bias  
 296 limits in Secs. 3.2 and 3.3, respectively.

### 297 3.2 Delta-T noise for a small temperature bias

298 We start our charge-noise analysis with the tunneling noise  $S_{TT}^{II}$  in (25c). As shown in Ap-  
 299 pendix G and further discussed in Sec. 5, for  $\lambda = \nu = 1$ ,  $S_{TT}^{II}$  coincides with the full noise of a  
 300 weakly-coupled two-terminal system connected to reservoirs described by Fermi functions at  
 301 temperatures  $T_1$  and  $T_2$ , thus providing a link to standard scattering theory for non-interacting  
 302 fermions.

303 By expanding the integrand in (25c) in powers of  $\Delta T/(2\bar{T})$  and integrating term by term  
 304 (see Appendix E for additional details of this approach), we obtain

$$S_{TT}^{II} = S_0^{II} \left[ 1 + \mathcal{C}^{(2)} \left( \frac{\Delta T}{2\bar{T}} \right)^2 + \mathcal{C}^{(4)} \left( \frac{\Delta T}{2\bar{T}} \right)^4 + \dots \right], \quad (27)$$

305 with the prefactor and two expansion coefficients given as

$$S_0^{II} = 4g_T(\bar{T})\bar{T}, \quad (28a)$$

$$C^{(2)} = \lambda \left\{ \frac{\lambda}{1+2\lambda} \left[ \frac{\pi^2}{2} - \psi^{(1)}(1+\lambda) \right] - 1 \right\}, \quad (28b)$$

$$C^{(4)} = \lambda \frac{\pi^4 \lambda^2 (4+3\lambda) - 12\pi^2 \lambda (2\lambda^2 + 3\lambda - 3) + 12(4\lambda^3 + 4\lambda^2 - 5\lambda - 3)}{24(4\lambda^2 + 8\lambda + 3)} \\ + \lambda^2 \frac{4\lambda^2 + 6\lambda - 6 - \pi^2 \lambda (4+3\lambda)}{8\lambda^2 + 16\lambda + 6} \psi^{(1)}(\lambda+1) + \lambda^3 \frac{4+3\lambda}{2(4\lambda^2 + 8\lambda + 3)} [\psi^{(1)}(\lambda+1)]^2 \\ + \lambda^3 \frac{4+3\lambda}{12(4\lambda^2 + 8\lambda + 3)} \psi^{(3)}(\lambda+1), \quad (28c)$$

306 where  $\psi^{(n)}(z)$  are polygamma functions. These expressions confirm those previously reported  
307 in Ref. [32] for  $\lambda = \nu$  and in Ref. [38] for more generic tunneling setups and scaling dimensions  
308  $\lambda$ . As noted in these works,  $C^{(2)}$  takes negative values for  $\lambda < 1/2$ . Moreover,  $|C^{(4)}| \ll |C^{(2)}|$   
309 (see Fig. 2a), so that in the small-temperature bias limit,  $|\Delta T| \ll \bar{T}$ , the sign of the correction  
310 to the equilibrium term can be directly read off from the sign of the coefficient  $C^{(2)}$ . Moreover,  
311 all odd coefficients vanish,  $C^{(2n+1)} = 0$ , as a consequence of equal edge structures on the  
312 top and bottom edge segments, together with the choice of a symmetric temperature bias,  
313 see Eq. (26). Linear terms in  $\Delta T$  can only arise for asymmetric temperature biases and/or  
314 unequal edge structures [40].

315 From an experimental perspective, the tunneling noise  $S_{TT}^{II}$  is not directly accessible, be-  
316 cause what is measured is either cross- or auto-correlations of current fluctuations detected  
317 in the drain contacts 3 and 4. Here, we choose to focus on the cross-correlations, as these  
318 have the advantage of being zero at equilibrium, in contrast to the auto-correlations which  
319 are finite. Before presenting the results in the FQH regime, we remark that for the integer  
320 case  $\lambda = \nu = 1$ , the cross-correlation  $S_{34}^{II}$  coincides with the *shot noise* component in a non-  
321 interacting two-terminal system (see Appendix G). Moving on to the FQH regime, we expand  
322 the cross-correlation delta- $T$  noises (25f)-(25g) in powers of the temperature bias, integrate  
323 term by term, and obtain

$$S_{34}^{II} = S_{43}^{II} = S_0^{II} \left[ (-C^{(2)} + \mathcal{D}^{(2)}) \left( \frac{\Delta T}{2\bar{T}} \right)^2 + (-C^{(4)} + \mathcal{D}^{(4)}) \left( \frac{\Delta T}{2\bar{T}} \right)^4 + \dots \right]. \quad (29)$$

324 Here, we have parametrized this noise expansion by introducing an additional set of coeffi-  
325 cients  $\mathcal{D}^{(n)}$ , in which the leading ones are

$$\mathcal{D}^{(2)} = \lambda \left\{ \frac{3\lambda}{1+2\lambda} \left[ \frac{\pi^2}{6} - \psi^{(1)}(1+\lambda) \right] - 1 \right\}, \quad (30a)$$

$$\mathcal{D}^{(4)} = -\frac{\lambda \{12 + \lambda[12 + \pi^4 + 12(\pi^2 - 2)\lambda]\}}{24(1+2\lambda)} + \frac{\lambda^2(5\pi^2 + 18\lambda)}{6(1+2\lambda)} \psi^{(1)}(1+\lambda), \\ -\frac{5\lambda^2}{2(1+2\lambda)} [\psi^{(1)}(1+\lambda)]^2 - \frac{5\lambda^2}{12(1+2\lambda)} \psi^{(3)}(1+\lambda) \\ + \frac{\lambda^2(1+\lambda^2)}{8[3+4\lambda(2+\lambda)]} \{ \pi^4 - 20\pi^2 \psi^{(1)}(2+\lambda) + 60[\psi^{(1)}(2+\lambda)]^2 + 10\psi^{(3)}(2+\lambda) \}. \quad (30b)$$

326 The origin of the  $\mathcal{D}^{(n)}$  coefficients can be traced to the temperature dependence of the differ-  
327 ential charge tunneling conductance (21) which enters in Eq. (25f) and (25g), in addition to  
328 the tunneling noise  $S_{TT}^{II}$ . To the best of our knowledge, expressions for the the cross-correlated  
329 delta- $T$  noise and the coefficients  $\mathcal{D}^{(2)}$  and  $\mathcal{D}^{(4)}$  have not been reported before. Notice again

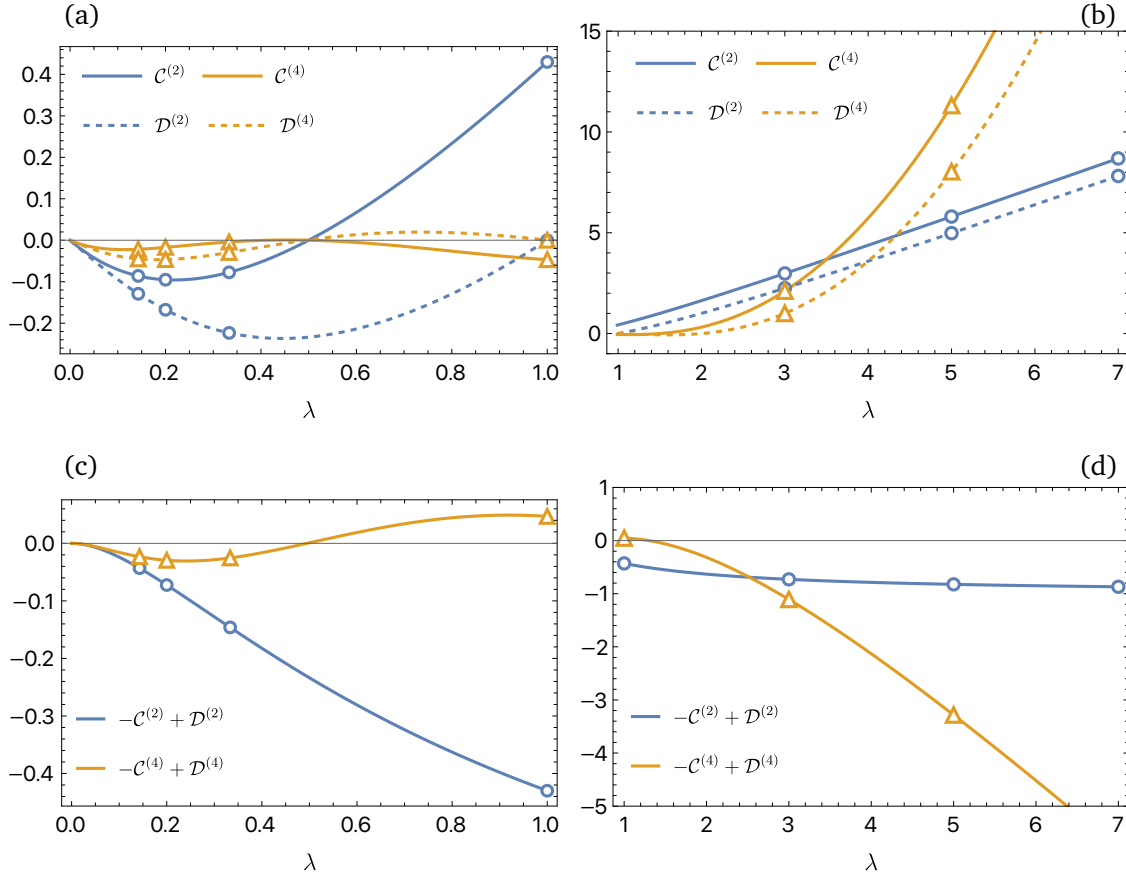


Figure 2: (a-b) Second- and fourth-order delta- $T$  noise expansion coefficients  $\mathcal{C}^{(2)}$ ,  $\mathcal{C}^{(4)}$ ,  $\mathcal{D}^{(2)}$ , and  $\mathcal{D}^{(4)}$  (Eq. (28b), (28c), (30a), and (30b), respectively) as functions of the scaling dimension  $\lambda$ . Panels (c-d) show the difference  $\mathcal{D}^{(n)} - \mathcal{C}^{(n)}$  that appears in the expansion for the full cross correlation noise (29). Triangles and circles mark the values for  $\lambda = \nu$  (panels a and c) and  $\lambda = 1/\nu$  (panels b and d) for fillings  $\nu = 1, 1/3, 1/5, 1/7$ .

330 the absence of terms with odd powers of  $\Delta T/(2\bar{T})$  in Eq. (29) due to the symmetric setup and  
 331 bias.

332 We plot the expansion coefficients (28b), (28c), (30a), and (30b) as functions of the scaling  
 333 dimension  $\lambda$  in Fig. 2(a-b). We also mark the values  $\lambda = \nu$  and  $\lambda = 1/\nu$  (for  $\nu = 1, 1/3, 1/5, 1/7$ ),  
 334 corresponding to ideal weak and strong backscattering limits. We thus confirm that the weak  
 335 back-scattering regime for Laughlin states, i.e.,  $\lambda < 1/2$ , produces negative delta- $T$  noise [32],  
 336  $S_{TT}^{II}/S_0^{II} < 1$ , since for such scaling dimensions  $\mathcal{C}^{(2)} < 0$  and  $|\mathcal{C}^{(4)}| < |\mathcal{C}^{(2)}|$ . For  $1/2 < \lambda \leq 1$ ,  
 337 we still have  $|\mathcal{C}^{(4)}| < |\mathcal{C}^{(2)}|$  but  $\mathcal{C}^{(2)} > 0$  so that  $S_{TT}^{II}/S_0^{II} \geq 1$ . In the strong back-scattering  
 338 regime for Laughlin states,  $\lambda > 1$ , we see that  $|\mathcal{C}^{(4)}| > |\mathcal{C}^{(2)}|$  for  $\lambda \gtrsim 3$ . For completeness, we  
 339 show in Fig. 2(c-d) the behavior of the combination  $-\mathcal{C}^{(n)} + \mathcal{D}^{(n)}$  (for  $n = 2, 4$ ) that appears  
 340 in the expansion of the cross-correlation noise  $S_{34}^{II}$  in Eq. (29). We see that the leading-order  
 341 correction is *always negative*, independently of the scaling dimension. Therefore, recalling that  
 342  $S_{34}^{II} = 0$  at equilibrium, the temperature induced cross correlation noise is always negative, in  
 343 contrast to the tunneling noise.

344 We find it further instructive to separately analyze the noise expansion terms for the special  
 345 and important case of non-interacting electrons, obtained here for  $\lambda = \nu = 1$ . Then, the

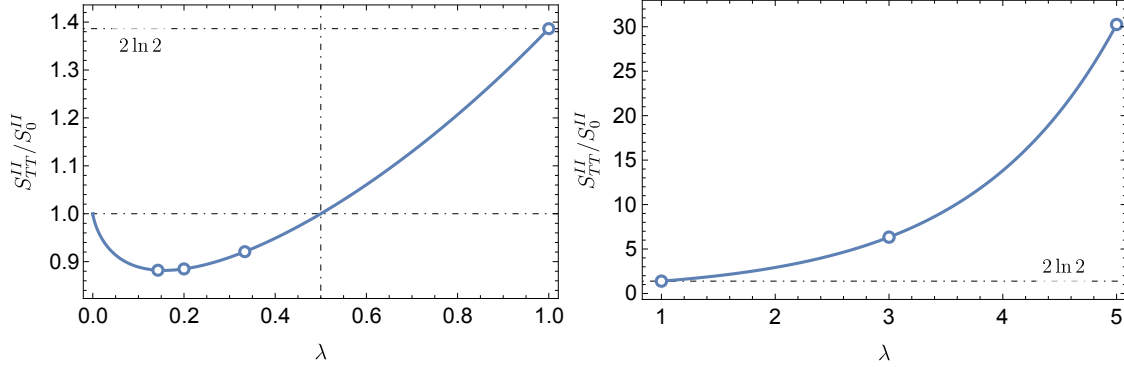


Figure 3: Tunneling delta- $T$  noise (32) in the large bias regime, normalized to the equilibrium noise  $S_0^{II}$ , as a function of the scaling dimension  $\lambda$ . Circles mark the values for  $\lambda = \nu$  for  $\nu = 1, 1/3, 1/5, 1/7$  (left panel) and  $\lambda = 1/\nu$  for  $\nu = 1, 1/3, 1/5$  (right panel). The free-electron value  $2 \ln 2$ , given by Eq. (34), is highlighted.

346 coefficients (28b), (28c), (30a), and (30b) reduce to

$$\mathcal{C}^{(2)} = \frac{\pi^2}{9} - \frac{2}{3}, \approx 0.43 \quad (31a)$$

$$\mathcal{C}^{(4)} = -\frac{7\pi^4}{675} + \frac{\pi^2}{9} - \frac{2}{15} \approx -0.05, \quad (31b)$$

$$\mathcal{D}^{(2)} = 0, \quad (31c)$$

$$\mathcal{D}^{(4)} = 0, \quad (31d)$$

347 where  $\mathcal{C}^{(2)}, \mathcal{C}^{(4)}$  are precisely those reported in Ref. [32]. The coefficients (31) may be obtained  
 348 also with a scattering approach (see Appendix G). We thus deduce that the finite coefficients  
 349  $\mathcal{D}^{(2)}$  and  $\mathcal{D}^{(4)}$  (which both vanish for in the non-interacting case  $\lambda = 1$ ) are a result of the  
 350 strongly correlated nature of the FQH edge, due to the non-trivial temperature dependence of  
 351 the differential tunneling conductance (21). In turn, this temperature dependence is a conse-  
 352 quence of the slow power-law decay of the dynamical correlations of the tunneling particles  
 353 in the FQH regime.

### 354 3.3 Delta-T noise for a large temperature bias

355 In the large bias limit, we choose  $T_1 = T_{\text{hot}} \gg T_2$ , effectively setting  $T_2 \rightarrow 0$ . Then, we find  
 356 that the tunneling charge-current noise (25c) reduces to

$$S_{TT}^{II} = 4g_T(T_{\text{hot}})k_B T_{\text{hot}} \mathcal{I}_{-1}(\lambda), \quad (32)$$

357 with the integral function

$$\mathcal{I}_n(\lambda) \equiv \frac{\Gamma(2\lambda)}{\pi^\lambda \Gamma(\lambda)^4} \int_0^{+\infty} dx e^{-x} x^{\lambda+n} \left| \Gamma\left(\frac{\lambda}{2} + \frac{ix}{\pi}\right) \right|^2. \quad (33)$$

358 For generic values of  $\lambda$ , we resort to a numerical integration of the function  $\mathcal{I}_{-1}(\lambda)$  and plot the  
 359 tunneling noise in Fig. 3. We observe that for scaling dimensions  $\lambda < 1/2$ , the non-equilibrium  
 360 delta- $T$  noise is always smaller than the equilibrium contribution  $S_0^{II}$ . This behavior is directly  
 361 linked to that of the tunneling conductance  $g_T(\bar{T})$  in Eq. (22), which is a *decreasing* function  
 362 of the temperature when  $\lambda < 1/2$ . Then, given that  $T_{\text{hot}} = 2\bar{T}$  in the large bias limit [see

363 discussion below Eq. (26)], the decrease in  $g_T(T_{\text{hot}})$  is the reason why  $S_{TT}^{II} < S_0^{II}$ , despite that  
 364 the function  $\mathcal{I}_{-1}(\lambda)$  grows with  $\lambda$  even for  $\lambda < 1/2$ .

365 An exact evaluation of Eq. (32) is possible for  $\lambda = \nu = 1$  for which  $\mathcal{I}_{-1}(1) = \ln 2$ , thus  
 366 reproducing the known result [29, 34, 92]

$$S_{TT}^{II} = 4D \frac{e^2}{h} k_B T_{\text{hot}} \ln 2 = 4D \frac{e^2}{h} k_B \bar{T} \times 2 \ln 2, \quad (34)$$

367 where we reinstated  $h$  and  $k_B$ , and identified the reflection probability  $D$  from Eq. (24).

368 We confirm the result (34) with a scattering approach in Eq. (G.14) in Appendix G. Equa-  
 369 tion (34) can be re-written in a form which is reminiscent of a fluctuation-dissipation relation,  
 370 by defining an effective noise temperature [29]

$$S_{TT}^{II} = 4D \frac{e^2}{h} k_B T_{\text{noise}}, \quad T_{\text{noise}} \equiv T_{\text{hot}} \ln 2. \quad (35)$$

371 The effective noise temperature  $T_{\text{noise}} = T_{\text{hot}} \ln 2$  in the large temperature bias limit has been  
 372 experimentally established [29] for non-interacting electrons in a two-terminal setup. We note  
 373 that a corresponding effective noise temperature in the FQH regime is not straightforward to  
 374 define, as in this case the charge tunneling conductance depends on the temperature, prevent-  
 375 ing a clear separation between conductance and temperature. We point out here that Ref. [93]  
 376 explored the possibility of defining an effective noise temperature associated with an effective  
 377 distribution induced by the tunneling process. This requires the introduction of a second QPC  
 378 (used as a detector), after which the noise is measured. We do not consider this situation here,  
 379 as it goes beyond the scope of our work.

380 For completeness, we also present the large-bias limit of the cross-correlation noise (25f).  
 381 It reads

$$\frac{S_{34}^{II}}{S_0^{II}} = -\frac{1}{2} \mathcal{I}_{-1}(\lambda) + \frac{2^{2\lambda-1}}{\pi^{\lambda+1}} \frac{\Gamma(2\lambda)}{\Gamma^4(\lambda)} \int_0^{+\infty} dx e^{-x} x^{\lambda-1} \left| \Gamma\left(\frac{\lambda}{2} + i\frac{x}{\pi}\right) \right|^2 \text{Im} \left[ \psi^{(0)}\left(\frac{\lambda}{2} + i\frac{x}{\pi}\right) \right], \quad (36)$$

382 where  $\mathcal{I}_{-1}(\lambda)$  is given in Eq. (33) and  $\psi^{(0)}(z)$  is the digamma function. For  $\lambda = 1$ , the ex-  
 383 pression reduces to  $S_{34}^{II} = -S_0^{II}(2 \ln 2 - 1)$ , corresponding (up to a sign) to the shot noise of a  
 384 temperature-biased, two-terminal, non-interacting system [24, 34].

### 385 3.4 Full delta-T noise and comparison to asymptotic limits

386 We gain further insights into the delta- $T$  noise by numerically computing the full noise ratio  
 387  $S_{TT}^{II}/S_0^{II}$  in Eq. (25c) and plotting it together with the asymptotic expansions (27) and (32).  
 388 The result is presented in Fig. 4. The most striking feature is the very contrasting curve shape  
 389 for non-interacting electrons,  $\nu = \lambda = 1$ , in comparison to the  $\nu = \lambda = 1/3$  and  $\nu = \lambda = 1/5$   
 390 FQH edge states. Whereas  $1 \leq S_{TT}^{II}/S_0^{II} \leq 2 \ln 2$  for  $\nu = \lambda = 1$  [see Eq. (34)], this ratio is  
 391 instead bounded as  $S_{TT}^{II}/S_0^{II} \leq 1$  for the Laughlin edges. This feature reflects the non-trivial  
 392 scaling dimension  $\lambda \neq 1$  of the tunneling quasiparticles in the FQH regime [32, 37, 38]. The  
 393 bounded noise in the FQH regime further highlights that the noise on top of the equilibrium  
 394 one is indeed negative in this case [32], i.e., the non-equilibrium conditions *reduce* the noise  
 395 compared to equilibrium.

396 We also observe an additional important and quite surprising feature. For  $\lambda = 1, 1/3, 1/5$ ,  
 397 the small bias expansions (27) are in fact excellent approximations within a surprisingly broad  
 398 range of the temperature bias ratio  $T_1/T_2$ . This result suggests that for these values, the coeffi-  
 399 cients  $\mathcal{C}^{(n)}$  in the expansion (27) decrease rapidly in magnitude with increasing  $n$ . Notably, for  
 400  $\lambda = 1/3$ , the leading order expansion [i.e., keeping only  $\mathcal{C}^{(2)}$  in Eq. (27)] remains an excellent  
 401 approximation to the full noise over two orders of magnitude of the temperature bias ratio.

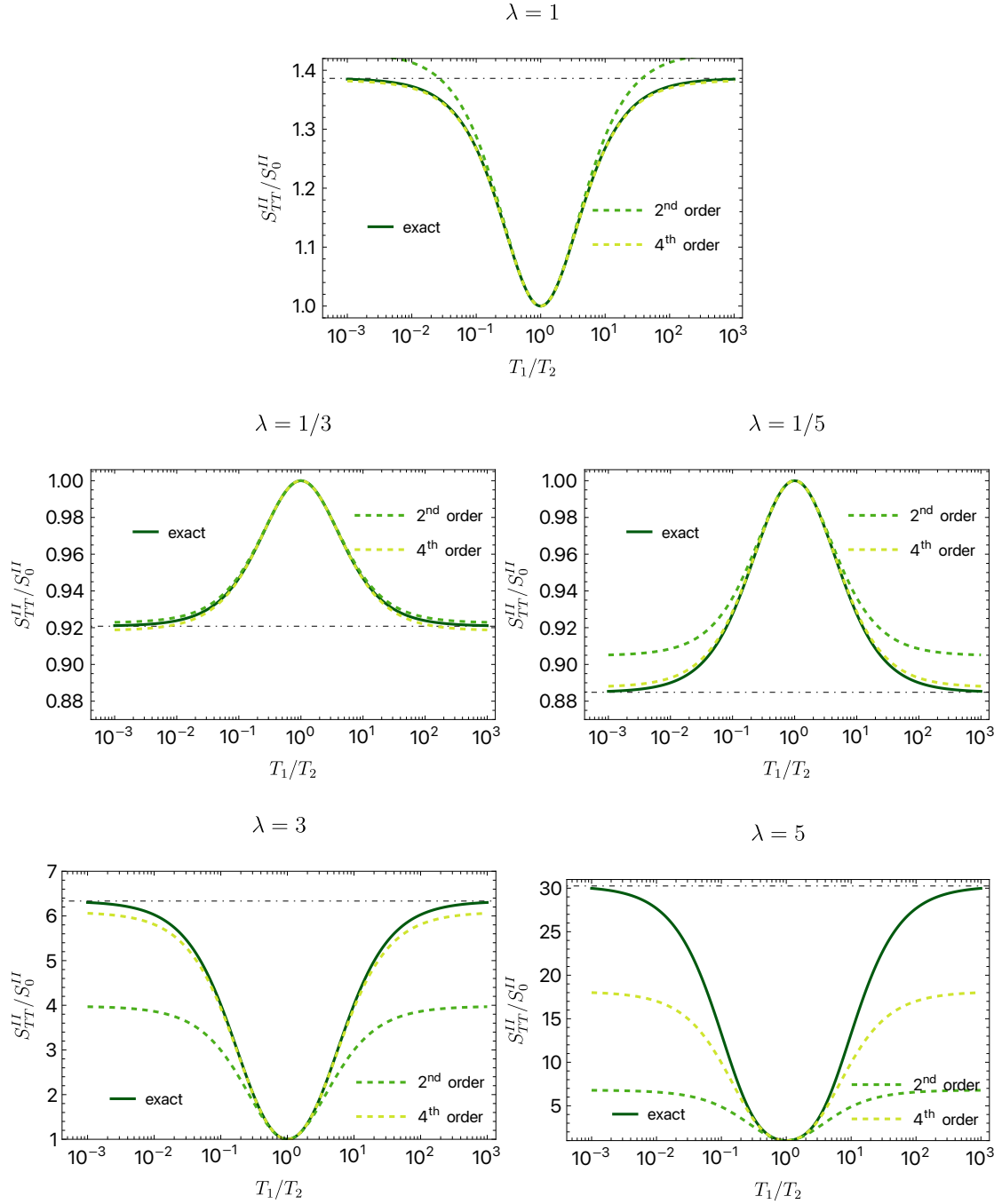


Figure 4: Numerically computed backscattering charge-current noise  $S_{TT}^{II}$ , normalized to  $S_0^{II}$  (solid, dark green line) for different scaling dimensions  $\lambda$ . The values  $\lambda = 1/3, 1/5$  correspond to the ideal ones in the weak backscattering regime at fillings  $\nu = 1/3, 1/5$ , while  $\lambda = 3, 5$  are the ideal values in the strong backscattering regime at the same filling. We also plot the small- $\Delta T$  expansions [see Eq. (27)] at second and fourth order, (light green, dashed and yellow, dashed curves, respectively). The large bias limits (32) are given as black, dot-dashed lines. The noise is plotted vs  $T_1/T_2 = [1 + \Delta T/(2\bar{T})]/[1 - \Delta T/(2\bar{T})]$ . Note that the large bias limit  $T_1/T_2 \gg 1$  is obtained for  $\Delta T \rightarrow 2\bar{T}$ ,  $T_1 \rightarrow T_{\text{hot}}$ , whereas in the opposite limit  $T_1/T_2 \ll 1$ ,  $T_2 \rightarrow T_{\text{hot}}$ .

402 We anticipate that this observation will be very useful in future modelling of delta- $T$  noise for  
 403 more complex FQH edge structures (see, e.g., Refs. [39, 41] for such cases). Furthermore, we  
 404 remark that the results in Fig. 4 strongly suggest that the asymptotic value (32) provides an  
 405 upper bound (for any temperatures  $T_1$  and  $T_2$ ) to the tunneling noise  $S_{TT}^{II}$  when  $\lambda > 1/2$ , but  
 406 a lower bound when  $\lambda < 1/2$ . We leave a rigorous proof of this conjecture, along the lines of  
 407 Refs. [34, 92, 94], for future work.

408 While we focused our numerical evaluation on the tunneling noise, the same analysis can  
 409 be repeated for the cross correlation  $S_{34}^{II}$ , and we find very similar results: The first two expan-  
 410 sion coefficients in (29) provide an excellent approximation for  $S_{34}^{II}$  over an extended range  
 411 of the temperature bias ratio. Moreover, the cross-correlation noise is always negative and  
 412 appears to be bounded from below by the large bias limit (36) for all scaling dimensions  $\lambda$ .

## 413 4 Heat currents and heat-current noise

414 In this section, we analyze the heat-current noise for a pure temperature bias, without any  
 415 voltage bias:  $V = 0$ . In the same manner as for the charge currents and the charge-current  
 416 noise (see Sec. 3), we derive zero-frequency expressions for heat currents and heat-current  
 417 noise (detailed calculations including finite frequency noise expressions are presented in Ap-  
 418 pendix B, which also includes the case  $V \neq 0$ ).

419 First, we obtain the average heat tunneling current in Eq. (3) as

$$J_T = -2i|\Lambda|^2 \int_{-\infty}^{+\infty} d\tau G_L(\tau) \partial_\tau G_R(\tau), \quad (37)$$

420 where the Green's functions are given in Eq. (19). In contrast to the charge tunneling cur-  
 421 rent (18), we see that the average heat tunneling current is finite even for  $V = 0$ . Indeed,  
 422 a vanishing average heat tunneling current requires also  $T_1 = T_2$ , i.e., no temperature bias.  
 423 From Eq. (37), we next define the heat tunneling conductance

$$g_T^Q(\bar{T}) = \lim_{\Delta T \rightarrow 0} \frac{\partial J_T}{\partial \Delta T} = \frac{\pi \lambda^2}{1 + 2\lambda} \frac{|\Lambda|^2}{2v_F^2} \bar{T} (2\pi \bar{T} \tau_0)^{2\lambda-2} \frac{\Gamma^2(\lambda)}{\Gamma(2\lambda)} = \gamma \kappa_0 \bar{T} g_T(\bar{T}) \frac{2\pi}{e^2}. \quad (38)$$

424 Here, in the final equality, we identified the charge tunneling conductance (22), and used that  
 425  $\kappa_0 \bar{T} = \pi \bar{T} / 6$  is the heat conductance quantum [in conventional units,  $\kappa_0 \bar{T} = \pi^2 k_B^2 \bar{T} / (3h)$ ].  
 426 Moreover, the prefactor

$$\gamma = \frac{\lambda^2}{v^2} \times \frac{3}{2\lambda + 1} \quad (39)$$

427 characterizes the deviation from the Wiedemann-Franz law [95–97] as

$$\frac{g_T^Q(\bar{T})}{g_T(\bar{T})\bar{T}} = \gamma L_0, \quad (40)$$

428 where  $L_0 = (\pi^2/3)(k_B/e)^2$  is the Lorenz number. The deviation from the Wiedemann-Franz  
 429 law ( $\gamma \neq 1$ ) in the FQH regime highlights that charge and heat are not carried by free electrons  
 430 in the QPC tunneling, but instead by fractionalized quasiparticles.



431 Next, we obtain the zero-frequency heat-current noise components as

$$S_{11}^{JJ} = 2 \frac{\pi^2 k_B^3}{3h} T_1^3, \quad (41a)$$

$$S_{22}^{JJ} = 2 \frac{\pi^2 k_B^3}{3h} T_2^3, \quad (41b)$$

$$S_{TT}^{JJ} = 4|\Lambda|^2 \int_{-\infty}^{+\infty} d\tau \partial_\tau G_R(\tau) \partial_\tau G_L(\tau), \quad (41c)$$

$$S_{33}^{JJ} = S_{11}^{JJ} + S_{TT}^{JJ} - 4k_B \lambda T_1 J_T - 8i|\Lambda|^2 k_B T_1 \int_{-\infty}^{+\infty} d\tau \tau \partial_\tau G_R(\tau) \partial_\tau G_L(\tau), \quad (41d)$$

$$S_{44}^{JJ} = S_{22}^{JJ} + S_{TT}^{JJ} + 4k_B \lambda T_2 J_T - 8i|\Lambda|^2 k_B T_2 \int_{-\infty}^{+\infty} d\tau \tau \partial_\tau G_L(\tau) \partial_\tau G_R(\tau), \quad (41e)$$

$$S_{34}^{JJ} = -S_{TT}^{JJ} + 2\lambda k_B (T_1 - T_2) J_T + 4i|\Lambda|^2 k_B (T_1 + T_2) \int_{-\infty}^{+\infty} d\tau \tau \partial_\tau G_R(\tau) \partial_\tau G_L(\tau), \quad (41f)$$

$$S_{43}^{JJ} = S_{34}^{JJ}. \quad (41g)$$

432 By plugging these expressions into Eq. (6), we see that they satisfy energy conservation. Next,  
433 we evaluate the expressions (41) for equilibrium  $T_1 = T_2 = \bar{T}$ . We then have

434  $S_{11}^{JJ} = S_{22}^{JJ} = S_{33}^{JJ} = S_{44}^{JJ} = 2\kappa_0 k_B \bar{T}^3$ ,  $S_{34}^{JJ} = S_{43}^{JJ} = 0$ , and  $S_{TT}^{JJ} = 4G_T^Q(\bar{T})\bar{T}^2$ , which are precisely  
435 the expected equilibrium expressions [48, 98]. We also have that for  $\lambda = 1$ , Eqs. (41) correctly  
436 reduce to the expressions for non-interacting electrons, obtained within scattering theory.

437 In the following subsections, we consider, just as for the delta- $T$  noise in Sec. 3, the two  
438 analytically tractable limits of small and large temperature biases. The results are presented  
439 below in Secs. 4.1 and 4.2, respectively.

#### 440 4.1 Heat-current noise for small temperature bias

441 In the small temperature bias regime,  $\Delta T \ll \bar{T}$  with  $T_{1,2} = \bar{T} \pm \Delta T/2$ , we expand the heat  
442 tunneling noise (41c) in powers of  $\Delta T/(2\bar{T})$ , and integrate term by term. We then find

$$S_{TT}^{JJ} = S_0^{JJ} \left[ 1 + C_Q^{(2)} \left( \frac{\Delta T}{2\bar{T}} \right)^2 + C_Q^{(4)} \left( \frac{\Delta T}{2\bar{T}} \right)^4 + \dots \right], \quad (42)$$

443 where the zeroth order, or equilibrium, heat tunneling noise reads

$$S_0^{JJ} = \frac{2\pi\lambda^2}{1+2\lambda} \frac{|\Lambda|^2}{v_F^2} \bar{T}^3 (2\pi\bar{T}\tau_0)^{2\lambda-2} \frac{\Gamma^2(\lambda)}{\Gamma(2\lambda)} = 4g_T^Q(\bar{T})\bar{T}^2, \quad (43)$$

444 where we identified the heat tunneling conductance Eq. (38) in the final equality. Equa-  
445 tion (43) manifests the fluctuation-dissipation theorem for zero-frequency heat transport [48,  
446 98].

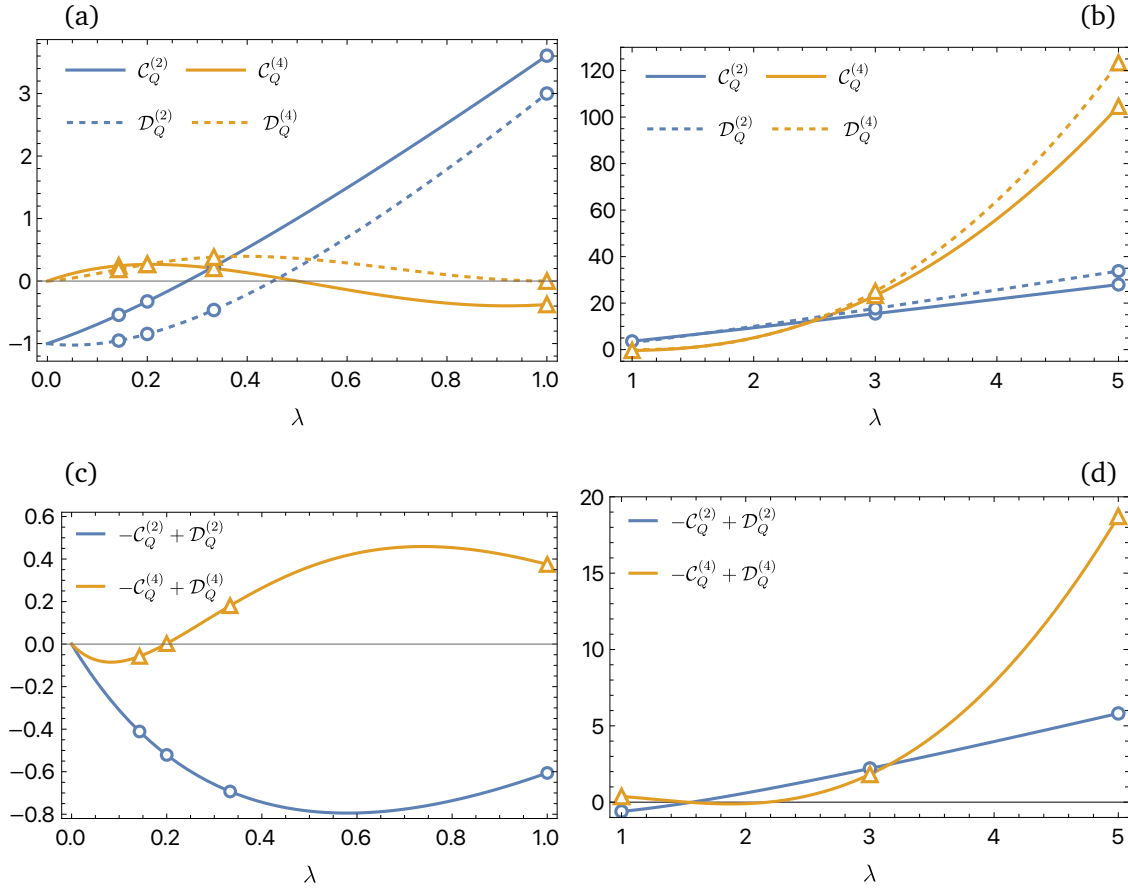


Figure 5: Second- and fourth-order delta- $T$  noise expansion coefficients  $C_Q^{(2)}$ ,  $C_Q^{(4)}$ ,  $D_Q^{(2)}$ , and  $D_Q^{(4)}$  (Eq. (47a), (47b), (47c), and (47d), respectively) as functions of the scaling dimension  $\lambda$ . Triangles and circles mark the values for  $\lambda = 1, 1/3, 1/5, 1/7$  (panels a and c) and  $\lambda = 1, 3, 5$  (panels b and d).

447 The heat-current noise expansion coefficients in Eq. (42) read

$$C_Q^{(2)} = \frac{(\pi^2(3\lambda + 4) - 2(2\lambda + 7))\lambda^2 - 2(3\lambda + 4)\lambda^2\psi^{(1)}(\lambda) + 8}{2\lambda(2\lambda + 3)}, \quad (44a)$$

$$\begin{aligned} C_Q^{(4)} = & \frac{\lambda\{12[(1 + 2\lambda)(2\lambda^2 + 13\lambda + 23) - \pi^2(2 + \lambda)(6\lambda^2 + 23\lambda - 10)]\}}{24(3 + 2\lambda)(5 + 2\lambda)} \\ & + \frac{\lambda\pi^4(15\lambda^3 + 60\lambda^2 + 64\lambda + 16)}{24(3 + 2\lambda)(5 + 2\lambda)} \\ & - \frac{\lambda[\pi^2(15\lambda^3 + 60\lambda^2 + 64\lambda + 16) - 2(2 + \lambda)(6\lambda^2 + 23\lambda - 10)]}{2(3 + 2\lambda)(5 + 2\lambda)}\psi^{(1)}(1 + \lambda) \\ & + \frac{\lambda(15\lambda^3 + 60\lambda^2 + 64\lambda + 16)}{2(3 + 2\lambda)(5 + 2\lambda)}[\psi^{(1)}(1 + \lambda)]^2 + \frac{\lambda(15\lambda^3 + 60\lambda^2 + 64\lambda + 16)}{12(3 + 2\lambda)(5 + 2\lambda)}\psi^{(3)}(1 + \lambda). \end{aligned} \quad (44b)$$

448 We plot these coefficients in Fig. 5. We see that the coefficient  $C_Q^{(2)}$  changes its sign at  
 449  $\lambda = \lambda^* \approx 0.28$  which, somewhat surprisingly, shows that  $C_Q^{(2)} < 0$  for all ideal Laughlin states,  
 450 *except*  $\nu = 1/3$  for which it is positive. This feature stands in contrast to the charge tunneling  
 451 noise expansion coefficient  $C^{(2)}$  (see Eq. (28b) and the discussion below it), which is negative

452 for all Laughlin states. However, we believe that this different behavior has no deeper meaning  
 453 and, in particular, it does not imply any fundamental differences between the 1/3 state and  
 454 the other Laughlin states. Rather, the difference between the delta- $T$  and heat-current noise  
 455 is their different dependence on the scaling dimensions. Ultimately, this feature is related to  
 456 the fact that the transported heat depends on the energy at which it is transferred, while the  
 457 charge does not [compare in particular Eqs. (68) and (71) in Sec. 5 below]. In turn, the scal-  
 458 ing dimension dependency affects the results of those integrals that arise when the noises are  
 459 expanded in powers of  $\Delta T$ .

460 Moving on to cross correlation heat-current noise (41f), we obtain the expansion

$$S_{34}^{JJ} = S_{43}^{JJ} = S_0^{JJ} \left[ (-C_Q^{(2)} + D_Q^{(2)}) \left( \frac{\Delta T}{2\bar{T}} \right)^2 + (-C_Q^{(4)} + D_Q^{(4)}) \left( \frac{\Delta T}{2\bar{T}} \right)^4 + \dots \right], \quad (45)$$

461 with the additional coefficients

$$D_Q^{(2)} = \frac{\lambda(4+3\lambda)[\pi^2 - 6\psi^{(1)}(1+\lambda)] + 2(1+2\lambda)(\lambda-3)}{2(3+2\lambda)}, \quad (46a)$$

$$\begin{aligned} D_Q^{(4)} = & \frac{3\lambda(1+2\lambda)(5-5\lambda-2\lambda^2)}{2(3+2\lambda)(5+2\lambda)} + \frac{\lambda(6\lambda^3+71\lambda^2+54\lambda-140)}{6(3+2\lambda)(5+2\lambda)} [6\psi^{(1)}(1+\lambda) - \pi^2] \\ & + \frac{\pi^2\lambda(16+64\lambda+60\lambda^2+15\lambda^3)}{24(3+2\lambda)(5+2\lambda)} [\pi^2 - 20\psi^{(1)}(1+\lambda)] \\ & + \frac{5\lambda(16+64\lambda+60\lambda^2+15\lambda^3)\{\psi^{(3)}(1+\lambda) + 6[\psi^{(1)}(1+\lambda)]^2\}}{12(3+2\lambda)(5+2\lambda)}. \end{aligned} \quad (46b)$$

462 For non-interacting electrons  $\lambda = 1$ , the expansion coefficients reduce to

$$C_Q^{(2)} = \frac{1}{15}(7\pi^2 - 15) \approx 3.6, \quad (47a)$$

$$C_Q^{(4)} = 2\pi^2 \left( \frac{7}{15} - \frac{31}{630}\pi^2 \right) \approx -0.37, \quad (47b)$$

$$D_Q^{(2)} = 3, \quad (47c)$$

$$D_Q^{(4)} = 0, \quad (47d)$$

463 in full agreement with the scattering approach, see Appendix G. Importantly, as shown in the  
 464 bottom panels of Fig. 5, the leading-order cross correlation expansion coefficient in Eq. (45),  
 465 i.e.,  $-C_Q^{(2)} + D_Q^{(2)}$  is *always* negative for all scaling dimensions  $\lambda \leq 1$ . In particular, it has the  
 466 same sign for all ideal Laughlin states, in contrast to the auto-correlation coefficient  $C_Q^{(2)}$ , which  
 467 may change sign as discussed above.

## 468 4.2 Heat-current noise for large temperature bias

469 Here, we consider the heat-current noise in the large bias limit  $T_1 = T_{\text{hot}} \gg T_2$ , so that the  
 470 cold temperature can effectively be set to  $T_2 \rightarrow 0$ . In this limit, we obtain the heat tunneling  
 471 noise (41c) as

$$S_{TT}^{JJ} = 4(k_B T_{\text{hot}})^2 g_T^Q(T_{\text{hot}}) \frac{8}{\pi^2} \frac{1+2\lambda}{\lambda^2} \mathcal{I}_1(\lambda), \quad (48)$$

472 with  $\mathcal{I}_1(\lambda)$  given in Eq. (33). We have not been able to evaluate this integral analytically for  
 473 generic  $\lambda$ , but for  $\lambda = 1$  we find

$$S_{TT}^{JJ} = \frac{|\Lambda|^2}{v_F^2} \frac{8T_{\text{hot}}^3}{\pi^2} \frac{3}{8} \pi \zeta(3) = \frac{3}{\pi} D\zeta(3) T_{\text{hot}}^3, \quad (49)$$

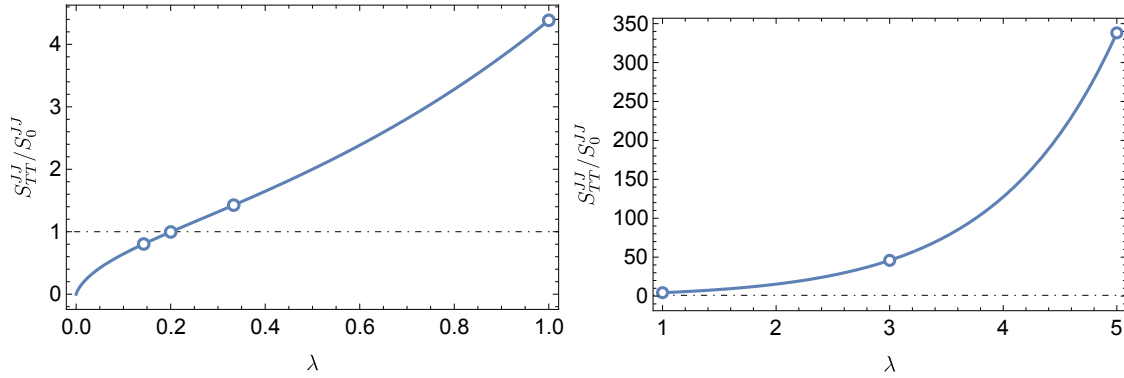


Figure 6: Tunneling heat delta- $T$  noise (48) in the large bias regime, normalized to the equilibrium noise  $S_0^{JJ}$  in Eq. (43), as a function of the scaling dimension  $\lambda$ . Circles mark the values for  $\lambda = \nu$  for  $\nu = 1, 1/3, 1/5, 1/7$  (left panel) and  $\lambda = 1/\nu$  for  $\nu = 1, 1/3, 1/5$  (right panel).

474 where  $\zeta(z)$  is the Riemann zeta function with  $\zeta(3) \approx 1.2$ . In the final equality in Eq. (49), we  
 475 identified the QPC reflection probability  $D$  from Eq. (24). The expression (49) is equivalent  
 476 to that which we obtain with a scattering approach (see Appendix G). The evolution of the  
 477 asymptotic value (48) as a function of the scaling dimension is shown in Fig. 6.

### 478 4.3 Full heat-current noise and comparison to asymptotic limits

479 Here, we numerically compute the noise ratio  $S_{TT}^{JJ}/S_0^{JJ}$  and plot it together with the asymptotic  
 480 limits (42) and (48) in Fig. 7. We first note the very contrasting behaviour between  $\nu = \lambda = 1$   
 481 and the Laughlin states with  $\lambda < 1/3$ . This feature reflects the distinct scaling dimension  
 482 dependence of the tunneling heat-current noise for  $\lambda > \lambda^*$  and  $\lambda < \lambda^*$ , where  $\lambda^* \approx 0.28$   
 483 marks the value where the dominant  $C_Q^{(2)}$  coefficient changes sign (see Sec. 4.1). We also see  
 484 that for  $\lambda = \nu = 1$  and  $\nu = 1/3$ , keeping four orders in the small bias expansion (42) is  
 485 enough to quite accurately capture the tunneling heat-current noise over a very broad range  
 486 of temperatures. In contrast, for  $\lambda = 1/5$ , terms beyond the fourth order are required for an  
 487 accurate approximation.

488 Another crucial difference in comparison to the charge tunneling noise is that, below the  
 489 scaling dimension  $\lambda^*$  (for which  $C_Q^{(2)} = 0$ ), the tunneling heat noise displays a non-monotonic  
 490 behavior as a function of the temperature ratio  $T_1/T_2$ , particularly pronounced in Fig. 7 for  
 491  $\lambda = 1/5$ . Such features are absent in the charge tunneling noise  $S_{TT}^{II}$ . The non-monotonic  
 492 behaviour of the tunneling heat noise allows us to conclude that the asymptotic large bias  
 493 expression in Eq. (48) is neither an upper nor a lower bound on the heat tunneling noise  
 494 when  $\lambda < \lambda^* \approx 0.28$ .

495 The conclusion of the above analysis is that the heat-current noise has a scaling dimension  
 496 dependence that is quite distinct from the delta- $T$  noise. As elaborated above, this follows  
 497 since the heat transferred across the QPC depends on the energy at which it occurs while  
 498 the charge transfer does not. Still, as detailed in the next section and in the same spirit of  
 499 Ref. [37], it is possible to use heat current fluctuations to define Fano factors [55] that allows  
 500 an extraction of the scaling dimension, thereby eliminating additional non-universal effects  
 501 possibly present in the tunneling amplitude.

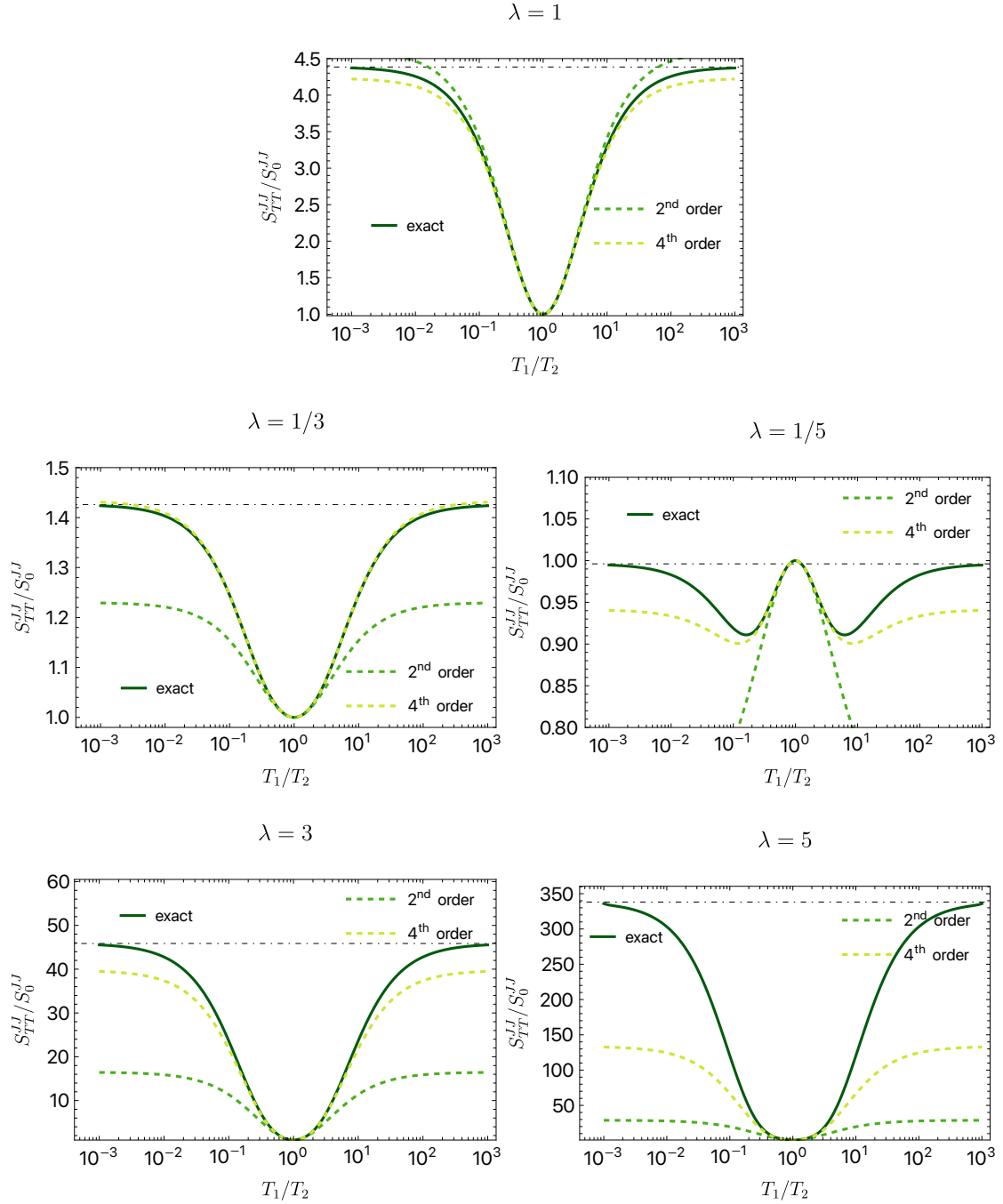


Figure 7: Numerically computed backscattering heat-current noise (solid, green line), normalized to  $S_0^{JJ}$  for different scaling dimensions  $\lambda$ . The values  $\lambda = 1/3, 1/5$  correspond to the ideal ones in the weak backscattering regime at fillings  $\nu = 1/3, 1/5$ , while  $\lambda = 3, 5$  are the ideal values in the strong backscattering regime at the same filling. We also plot the small- $\Delta T$  expansions [see Eq. (42)] to second and fourth order (green, dashed and yellow, dashed curves, respectively). The large bias limits (48) are given as black, dot-dashed lines. The noise is plotted vs  $T_1/T_2 = [1 + \Delta T/(2\bar{T})]/[1 - \Delta T/(2\bar{T})]$ . Note that for  $T_1/T_2 \gg 1$ ,  $T_1 \rightarrow T_{\text{hot}}$ , whereas in the opposite limit  $T_1/T_2 \ll 1$ ,  $T_2 \rightarrow T_{\text{hot}}$ .

#### 502 4.4 Generalized heat Fano factors

503 In Ref. [55], for the setup in Fig. 1, the authors define a “heat Fano factor” as

$$\mathcal{F}^J \equiv \frac{\Delta S_{33}^{JJ}}{2J_T}, \quad (50)$$

504 where  $\Delta S_{33}^{JJ} \equiv S_{33}^{JJ} - S_{11}^{JJ}$  is the excess heat-current noise in drain contact 3. The Fano fac-  
 505 tor (50) can be viewed as a heat transport analogue of the usual Fano factor in weak FQH  
 506 tunneling used to detect fractional charges [67–69]. In contrast with the standard Fano factor,  
 507 which involves both the scaling dimension and the charge of the tunneling quasiparticles [37],  
 508 the heat Fano factor has the advantage of providing a way to extract the scaling dimension  
 509 without any reference to the charge of the tunneling quasiparticles, thus providing a very ap-  
 510 pealing complementary tool for investigating complex FQH edge structures, especially those  
 511 involving neutral modes [70–73]. In the small temperature bias regime, with the parametriza-  
 512 tion  $T_1 = T_{\text{cold}}$  and  $T_2 = T_{\text{cold}} + \Delta T$ , Ref. [55] reports that the heat Fano factor evaluates to  
 513

$$\mathcal{F}^J = (2\lambda + 1)T_{\text{cold}} + \mathcal{O}\left(\frac{\Delta T}{T_{\text{cold}}}\right), \quad (51)$$

514 thereby providing a measure of the scaling dimension  $\lambda$ . The result (51) follows as both  $\Delta S_{33}^{JJ}$   
 515 and the tunneling current  $J_T$  are linear in  $\Delta T$  to leading order.

516 In this section, we generalize the Fano factor (50) by introducing additional heat Fano  
 517 factors as

$$\mathcal{F}_{\alpha\beta}^J = \frac{\Delta S_{\alpha\beta}^{JJ}}{2J_T}, \quad \alpha, \beta = 3, 4, \quad (52)$$

518 where  $\Delta S_{\alpha\beta}^{JJ}$  are excess heat-current noises, in which the equilibrium contributions, if present,  
 519 are subtracted. More specifically, we have  $\Delta S_{44}^{JJ} \equiv S_{44}^{JJ} - S_{22}^{JJ}$  and  $\Delta S_{34}^{JJ} = \Delta S_{43}^{JJ} \equiv S_{43}^{JJ}$ , since  
 520 the cross-correlation heat-current noises vanish in equilibrium. Due to energy conservation,  
 521 Eq. (6) dictates that, in the absence of voltage bias,

$$\mathcal{F}_{44}^J + \mathcal{F}_{33}^J + 2\mathcal{F}_{34}^J = 0, \quad (53)$$

522 so that there are only two independent heat Fano factors. Moreover, the explicit expressions  
 523 for the heat Fano factors may depend on the chosen parametrization of the temperature biases.  
 524 To investigate this, we next derive explicit results for the generic heat Fano factors (52) for  
 525 different parametrizations and temperature bias strengths.

##### 526 4.4.1 Small bias regime

527 **Symmetric temperature bias:** Here, we choose the symmetric temperature bias parametriza-  
 528 tion (26). We then expand the heat tunneling current (37) to leading order in  $\Delta T/(2\bar{T}) \ll 1$   
 529 and find

$$J_T = S_0^{JJ} \times \frac{1}{2\bar{T}} \frac{\Delta T}{2\bar{T}} + \mathcal{O}\left[\left(\frac{\Delta T}{2\bar{T}}\right)^2\right], \quad (54)$$

530 where  $S_0^{JJ} = 4g_T^Q(\bar{T})\bar{T}^2$  is the equilibrium heat tunneling noise (43). Combining Eq. (54) with  
 531 the expanded cross-correlation heat-current noise (45), we obtain the “crossed” heat Fano  
 532 factor as

$$\mathcal{F}_{34}^J = \frac{1}{2} \left[ -\mathcal{C}_Q^{(2)} + \mathcal{D}_Q^{(2)} \right] \Delta T, \quad (55)$$

533 with the scaling-dimension-dependent coefficients  $\mathcal{C}_Q^{(2)}$  and  $\mathcal{D}_Q^{(2)}$  given in Eq. (44a) and (46a),  
 534 respectively. We see that the Fano factor (55) depends on the temperature difference  $\Delta T$ , in

535 contrast with Eq. (51) which was derived in Ref. [55]. The reason for this is that the excess  
 536 auto-correlations satisfy  $\Delta S_{33}^{JJ} = -\Delta S_{44}^{JJ}$  to linear order in  $\Delta T$ . This observation, combined  
 537 with the sum rule (53), shows that keeping second-order terms in  $\Delta T$  is required to get a finite  
 538 Fano factor for the cross correlations. Explicitly, we find

$$\Delta S_{33}^{JJ} = S_0^{JJ} \left\{ -(2\lambda + 1) \left( \frac{\Delta T}{2\bar{T}} \right) + [C_Q^{(2)} - D_Q^{(2)}] \left( \frac{\Delta T}{2\bar{T}} \right)^2 \right\}, \quad (56a)$$

$$\Delta S_{44}^{JJ} = S_0^{JJ} \left\{ +(2\lambda + 1) \left( \frac{\Delta T}{2\bar{T}} \right) + [C_Q^{(2)} - D_Q^{(2)}] \left( \frac{\Delta T}{2\bar{T}} \right)^2 \right\}, \quad (56b)$$

539 which upon division with  $2J_T$  from Eq. (54) results in the two additional heat Fano factors

$$\mathcal{F}_{33}^J = -(2\lambda + 1)\bar{T} + \frac{1}{2} [C_Q^{(2)} - D_Q^{(2)}] \Delta T, \quad (57a)$$

$$\mathcal{F}_{44}^J = +(2\lambda + 1)\bar{T} + \frac{1}{2} [C_Q^{(2)} - D_Q^{(2)}] \Delta T. \quad (57b)$$

540 For non-interacting electrons,  $\lambda = 1$ , we find for the symmetric bias

$$\mathcal{F}_{33}^J|_{\lambda=1} = -3\bar{T} - \left( 2 - \frac{7\pi^2}{30} \right) \Delta T, \quad (58a)$$

$$\mathcal{F}_{44}^J|_{\lambda=1} = +3\bar{T} - \left( 2 - \frac{7\pi^2}{30} \right) \Delta T, \quad (58b)$$

$$\mathcal{F}_{34}^J|_{\lambda=1} = \left( 2 - \frac{7\pi^2}{30} \right) \Delta T. \quad (58c)$$

541 **Asymmetric temperature bias:** Here, we pick the alternative asymmetric bias parametriza-  
 542 tion  $T_1 = T_{\text{cold}} + \Delta T$  and  $T_2 = T_{\text{cold}}$ . Noticing that  $\bar{T} = T_{\text{cold}} + \Delta T/2$ , and keeping terms up to  
 543 second order in  $\Delta T$  in expressions found in Eq. (55) and Eq. (57), we obtain

$$\mathcal{F}_{33}^J = -(2\lambda + 1)T_{\text{cold}} + \frac{1}{2} [C_Q^{(2)} - D_Q^{(2)} - (1 + 2\lambda)] \Delta T, \quad (59a)$$

$$\mathcal{F}_{44}^J = +(2\lambda + 1)T_{\text{cold}} + \frac{1}{2} [C_Q^{(2)} - D_Q^{(2)} + (1 + 2\lambda)] \Delta T, \quad (59b)$$

$$\mathcal{F}_{34}^J = \mathcal{F}_{43}^J = \frac{1}{2} [-C_Q^{(2)} + D_Q^{(2)}] \Delta T, \quad (59c)$$

544 which thus extends the Fano factor from Ref. [55] with a correction that is linear in  $\Delta T$ . Note  
 545 that an explicit calculation of the Fano factors with the asymmetric parametrization requires  
 546 an expansion to second order in  $\Delta T$  also for the tunneling current. We also remark that the  
 547 opposite sign in the leading term of  $\mathcal{F}_{33}^J$  compared to the result (50) in Ref. [55] follows from  
 548 the fact that the authors choose  $T_1$  as the coldest temperature, which leads to a sign change  
 549 in the tunneling current. For  $\lambda = 1$ , we have for the asymmetric bias

$$\mathcal{F}_{33}^J|_{\lambda=1} = -3T_{\text{cold}} + \left( \frac{7\pi^2}{30} - 5 \right) \Delta T, \quad (60a)$$

$$\mathcal{F}_{44}^J|_{\lambda=1} = +3T_{\text{cold}} + \left( \frac{7\pi^2}{30} + 1 \right) \Delta T, \quad (60b)$$

$$\mathcal{F}_{34}^J|_{\lambda=1} = \left( 2 - \frac{7\pi^2}{30} \right) \Delta T. \quad (60c)$$

#### 550 4.4.2 Large bias regime

551 For the large temperature bias, we take  $T_1 = T_{\text{hot}}$  and  $T_2 \rightarrow 0$ . Then, the heat-current  
552 noises (41d)-(41f) simplify to

$$\Delta S_{33}^{JJ} = S_{TT}^{JJ} - 8\lambda T_{\text{hot}} J_T, \quad (61a)$$

$$\Delta S_{44}^{JJ} = S_{TT}^{JJ}, \quad (61b)$$

$$\Delta S_{34}^{JJ} = -S_{TT}^{JJ} + 4\lambda T_{\text{hot}} J_T. \quad (61c)$$

553 Plugging into these expressions the heat tunneling current (37) in the large bias regime,

$$J_T = T_{\text{hot}} g_T^Q(T_{\text{hot}}) \frac{4}{\pi^2} \frac{1+2\lambda}{\lambda^2} \mathcal{I}_0(\lambda) \quad (62)$$

554 and the tunneling heat-current noise  $S_{TT}^{JJ}$  from Eq. (48), we find

$$\mathcal{F}_{33}^J = 2T_{\text{hot}} \left[ \frac{\mathcal{I}_1(\lambda)}{\mathcal{I}_0(\lambda)} - 2\lambda \right], \quad (63a)$$

$$\mathcal{F}_{44}^J = 2T_{\text{hot}} \frac{\mathcal{I}_1(\lambda)}{\mathcal{I}_0(\lambda)}, \quad (63b)$$

$$\mathcal{F}_{34}^J = 2T_{\text{hot}} \left[ \lambda - \frac{\mathcal{I}_1(\lambda)}{\mathcal{I}_0(\lambda)} \right], \quad (63c)$$

555 with the integral functions  $\mathcal{I}_n(\lambda)$  from Eq. (33). For free electrons, the large bias heat Fano  
556 factors reduce to

$$\mathcal{F}_{33}^J|_{\lambda=1} = 2T_{\text{hot}} \left[ \frac{9\zeta(3)}{\pi^2} - 2 \right] \approx -1.8T_{\text{hot}}, \quad (64a)$$

$$\mathcal{F}_{44}^J|_{\lambda=1} = 2T_{\text{hot}} \left[ \frac{9\zeta(3)}{\pi^2} \right] \approx 2.2T_{\text{hot}}, \quad (64b)$$

$$\mathcal{F}_{34}^J|_{\lambda=1} = 2T_{\text{hot}} \left[ 1 - \frac{9\zeta(3)}{\pi^2} \right] \approx -0.2T_{\text{hot}}. \quad (64c)$$

557 We note that the different form of  $\mathcal{F}_{33}^J$  and  $\mathcal{F}_{44}^J$  is simply due to the chosen bias parametriza-  
558 tion. By inverting the temperature bias (i.e., taking instead  $T_1 \rightarrow 0$  and  $T_2 = T_{\text{hot}}$ ), we simply  
559 get  $\mathcal{F}_{33}^J \leftrightarrow -\mathcal{F}_{44}^J$ , while the cross-correlation noise,  $\mathcal{F}_{34}^J$ , does not change. This feature is very  
560 distinct from voltage-biased charge-current noise, where the noise and Fano factor depend on  
561 the voltage *difference* between the source contacts. Our results in this subsection thus highlight  
562 that temperature biased induced noise behaves very differently, as there is no corresponding  
563 “gauge invariance” for the temperature bias.

564 Just as for the noise, it is instructive to compare the derived asymptotic limits for the Fano  
565 factors with the exact results obtained by numerical integration of both the tunneling current  
566 and the noise. We plot the exact results for all Fano factors as a function of  $T_1/T_2$  in Fig. 8,  
567 together with the asymptotic expressions that we have derived in the previous sections. As  
568 expected,  $\mathcal{F}_{34}^J$  vanishes when  $T_1 = T_2$ , while the other two Fano factors do not and approach  
569 the values  $\pm(2\lambda + 1)\bar{T}$ , as derived in Eq. (57). The dashed lines show the effect of the linear-  
570 in- $\Delta T$  corrections of Eq. (57), which must be included to better estimate the Fano factors,  
571 even for small  $\Delta T$ . Finally, we also see that the symmetry  $\mathcal{F}_{33}^J \leftrightarrow -\mathcal{F}_{44}^J$  upon exchange of  
572  $T_1 \leftrightarrow T_2$  is valid for generic values of  $T_1/T_2$  and not only in the large bias regime as discussed  
573 previously. This property can be proven explicitly by manipulating the integral expressions for  
574  $J_T$ ,  $S_{33}^{JJ}$ , and  $S_{44}^{JJ}$  (Eqs. (37), (41d), and (41e), respectively).



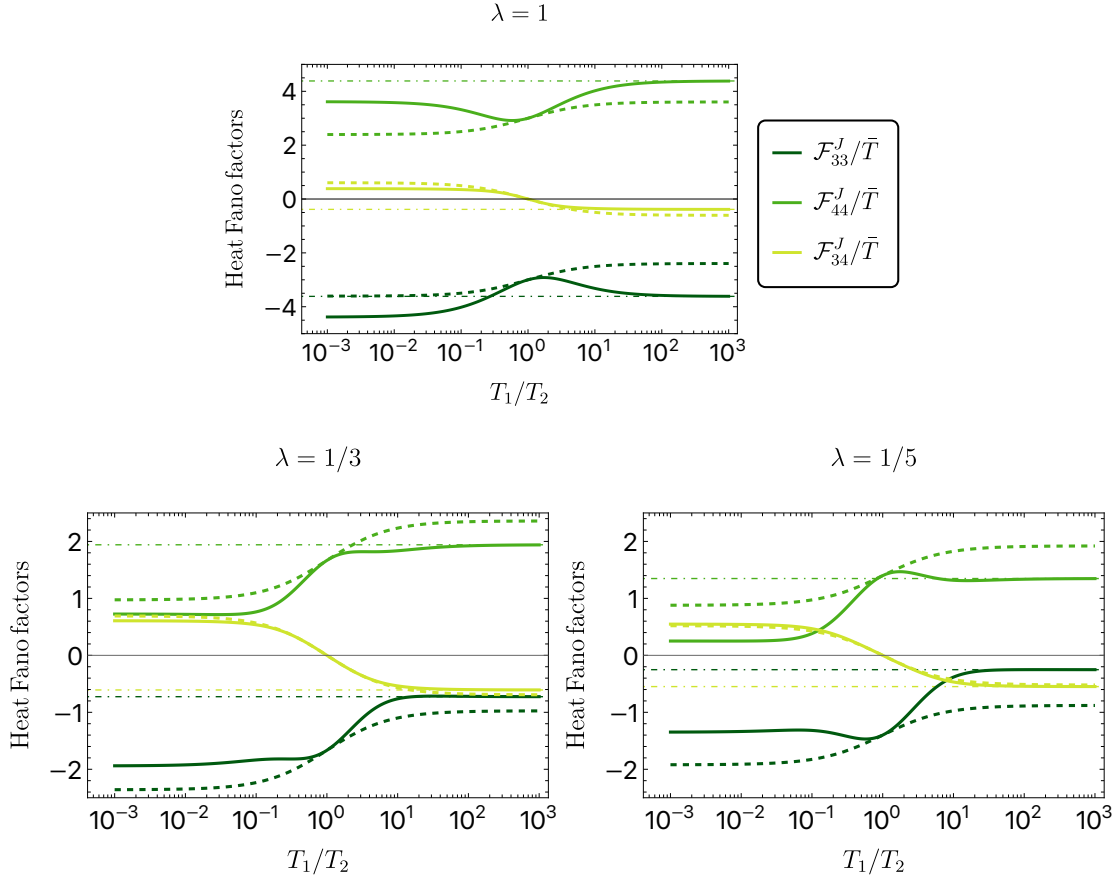


Figure 8: Numerically computed heat Fano factors normalized to  $\bar{T} = (T_1 + T_2)/2$ , for different scaling dimensions  $\lambda$ . The full lines are the exact results for  $\mathcal{F}_{33}^J$ ,  $\mathcal{F}_{44}^J$ , and  $\mathcal{F}_{34}^J$ , while the dashed lines refer to the small- $\Delta T$  results (55) and (57). The large bias limits (63) are shown as horizontal, dot-dashed lines. The Fano factors are plotted as a function of  $T_1/T_2 = [1 + \Delta T/(2\bar{T})]/[1 - \Delta T/(2\bar{T})]$ . The legend in the box applies to all plots.

## 575 5 Effective single-particle picture

576 To gain additional insights into the properties of the delta- $T$  and heat-current noise, we find  
 577 it useful to introduce an effective density of states (EDOS) [38, 99, 100]. We define the EDOS  
 578  $D_\lambda(E)$  by the relation

$$\frac{P_\alpha(E)}{2\pi a} = D_\lambda(E, T_\alpha) f_\alpha(-E), \quad (65)$$

579 where  $f_\alpha(E) = [\exp(E/T_\alpha) + 1]^{-1}$  is the Fermi-Dirac distribution at zero electrochemical po-  
 580 tential  $\mu_\alpha = 0$  and  $P_\alpha(E)$  is the quasiparticle Green's function (19) in energy space (see Ap-  
 581 pendix F for details). Alternatively, one may interpret the product  $D_\lambda(E, T_\alpha) f_\alpha(-E)$  as an  
 582 effective anyon distribution, an approach recently pursued in Ref. [101]. Straightforward ma-  
 583 nipulation of  $P_\alpha(E)$  gives the explicit expression

$$D_\lambda(E, T) = \frac{1}{v_F} \left( \frac{2\pi a}{v_F} \right)^{\lambda-1} T^{\lambda-1} \frac{\left| \Gamma\left(\frac{\lambda}{2} + i\frac{E}{2\pi T}\right) \right|^2}{\Gamma(\lambda) \left| \Gamma\left(\frac{1}{2} + i\frac{E}{2\pi T}\right) \right|^2}, \quad (66)$$

584 along with its zero-temperature limit

$$D_\lambda(E, 0) = \frac{1}{v_F \Gamma(\lambda)} \left( \frac{a}{v_F} \right)^{\lambda-1} |E|^{\lambda-1}. \quad (67)$$

585 For non-interacting electrons,  $D_1(E, T) = 1/v_F$ , which, notably, has no energy and temperature  
586 dependencies.

587 With the EDOS (66), we use a Fourier transform to write the charge tunneling noise  $S_{TT}^{II}$   
588 in Eq. (25c) as

$$S_{TT}^{II} = \frac{4e^2 v^2 |\Lambda|^2}{(2\pi a)^2} \frac{1}{2\pi} \int_{-\infty}^{+\infty} dE P_1(E) P_2(-E) \equiv \frac{4v^2 e^2}{2\pi} \int_{-\infty}^{+\infty} dE D_{\text{eff}}(E) f_1(-E) f_2(E). \quad (68)$$

589 Here, in the final equality, we defined the effective energy-dependent tunneling probability

$$D_{\text{eff}}(E) \equiv |\Lambda|^2 D_\lambda(E, T_1) D_\lambda(-E, T_2), \quad (69)$$

590 which reduces to  $D_{\text{eff}}(E) = |\Lambda|^2 / v_F^2 = D$  [see Eq. (24)] for  $\lambda = \nu = 1$ . In this case, the  
591 expression (68) is fully equivalent to the scattering formula in Eq. (G.9) (see Appendix G), for  
592 weak tunneling. By inspecting Eqs. (66) and (69), we see that both  $D_\lambda(E, T_\alpha)$  and  $D_{\text{eff}}(E)$  are  
593 even functions of energy. This feature is a consequence of the particle-hole symmetry inherent  
594 to the linearized bosonic spectrum, which is a key feature of the chiral Luttinger model. By  
595 using this symmetry, we further express the tunneling charge noise (68) as

$$S_{TT}^{II} = 2(e\nu)^2 (\Gamma_{1 \rightarrow 2} + \Gamma_{2 \rightarrow 1}), \quad (70a)$$

$$\Gamma_{1 \rightarrow 2} \equiv \frac{1}{2\pi} \int_{-\infty}^{+\infty} dE D_{\text{eff}}(E) f_1(E) [1 - f_2(E)], \quad (70b)$$

$$\Gamma_{2 \rightarrow 1} \equiv \frac{1}{2\pi} \int_{-\infty}^{+\infty} dE D_{\text{eff}}(E) f_2(E) [1 - f_1(E)]. \quad (70c)$$

596 Here,  $\Gamma_{1 \rightarrow 2}$  are tunneling rates, in terms of which the charge tunneling current (18) reads  
597  $I_T = -2e\nu(\Gamma_{1 \rightarrow 2} - \Gamma_{2 \rightarrow 1})$ . **The rewriting of the tunneling noise in the form of Eq. (70) makes  
598 the result analogous to a conventional Landauer-Büttiker formula, where the EDOS plays the  
599 role of the transmission function.**

600 The expressions for the tunneling current and the associated noise in terms of rates are a  
601 special instance of a general behavior of weak tunneling links [102]. An advantage of writing  
602 the tunneling noise in this way is that it permits a transparent interpretation of the large tem-  
603 perature bias regime discussed in Sec. 3.3. Indeed, setting  $T_2 = 0$ , the rates  $\Gamma_{1 \rightarrow 2}$  and  $\Gamma_{2 \rightarrow 1}$   
604 select only negative and positive energies, respectively. For free-electron tunneling, this limit  
605 permits a clear interpretation of the non-interacting tunneling noise (34) as being proportional  
606 to the sum of electron and hole fluxes emanating from the hot source contact [92]. By analogy,  
607 the strongly correlated expression (32) can, via Eq. (70), viewed as a sum of fluxes of fraction-  
608 ally charged quasi-particles and quasi-holes, mediated by the effective tunneling probability  
609  $D_{\text{eff}}(E)$  in Eq. (69).

610 Analogously to the delta- $T$  noise, we can also express the heat-current noise by exploiting  
611 the EDOS. In particular, the heat tunneling noise (41c) can be written as

$$S_{TT}^{JJ} = \frac{4}{2\pi} \int_{-\infty}^{+\infty} dE E^2 D_{\text{eff}}(E) f_1(-E) f_2(E), \quad (71)$$

612 which reduces to the scattering formula Eq. (G.9) when  $\lambda = \nu = 1$  (see Appendix G). However,  
613 in contrast to the charge noise, it is not possible to introduce rates in such a way that the

614 tunneling current is given by their difference and the noise by their sum. The reason for this is  
 615 that the transported heat depends on the energy at which it is transferred. As a consequence,  
 616 the rates for the heat transfers includes integration over  $ED_{\text{eff}}(E)$ , while the noise instead  
 617 includes integration over  $E^2D_{\text{eff}}(E)$ . For non-interacting systems, this fact was recently noted  
 618 in Ref. [92], and we thus establish here the same property also for weak tunneling in the FQH  
 619 regime.

620 The above approach shows that by introducing  $D_{\text{eff}}(E)$ , we can put our perturbative ap-  
 621 proach to weak tunneling in the FQH regime on a similar footing as non-interacting particles  
 622 treated with a scattering approach. As such, insofar as the tunneling currents and the associ-  
 623 ated noise are concerned, we may view the FQH setup in Fig. 1 as two fermionic reservoirs (the  
 624 sources) bridged by a conductor fully captured in terms of the energy-dependent transmission  
 625  $D_{\text{eff}}(E)$ . With the EDOS and the effective tunneling probability, we see that the non-trivial  
 626 scaling dimension behavior of the tunneling delta- $T$  and heat-current noises,  $S_{TT}^{II}$  and  $S_{TT}^{JJ}$ , re-  
 627 spectively, comes entirely from the correlation-induced energy and temperature dependence in  
 628  $D_{\text{eff}}(E)$ . Furthermore, the peculiar feature of negative excess charge noise can with the EDOS  
 629 be seen to be essentially the same energy filtering mechanism that was identified in scattering  
 630 theory in Ref. [103] (see also Ref. [38] for a discussion).

## 631 6 Mixed noise

632 While our focus in this work is on delta- $T$  and heat-current noise —corresponding to Eq. (1),  
 633 with both involved operators referring to either charge, or heat current— we may consider also  
 634 correlations between a charge current operator and a heat current operator. Such quantities  
 635 are known as mixed noise (see e.g. Ref. [58]). Explicitly, the mixed charge-heat noise is  
 636 defined as

$$S_{\alpha\beta}^{IJ}(\omega) = \int_{-\infty}^{+\infty} dt \langle \{\delta\hat{I}_\alpha(t), \delta\hat{J}_\beta(0)\} \rangle e^{i\omega t}, \quad (72)$$

637 with  $\alpha, \beta$  labelling the drain contacts 3 and 4.

638 In this section, we comment briefly on this type of noise for the QPC device in Fig. 1.  
 639 Before presenting our results in the FQH regime, we recall previously known results, based on  
 640 scattering theory, for non-interacting systems. In this case, it was shown in Ref. [58] that, near  
 641 equilibrium, the zero-frequency mixed noise is closely related to thermoelectric conversion.  
 642 More specifically, at equilibrium temperature  $\bar{T}$ , one finds for a non-interacting electron system

$$S_0^{IJ}(0) = 2k_B \bar{T}^2 \mathcal{S} g_T(\bar{T}), \quad (73)$$

643 where  $g_T(\bar{T})$  is the charge tunneling conductance and  $\mathcal{S}$  is the Seebeck coefficient. It is well-  
 644 known that finite thermoelectric conversion (i.e.,  $\mathcal{S} \neq 0$ ) always requires some sort of energy  
 645 filtering mechanism (via an energy-dependent transmission) of the transferred particles and  
 646 holes, i.e., a mechanism that breaks particle-hole symmetry, see e.g., Ref. [104]. This feature  
 647 suggests that, also in the FQH regime, particle-hole symmetry breaking is required to generate  
 648 non-vanishing mixed noise. In the following, we show that this is indeed the case. When  
 649 we evaluate the mixed noise, we exclude band curvature effects, or an asymmetric tunneling  
 650 amplitude  $\Lambda(E) \neq \Lambda(-E)$ . Instead, we focus on the simple option of breaking particle-hole  
 651 symmetry with a finite voltage bias  $V \neq 0$  on top of the temperature bias.

652 With the same approach we used for the charge and heat noises, we compute (details are  
 653 provided in Appendix C) all possible combinations  $S_{\alpha\beta}^{IJ}$ , with  $\alpha, \beta = 3, 4$ . At zero frequency,  
 654 we have

$$S_{33}^{IJ}(0) = +M_{TT} - \frac{V}{2} S_{TT}^{II} - 2T_1(1 + \lambda)I_T + 4T_1\partial_V \langle \hat{J}_3^{(2)} \rangle, \quad (74a)$$

$$S_{44}^{IJ}(0) = +M_{TT} + \frac{V}{2}S_{TT}^{II} + 2T_2(1 + \lambda)I_T - 4T_2\partial_V \langle \hat{j}_4^{(2)} \rangle, \quad (74b)$$

$$S_{34}^{IJ}(0) = -M_{TT} - \frac{V}{2}S_{TT}^{II} - 2\lambda T_2 I_T + 2(T_1 + T_2)\partial_V \langle \hat{j}_4^{(2)} \rangle, \quad (74c)$$

$$S_{43}^{IJ}(0) = -M_{TT} + \frac{V}{2}S_{TT}^{II} + 2\lambda T_1 I_T - 2(T_1 + T_2)\partial_V \langle \hat{j}_3^{(2)} \rangle. \quad (74d)$$

655 Here, we introduced the tunneling-induced components of the average heat currents in the  
 656 drains in the presence of a finite voltage bias, denoted  $\langle \hat{j}_\alpha^{(2)} \rangle$ . We obtain these components  
 657 from the perturbative expansion in Eq. (15b) (see also Eq. (B.7) in Appendix B) as

$$\langle \hat{j}_3^{(2)} \rangle = 2i|\Lambda|^2 \int_{-\infty}^{+\infty} d\tau \cos(e\nu V \tau) G_L(\tau) \partial_\tau G_R(\tau), \quad (75a)$$

$$\langle \hat{j}_4^{(2)} \rangle = 2i|\Lambda|^2 \int_{-\infty}^{+\infty} d\tau \cos(e\nu V \tau) G_R(\tau) \partial_\tau G_L(\tau). \quad (75b)$$

658 For  $V = 0$ , they reduce to  $\langle \hat{j}_4^{(2)} \rangle = -\langle \hat{j}_3^{(2)} \rangle = J_T$ , i.e., the heat tunneling current (37). In  
 659 Eq. (74), we also introduced the integral

$$M_{TT} = 2e\nu|\Lambda|^2 \int_{-\infty}^{+\infty} d\tau \sin(e\nu V \tau) [G_L(\tau) \partial_\tau G_R(\tau) - G_R(\tau) \partial_\tau G_L(\tau)]. \quad (76)$$

660 The first two terms on each line in Eq. (74) represent contributions from correlations of the  
 661 first-order correction to the charge and heat currents, namely  $\hat{I}_\alpha^{(1)}$  and  $\hat{J}_\beta^{(1)}$ , cf. Eqs. (C.3-C.4)  
 662 in Appendix C. As a consequence, these terms are of similar nature as the tunneling charge  
 663 noise, as they involve correlations between the tunneling charge current and the heat transfer  
 664 between the upper and lower edge (note, however, that due to lack of heat conservation at  
 665  $V \neq 0$ , the tunneling heat current from the upper to the lower edge is not the same as the  
 666 tunneling heat current in the opposite direction, i.e.,  $\langle \hat{j}_3^{(1)} \rangle \neq -\langle \hat{j}_4^{(1)} \rangle$ ).

667 To the best of our knowledge, the full expressions in Eq. (74) have not been previously  
 668 reported, especially the terms stemming from the correlations between the tunneling currents  
 669 and the unperturbed currents that flow unimpeded along the edges (these are the crossed  
 670 terms denoted by  $M_{\alpha\beta}^{(02)}$  and  $M_{\alpha\beta}^{(20)}$  in Appendix C). We see that all the terms involved in the  
 671 mixed noises in Eq. (74) vanish when particle-hole symmetry is restored, i.e., by taking  $V = 0$ .  
 672 This feature is in agreement with the intuitive anticipation stated at the beginning of this  
 673 Section, that a finite mixed noise requires the breaking of particle-hole symmetry.

674 Importantly, just as for for the charge and heat noises (see Sec. 5), the ‘‘tunneling’’ con-  
 675 tributions,  $M_{TT} \pm VS_{TT}^{II}/2$ , can be written in a form that is reminiscent of a scattering-theory  
 676 expression for non-interacting systems, thus providing a link to the thermoelectric response.  
 677 Explicitly, defining the electrochemical potentials  $\mu_{1,2}$  so that  $\mu_1 - \mu_2 = e\nu V$ , we find that

$$M_{TT} \mp \frac{V}{2}S_{TT}^{II} = 2e\nu|\Lambda|^2 \int_{-\infty}^{+\infty} \frac{dE}{2\pi} (E - \mu_{1,2}) D_\lambda(E - \mu_1, T_1) D_\lambda(E - \mu_2, T_2) \\ \times \{f_1(E - \mu_1)[1 - f_2(E - \mu_2)] + f_2(E - \mu_2)[1 - f_1(E - \mu_1)]\}, \quad (77)$$

678 with  $f_\alpha(E) = [1 + \exp(E/T_\alpha)]^{-1}$  and  $D_\lambda(E, T_\alpha)$  given in Eq. (66). **In arriving at Eq. (77), we**  
 679 **have used that  $D_\lambda(E - \mu_j, T_j) = D_\lambda(-E + \mu_j, T_j)$ .** Furthermore, for  $\lambda = 1$ , Eq. (77) matches  
 680 exactly the scattering theory result (at weak and energy-independent transmission) for a two-  
 681 terminal system with reservoirs at temperatures  $T_{1,2}$  and chemical potentials  $\mu_{1,2}$  (see, e.g.,

Eq. (13) in Ref. [58]). When  $\lambda \neq 1$ , the effect of strong correlations is fully captured by the effective density of states  $D_\lambda(E, T_\alpha)$ .

The above analogy with scattering theory allows us to establish the thermoelectric relation (73) also for edges in the FQH effect, at least when we analyze the tunneling contributions. Indeed, we can formally show that in equilibrium, i.e., in the limit  $V, \Delta T \rightarrow 0$ , Eq. (77) is related to the Seebeck coefficient  $\mathcal{S}$ . We achieve this connection by differentiating the charge tunneling current (18) with respect to the temperature bias  $\Delta T$  and evaluating the result at equilibrium, which defines the thermoelectric conductance

$$L \equiv \left. \frac{\partial I_T}{\partial \Delta T} \right|_{\substack{V \rightarrow 0 \\ \Delta T \rightarrow 0}} = e \nu |\Lambda|^2 \int_{-\infty}^{+\infty} \frac{dE}{2\pi} D_\lambda^2(E, \bar{T}) \frac{E}{\bar{T}^2} f(E) [1 - f(E)], \quad (78)$$

with the global equilibrium Fermi distribution  $f_1(E) = f_2(E) \equiv f(E) = [1 + \exp(E/\bar{T})]^{-1}$ . It is known [104] that  $L$  is related to the Seebeck coefficient  $\mathcal{S}$  and the charge tunneling conductance as  $L = \mathcal{S} g_T(\bar{T})$ . Considering then Eq. (77) in the limit  $V, \Delta T \rightarrow 0$ , we find that

$$M_{TT} \pm \frac{V}{2} S_{TT}^{II} \rightarrow S_0^{IJ}(0) = 4\bar{T}^2 L, \quad (79)$$

which shows that Eq. (73) holds also in the FQH regime. However, as elaborated above, we have in our model  $\mathcal{S} = 0$  due to the intrinsic particle-hole symmetry. Indeed, given the symmetry  $D_\lambda(E, \bar{T}) = D_\lambda(-E, \bar{T})$ , the integrand in (78) is odd, so that the relation  $S_0^{IJ} = \mathcal{S} = L = 0$  becomes trivial. Nonetheless, it follows that measuring a nonzero mixed noise is a clear signature of mechanisms that violate particle-hole symmetry, resulting in an asymmetric effective density of states.

Complementary to the analogy with scattering theory, we further establish another relation between the mixed noise and the thermoelectric conductance in the linear response regime, i.e., for  $eV/\bar{T} \ll 1$  but finite. This connection is possible since in linear response all mixed noise terms in Eq. (74) become proportional to  $eV/\bar{T}$ . Likewise, also the finite-bias thermoelectric conductance  $\tilde{L} = \partial_{\Delta T} I_T|_{\Delta T \rightarrow 0}$  [notice the difference compared to the definition of  $L$  in (78)] becomes proportional to  $eV/\bar{T}$ . It follows that

$$S_{33}^{IJ}(0) = -S_{44}^{IJ}(0) = 2\lambda \bar{T}^2 \tilde{L}, \quad (80a)$$

$$S_{34}^{IJ}(0) = -S_{43}^{IJ}(0) = 2(\lambda - 1) \bar{T}^2 \tilde{L}, \quad (80b)$$

to leading order in  $eV/\bar{T}$ . The explicit derivation of Eq. (80) is provided in Appendix C. Taking the limit  $V \rightarrow 0$  in Eq. (80) produces vanishing left- and right-hand sides, in agreement with the previous analysis at equilibrium.

Since our main focus of this paper FQH tunneling induced by a pure temperature biases (in which case the mixed noise vanishes, as discussed above), we leave a broader analysis of the mixed noise correlators, with both temperature and voltage biases present, for future studies.

## 7 Summary and Outlook

With the chiral Luttinger liquid model, we computed quantum transport observables in a QPC device (see Fig. 1) in the FQH regime at Laughlin fillings  $\nu = (2n+1)^{-1}$ . Focusing on the more unconventional configuration with a temperature bias between the source contacts, we derived detailed expressions for charge and heat currents entering the drain contacts, their auto- and cross-correlation noises, as well as mixed charge- and heat-current correlation noise. We complemented our calculations with an interpretation of the transport in terms of an effective density of states. This interpretation highlights a key aspect of temperature-biased noise: In

719 essence, injecting particles into the QPC region via edge states results in noise that, when the  
720 edge temperatures are different, explicitly probes the scaling dimensions dependence of the  
721 effective density of states. Our findings thereby explicitly show how the scaling dimensions of  
722 the tunneling particles enter these unconventional noise observables, including delta- $T$  noise,  
723 heat-current noise, and mixed noise. As such, our work provides novel opportunities to ex-  
724 tract the elusive scaling dimensions of quasiparticles in the FQH effect. In turn, these scaling  
725 dimensions are paramount to identify the anyonic statistics of these quasiparticles.

726 What are then the advantages and disadvantages of the different types of noise? The delta-  
727  $T$  noise is the simplest temperature-biased noise to measure and has already been implemented  
728 in the FQH regime (see e.g., Ref. [31]). As its major feature, it detects only the scaling dimen-  
729 sions for tunneling of charged particles, although these scaling dimensions could be indirectly  
730 affected by the presence of neutral modes. As such, for more complex edge structures, it might  
731 be difficult to use delta- $T$  noise to isolate the scaling dimensions of a certain type of anyonic  
732 quasiparticles. In comparison, the heat-current noise directly reflects the contributions from  
733 both charge and neutral modes. Its experimental access is however more demanding (see dis-  
734 cussion below). The mixed noise is mostly-advantageous in detecting the particle-hole sym-  
735 metry of the system. Indeed, in particle-hole symmetric systems, like the presently considered  
736 low-energy dynamics of the FQH edge, the mixed noise vanishes in the absence of a voltage  
737 bias. Finite mixed noise due to a pure temperature bias, thus probes not only scaling dimen-  
738 sions via the effective density of states, but is also a signal of breaking particle-hole symmetry,  
739 e.g., deviations from the linear edge mode spectrum. Remarkably, this connection to particle-  
740 hole symmetry bridges the mixed noise to Seebeck coefficients, a quantity that also requires  
741 the presence of particle-hole symmetry breaking. However, among the observables considered  
742 in this work, mixed noise is probably the most difficult one to access experimentally, despite  
743 its connection to thermoelectric response, as derived in Eq. (80).

744 Our work is further potentially applicable to other platforms that support edge states. First,  
745 it paves the way for generalized noises as a tool to identify scaling dimensions of more involved  
746 FQH edges, including hierarchical states like  $\nu = 2/5$  and  $\nu = 2/3$  or as a tool to distinguish  
747 candidate states for non-Abelian states, e.g., at  $\nu = 5/2$  and  $\nu = 12/5$ . Second, our calcula-  
748 tions can be adapted to describe temperature-biased noise in related strongly correlated one-  
749 dimensional systems, such as disordered FQH line junctions [41, 74–77], disordered quantum  
750 wires [78], and quantum spin Hall edges [79].

751 We end by discussing the feasibility to experimentally measure our proposed noise compo-  
752 nents. FQH setups with temperature gradients across QPCs have been realized in GaAs-based  
753 devices (see e.g. Ref. [31]) and charge currents, heat currents, and charge noise are by now  
754 routinely measured. To also measure heat-current noise, it was proposed in Refs. [55, 105]  
755 that edge-coupled quantum dots, via thermoelectricity, may convert edge channel heat-current  
756 fluctuations to more easily measurable charge-current fluctuations. Alternatively, heat-current  
757 noise and mixed noise can be converted [1] to temperature fluctuations in a floating probe  
758 contact. A similar strategy could be used to access the mixed noise by monitoring electrical  
759 potential and temperature fluctuations in the floating probe [51]. Another indirect way to  
760 measure the mixed noise would be via the Seebeck coefficient. Devices with such implemen-  
761 tations in the FQH regime remain, to the best of our knowledge, yet to be fabricated, but we  
762 believe they might be within reach with current experimental techniques.

## 763 Acknowledgments

764 We thank Jinhong Park and Giacomo Rebola for useful comments on the manuscript.

765 **Funding information** C.S acknowledges support from the Area of Advance Nano at Chalmers  
 766 University of Technology and from the Swedish Vetenskapsrådet via Project No. 2023-04043.  
 767 G.Z. acknowledges the support from National Natural Science Foundation of China (Grant  
 768 No. 12374158) and Innovation Program for Quantum Science and Technology (Grant No.  
 769 2021ZD0302400). This project has received funding from the European Union's Horizon 2020  
 770 research and innovation programme under grant agreement No 101031655 (TEAPOT).

## 771 A Derivations of charge currents and delta-T noise

### 772 A.1 Currents

773 As our starting point, we recall that the unperturbed operators representing the charge currents  
 774 entering the drain contacts 3 and 4 are given by

$$\hat{I}_3^{(0)}(t) = \frac{ev_F\sqrt{\nu}}{2\pi} \partial_x \hat{\phi}_R(x_3, t) + \frac{e^2\nu}{2\pi} V_1, \quad (\text{A.1})$$

$$\hat{I}_4^{(0)}(t) = -\frac{ev_F\sqrt{\nu}}{2\pi} \partial_x \hat{\phi}_L(x_4, t) + \frac{e^2\nu}{2\pi} V_2, \quad (\text{A.2})$$

775 where  $x_3$  and  $x_4$  are the locations of the drains and  $V_{1,2}$  are the voltages applied at the source  
 776 contacts. The corrections induced by the tunneling are given in Eqs. (15), which we evaluate  
 777 at leading order to

$$\hat{I}_3^{(1)}(t) = ie\nu[\Lambda e^{-ie\nu V\tilde{t}} \hat{\psi}_R^\dagger(\tilde{t}) \hat{\psi}_L(\tilde{t}) - \Lambda^* e^{ie\nu V\tilde{t}} \hat{\psi}_L^\dagger(\tilde{t}) \hat{\psi}_R(\tilde{t})] \quad (\text{A.3a})$$

$$\hat{I}_4^{(1)}(t) = -ie\nu[\Lambda e^{-ie\nu V\tilde{t}} \hat{\psi}_R^\dagger(\tilde{t}) \hat{\psi}_L(\tilde{t}) - \Lambda^* e^{ie\nu V\tilde{t}} \hat{\psi}_L^\dagger(\tilde{t}) \hat{\psi}_R(\tilde{t})]. \quad (\text{A.3b})$$

778 Here,  $V = V_1 - V_2$  is the voltage bias between the two edges and  $\tilde{t} = t - x_3/\nu_F$ ,  $\bar{t} = t + x_4/\nu_F$ .  
 779 Notice that  $\hat{I}_3^{(1)}(t) = -\hat{I}_4^{(1)}(t)$  when  $x_3 = -x_4$ , reflecting current conservation. The expres-  
 780 sions (A.3) are valid “downstream” of the QPC on the respective edge (i.e., for  $x_3 > 0$  and  
 781  $x_4 < 0$ ), because corrections to the unperturbed currents may only occur on these sides of the  
 782 QPC due to the chiral propagation along the edge. Due to the imbalance of Klein factors in  
 783 Eq. (A.3), the first-order corrections vanish when taking the average:

$$\langle \hat{I}_3^{(1)}(t) \rangle = \langle \hat{I}_4^{(1)}(t) \rangle = 0. \quad (\text{A.4})$$

784 Moving on to the second-order corrections, we find that they are given by

$$\begin{aligned} \hat{I}_3^{(2)}(t) = & e\nu|\Lambda|^2 \int_{-\infty}^{\tilde{t}} dt'' e^{-ie\nu V(t''-\tilde{t})} [\hat{\psi}_R^\dagger(t'') \hat{\psi}_L(t''), \hat{\psi}_L^\dagger(\tilde{t}) \hat{\psi}_R(\tilde{t})] \\ & - e\nu|\Lambda|^2 \int_{-\infty}^{\tilde{t}} dt'' e^{ie\nu V(t''-\tilde{t})} [\hat{\psi}_L^\dagger(t'') \hat{\psi}_R(t''), \hat{\psi}_R^\dagger(\tilde{t}) \hat{\psi}_L(\tilde{t})], \end{aligned} \quad (\text{A.5a})$$

$$\begin{aligned} \hat{I}_4^{(2)}(t) = & -e\nu|\Lambda|^2 \int_{-\infty}^{\tilde{t}} dt'' e^{-ie\nu V(t''-\tilde{t})} [\hat{\psi}_R^\dagger(t'') \hat{\psi}_L(t''), \hat{\psi}_L^\dagger(\tilde{t}) \hat{\psi}_R(\tilde{t})] \\ & + e\nu|\Lambda|^2 \int_{-\infty}^{\tilde{t}} dt'' e^{ie\nu V(t''-\tilde{t})} [\hat{\psi}_L^\dagger(t'') \hat{\psi}_R(t''), \hat{\psi}_R^\dagger(\tilde{t}) \hat{\psi}_L(\tilde{t})], \end{aligned} \quad (\text{A.5b})$$

785 where we only kept the terms with balanced Klein factors. Just as for the first-order correc-  
 786 tions, we have  $\hat{I}_3^{(2)}(t) = -\hat{I}_4^{(2)}(t)$  if  $x_3 = -x_4$ . Taking the averages, and making the change of

787 variable  $\tau = t'' - \tilde{t}$  (for  $\alpha = 3$ ) and  $\tau = t'' - \bar{t}$  (for  $\alpha = 4$ ), we get

$$\langle \hat{I}_3^{(2)}(t) \rangle = -2ie\nu|\Lambda|^2 \int_{-\infty}^{+\infty} d\tau \sin(e\nu V\tau) G_R(\tau) G_L(\tau) \equiv -I_T, \quad (\text{A.6a})$$

$$\langle \hat{I}_4^{(2)}(t) \rangle = +2ie\nu|\Lambda|^2 \int_{-\infty}^{+\infty} d\tau \sin(e\nu V\tau) G_R(\tau) G_L(\tau) \equiv I_T, \quad (\text{A.6b})$$

788 where we identified the charge tunneling current in Eq. (18). Note that the average cur-  
789 rents (A.6) do not depend on time, as expected for the constant voltage bias, and the currents  
790 are equal and opposite, as required by charge current conservation. Gathering the above re-  
791 sults, we have that the average charge currents that enter the drains are given by

$$\langle \hat{I}_3 \rangle = \frac{e^2\nu}{2\pi} V_1 - I_T, \quad (\text{A.7})$$

$$\langle \hat{I}_4 \rangle = \frac{e^2\nu}{2\pi} V_2 + I_T. \quad (\text{A.8})$$

## 792 A.2 Zeroth order (or equilibrium) charge-current noise

793 Similarly to the charge current, we decompose the charge-current noise  $S_{\alpha\beta}^{II}$  as

$$S_{\alpha\beta}^{II} = S_{\alpha\beta}^{(00)} + S_{\alpha\beta}^{(11)} + S_{\alpha\beta}^{(02)} + S_{\alpha\beta}^{(20)} + \mathcal{O}(|\Lambda|^4), \quad (\text{A.9})$$

794 where

$$S_{\alpha\beta}^{(ij)}(t_1 - t_2) = \langle \{ \hat{I}_\alpha^{(i)}(t_1), \hat{I}_\beta^{(j)}(t_2) \} \rangle - 2 \langle \hat{I}_\alpha^{(i)}(t_1) \rangle \langle \hat{I}_\beta^{(j)}(t_2) \rangle. \quad (\text{A.10})$$

795 Here, the two superscripts  $i, j$  denote the order of the current operator expansion terms in  
796 Eq. (14), while the subscripts  $\alpha, \beta$  take the values 3 or 4, describing the drain contacts. We  
797 further note that the ‘‘crossed’’ terms  $S_{\alpha\beta}^{(02)}$  and  $S_{\alpha\beta}^{(20)}$  represent cross-correlations between the  
798 unperturbed currents along the edges and the tunneling current induced by the QPC. These  
799 terms are nothing but the contributions  $S_{\alpha T}^{II}$  and  $S_{T\alpha}^{II}$  appearing in Eq (4).

800 Next, we compute the zeroth order noise terms in (A.10). We start with

$$\begin{aligned} S_{44}^{(00)}(t_1 - t_2) &= \frac{e^2\nu}{(2\pi)^2} \langle \partial_{t_1} \hat{\phi}_L(\tilde{t}_1) \partial_{t_2} \hat{\phi}_L(\tilde{t}_2) \rangle + (t_1 \leftrightarrow t_2) \\ &= \frac{e^2\nu}{(2\pi)^2} \frac{-\pi^2 T_2^2}{\sinh^2[\pi T_2(i\tau_0 - (t_1 - t_2))]} + (t_1 \leftrightarrow t_2), \end{aligned} \quad (\text{A.11})$$

801 where we used the expression (20) for the bosonic Green’s function. Next, by Fourier trans-  
802 forming with respect to the time difference  $\tau \equiv t_1 - t_2$ , we get

$$S_{44}^{(00)}(\omega) = \frac{e^2\nu}{(2\pi)^2} \int_{-\infty}^{+\infty} d\tau \left[ \frac{-\pi^2 T_2^2 e^{i\omega\tau}}{\sinh^2[\pi T_2(i\tau_0 - \tau)]} + (\tau \rightarrow -\tau) \right] = \frac{e^2\nu}{2\pi} \omega \coth \left[ \frac{\omega}{2T_2} \right]. \quad (\text{A.12})$$

803 In the zero-frequency limit, this expression reduces to the expected Johnson-Nyquist expres-  
804 sion

$$S_{44}^{(00)}(\omega \rightarrow 0) = 2 \frac{e^2\nu}{2\pi} T_2. \quad (\text{A.13})$$

805 This expression coincides with  $S_{22}^{II}$  in the main text, cf. Eq. (25b), as it represents the fluctu-  
806 ations reaching drain 2 in the absence of tunneling. The results for  $S_{33}^{(00)}(\omega)$  and  $S_{33}^{(00)}(0)$  are  
807 obtained from Eqs. (A.12) and (A.13), respectively, by substituting  $T_2 \rightarrow T_1$ , yielding Eq. (25a).  
808 Identical calculations for the cross-correlation noises lead to

$$S_{34}^{(00)}(\omega) = S_{43}^{(00)}(\omega) = 0, \quad (\text{A.14})$$

809 since at zeroth order, the two bosonic fields  $\hat{\phi}_{R/L}$  are uncorrelated.



### 810 A.3 First order, or tunneling, charge-current noise

811 The first order term in the noise (A.10) reads

$$S_{\alpha\beta}^{(11)}(t_1 - t_2) = \left\langle \left\{ \hat{I}_\alpha^{(1)}(t_1), \hat{I}_\beta^{(1)}(t_2) \right\} \right\rangle - 2 \left\langle \hat{I}_\alpha^{(1)}(t_1) \right\rangle \left\langle \hat{I}_\beta^{(1)}(t_2) \right\rangle, \quad (\text{A.15})$$

812 where we used that the first-order corrections to the average current vanish. By next using the  
813 first order corrections (A.3), we see that

$$S_{44}^{(11)}(t_1 - t_2) = S_{33}^{(11)}(t_1 - t_2) = -S_{34}^{(11)}(t_1 - t_2) = -S_{43}^{(11)}(t_1 - t_2), \quad (\text{A.16})$$

814 so there is only one independent term. Inserting Eq. (A.3b) into Eq. (A.15) we obtain

$$S_{44}^{(11)}(t_1 - t_2) = 2(e\nu)^2 |\Lambda|^2 \cos[e\nu V(t_1 - t_2)] G_R(t_1 - t_2) G_L(t_1 - t_2) + (t_1 \leftrightarrow t_2), \quad (\text{A.17})$$

815 and thus, after a Fourier transform, we arrive at

$$S_{44}^{(11)}(\omega \rightarrow 0) = 4(e\nu)^2 |\Lambda|^2 \int_{-\infty}^{+\infty} d\tau \cos(e\nu V\tau) G_R(\tau) G_L(\tau) \equiv S_{TT}^I, \quad (\text{A.18})$$

816 which defines the tunneling current noise  $S_{TT}^I$  in Eq. (25c).

### 817 A.4 Crossed charge-current noise terms $S_{\alpha\beta}^{(02)} + S_{\alpha\beta}^{(20)}$

818 Here, we compute the remaining last terms in the noise expansion (A.10). These terms rep-  
819 resent correlations between the unperturbed currents on the edge and the tunneling current  
820 induced by the QPC.

#### 821 A.4.1 $S_{44}^{(02)} + S_{44}^{(20)}$

822 We start with the contribution  $S_{44}^{(02)}$ . By using the previously found expressions for the current  
823 operators, Eqs. (A.2) and (A.5b), and recalling that  $\nu_F \partial_x \hat{\phi}_L = \partial_t \hat{\phi}_L$ , due to chiral propagation,  
824 we obtain [37, 84, 85]

$$\begin{aligned} S_{44}^{(02)}(t_{12}) = & -\frac{2i|\Lambda|^2(e\nu)^2}{2\pi} \int_{-\infty}^{\bar{t}_2} dt'' \cos[e\nu V(t'' - \bar{t}_2)] \left[ G_R(t'' - \bar{t}_2) G_L(t'' - \bar{t}_2) \mathcal{K}(\bar{t}_1, t'', \bar{t}_2) \right. \\ & \left. + G_R(\bar{t}_2 - t'') G_L(\bar{t}_2 - t'') \mathcal{K}(\bar{t}_1, \bar{t}_2, t'') \right] \\ & + \frac{2i(e\nu)^2 |\Lambda|^2}{2\pi} \int_{-\infty}^{\bar{t}_2} dt'' \cos[e\nu V(t'' - \bar{t}_2)] \left[ G_R(t'' - \bar{t}_2) G_L(t'' - \bar{t}_2) \mathcal{K}(-\bar{t}_1, -t'', -\bar{t}_2) \right. \\ & \left. + G_R(\bar{t}_1 - t'') G_L(\bar{t}_2 - t'') \mathcal{K}(-\bar{t}_1, -\bar{t}_2, -t'') \right], \end{aligned} \quad (\text{A.19})$$

825 where we abbreviated  $t_{12} = t_1 - t_2$ ,  $\bar{t}_i = t_i + x_4/\nu_F$  for  $i = 1, 2$ , and also defined the function

$$\mathcal{K}(t_1, t_2, t_3) = \pi T_2 \{ \coth[\pi T_2(i\tau_0 - (t_1 - t_2))] - \coth[\pi T_2(i\tau_0 - (t_1 - t_3))] \}. \quad (\text{A.20})$$

826 Finally, taking advantage of the permutation identity  $\mathcal{K}(1, 3, 2) = -\mathcal{K}(1, 2, 3)$  and introducing  
827 the variable  $\tau = t'' - \bar{t}_2$ , we arrive at

$$\begin{aligned} S_{44}^{(02)}(t_{12}) = & -\frac{2i(e\nu)^2 |\Lambda|^2}{2\pi} \int_{-\infty}^0 d\tau \cos(e\nu V\tau) \mathcal{K}_0(t_{12}, \tau) [G_R(\tau) G_L(\tau) - G_R(-\tau) G_L(-\tau)] \\ & - \frac{2i(e\nu)^2 |\Lambda|^2}{2\pi} \int_0^{+\infty} d\tau \cos(e\nu V\tau) \mathcal{K}_0(-t_{12}, \tau) [G_R(\tau) G_L(\tau) - G_R(-\tau) G_L(-\tau)] \end{aligned} \quad (\text{A.21})$$

828 in which

$$\mathcal{K}_0(t_{12}, \tau) \equiv \mathcal{K}(\bar{t}_1, \bar{t}_2 + \tau, \bar{t}_2) = \pi T_2 \{ \coth[\pi T_2(i\tau_0 - (t_{12} - \tau))] - \coth[\pi T_2(i\tau_0 - t_{12})] \}. \quad (\text{A.22})$$

829 Equation (A.21) explicitly shows that the noise only depends on the time difference  $t_{12} = t_1 - t_2$ ,  
830 as expected in the steady state.

831 The procedure to evaluate  $S_{44}^{(20)}$  is identical to that for  $S_{44}^{(02)}$ . We find

$$\begin{aligned} S_{44}^{(20)}(t_{12}) = & -\frac{2i(e\nu)^2|\Lambda|^2}{2\pi} \int_0^{+\infty} d\tau \cos(e\nu V\tau) \mathcal{K}_0(t_{12}, \tau) [G_R(\tau)G_L(\tau) - G_R(-\tau)G_L(-\tau)] \\ & -\frac{2i(e\nu)^2|\Lambda|^2}{2\pi} \int_{-\infty}^0 d\tau \cos(e\nu V\tau) \mathcal{K}_0(-t_{12}, \tau) [G_R(\tau)G_L(\tau) - G_R(-\tau)G_L(-\tau)]. \end{aligned} \quad (\text{A.23})$$

832 We can therefore combine Eqs. (A.21) and (A.23) into a single integral

$$\begin{aligned} S_{44}^{(02+20)}(t_{12}) = & -\frac{2i(e\nu)^2|\Lambda|^2}{2\pi} \int_{-\infty}^{+\infty} d\tau \cos(e\nu V\tau) G_R(\tau)G_L(\tau) [\mathcal{K}_0(t_{12}, \tau) - \mathcal{K}_0(t_{12}, -\tau)] \\ & -\frac{2i(e\nu)^2|\Lambda|^2}{2\pi} \int_{-\infty}^{+\infty} d\tau \cos(e\nu V\tau) G_R(\tau)G_L(\tau) [\mathcal{K}_0(-t_{12}, \tau) - \mathcal{K}_0(-t_{12}, -\tau)], \end{aligned} \quad (\text{A.24})$$

833 and we obtain the finite-frequency expression by Fourier transforming with respect to the time  
834 difference  $t_{12}$ . The final result thus involves the function

$$\mathcal{K}_0(\omega, \tau) = \int_{-\infty}^{+\infty} dt_{12} e^{i\omega t_{12}} \mathcal{K}_0(t_{12}, \tau), \quad (\text{A.25})$$

835 which can be evaluated with the residue theorem. We obtain

$$S_{44}^{(02+20)}(\omega) = -4i(e\nu)^2|\Lambda|^2 \coth\left(\frac{\omega}{2T_2}\right) \int_{-\infty}^{+\infty} d\tau \cos(e\nu V\tau) G_R(\tau)G_L(\tau) \sin(\omega\tau). \quad (\text{A.26})$$

836 Taking the zero-frequency limit, we get

$$S_{44}^{(02+20)}(0) = -4T_2 \times 2i(e\nu)^2|\Lambda|^2 \int_{-\infty}^{+\infty} d\tau \cos(e\nu V\tau) \tau G_R(\tau)G_L(\tau) = -4T_2 \frac{\partial I_T}{\partial V}, \quad (\text{A.27})$$

837 where in the final equality, we identified the differential charge tunneling conductance (21).

#### 838 **A.4.2** $S_{33}^{(02)} + S_{33}^{(20)}$

839 We evaluate these terms by following an identical procedure as in the previous subsection.  
840 The result is simply obtained by the substitutions  $L \rightarrow R$  and  $T_2 \rightarrow T_1$ :

$$S_{33}^{(02+20)}(\omega) = -4i(e\nu)^2|\Lambda|^2 \coth\left(\frac{\omega}{2T_1}\right) \int_{-\infty}^{+\infty} d\tau \cos(e\nu V\tau) G_R(\tau)G_L(\tau) \sin(\omega\tau), \quad (\text{A.28})$$

$$S_{33}^{(02+20)}(0) = -4T_1 \times 2i(e\nu)^2|\Lambda|^2 \int_{-\infty}^{+\infty} d\tau \cos(e\nu V\tau) \tau G_R(\tau)G_L(\tau) = -4T_1 \frac{\partial I_T}{\partial V}. \quad (\text{A.29})$$

841 **A.4.3**  $S_{34}^{(02)} + S_{34}^{(20)}$  and  $S_{43}^{(02)} + S_{43}^{(20)}$

842 The evaluation of these contributions is very similar to the calculation of the previous terms.  
 843 The only difference is that we find not only the function  $\mathcal{K}_0$  defined in Eq. (A.22), but also a  
 844 corresponding one with  $T_1$  instead of  $T_2$ . As a result, the final expression reads

$$S_{34}^{(02+20)}(\omega) = 2i(e\nu)^2|\Lambda|^2 \left[ \coth\left(\frac{\omega}{2T_1}\right) + \coth\left(\frac{\omega}{2T_2}\right) \right] \int_{-\infty}^{+\infty} d\tau \cos(e\nu V\tau) G_R(\tau) G_L(\tau) \sin(\omega\tau). \quad (\text{A.30})$$

845 The zero-frequency limit is therefore

$$S_{34}^{(02+20)}(0) = 2(T_1 + T_2) \times 2i(e\nu)^2|\Lambda|^2 \int_{-\infty}^{+\infty} d\tau \cos(e\nu V\tau) \tau G_R(\tau) G_L(\tau) = 2(T_1 + T_2) \frac{\partial I_T}{\partial V}. \quad (\text{A.31})$$

846 **A.5 Summary of charge current fluctuations**

847 Gathering the results from all above subsections in Appendix A, we have that the tunneling  
 848 current, tunneling conductance, and the associated noise to leading order in the tunneling  
 849 amplitude  $\Lambda$  are given by

$$I_T = 2ie\nu|\Lambda|^2 \int_{-\infty}^{+\infty} d\tau \sin(e\nu V\tau) G_R(\tau) G_L(\tau), \quad (\text{A.32a})$$

$$\frac{\partial I_T}{\partial V} = 2i(e\nu)^2|\Lambda|^2 \int_{-\infty}^{+\infty} d\tau \tau \cos(e\nu V\tau) G_R(\tau) G_L(\tau), \quad (\text{A.32b})$$

$$S_{TT}^{II} = 4(e\nu)^2|\Lambda|^2 \int_{-\infty}^{+\infty} d\tau \cos(e\nu V\tau) G_R(\tau) G_L(\tau). \quad (\text{A.32c})$$

850 These expressions are stated in Eqs. (18), (21), and Eq. (25c) in the main text. The expressions  
 851 for the auto- and cross-correlated charge-current noises at zero frequency,  $S_{\alpha\beta}^{II}(0)$ , are summa-  
 852 rized in Tab. 1. It can readily be checked that these noise components obey the conservation  
 law (6).

$S_{\alpha\beta}^{II}(0)$	3	4
3	$2\frac{e^2\nu}{h}k_B T_1 + S_{TT}^{II} - 4k_B T_1 \frac{\partial I_T}{\partial V}$	$2k_B(T_1 + T_2) \frac{\partial I_T}{\partial V} - S_{TT}^{II}$
4	$2k_B(T_1 + T_2) \frac{\partial I_T}{\partial V} - S_{TT}^{II}$	$2\frac{e^2\nu}{h}k_B T_2 + S_{TT}^{II} - 4k_B T_2 \frac{\partial I_T}{\partial V}$

Table 1: Auto- and cross-correlation charge-current noise at zero frequency  $S_{\alpha\beta}^{II}$  with the drain reservoir indices  $\alpha, \beta = 3, 4$  (see Fig. 1). All expressions are given to  $\mathcal{O}(|\Lambda|^2)$  in the tunneling amplitude  $\Lambda$ .

853

## 854 B Derivations of heat currents and heat-current noise

### 855 B.1 Currents

856 The unperturbed operators representing the heat currents entering the drain contacts 3 and 4  
857 are given by

$$\hat{j}_3^{(0)}(t) = \frac{v_F^2}{4\pi} [\partial_x \hat{\phi}_R(x_3, t)]^2 - \frac{q^2 \nu}{4\pi} V_1^2, \quad (\text{B.1a})$$

$$\hat{j}_4^{(0)}(t) = \frac{v_F^2}{4\pi} [\partial_x \hat{\phi}_L(x_4, t)]^2 - \frac{q^2 \nu}{4\pi} V_2^2. \quad (\text{B.1b})$$

858 The corresponding average values are readily obtained as

$$\langle \hat{j}_3^{(0)}(t) \rangle = \frac{\pi T_1^2}{12} - \frac{q^2 \nu}{4\pi} V_1^2, \quad (\text{B.2a})$$

$$\langle \hat{j}_4^{(0)}(t) \rangle = \frac{\pi T_2^2}{12} - \frac{q^2 \nu}{4\pi} V_2^2. \quad (\text{B.2b})$$

859 Here, we identified the free boson stress energy tensor  $\hat{\mathcal{T}}_{R,L}(t) = [\partial_x \hat{\phi}_{R,L}(x_{3,4}, t)]^2/2$ , and used  
860 that  $\langle \hat{\mathcal{T}}_{R,L}(t) \rangle = \pi^2 T_{1,2}^2/(6v_F^2)$  at finite temperature [60, 106]. We find the corrections to the  
861 unperturbed current operators by evaluating the commutators in Eq. (15). At first order, we  
862 find

$$\hat{j}_3^{(1)}(t) = -\left\{ \Lambda e^{-ie\nu V \tilde{t}} [\partial_t \hat{\psi}_R^\dagger(\tilde{t})] \hat{\psi}_L(\tilde{t}) + \Lambda^* e^{ie\nu V \tilde{t}} \hat{\psi}_L^\dagger(\tilde{t}) [\partial_t \hat{\psi}_R(\tilde{t})] \right\}, \quad (\text{B.3a})$$

$$\hat{j}_4^{(1)}(t) = -\left\{ \Lambda e^{-ie\nu V \tilde{t}} \hat{\psi}_R^\dagger(\tilde{t}) [\partial_t \hat{\psi}_L(\tilde{t})] + \Lambda^* e^{ie\nu V \tilde{t}} [\partial_t \hat{\psi}_L^\dagger(\tilde{t})] \hat{\psi}_R(\tilde{t}) \right\}, \quad (\text{B.3b})$$

863 where  $\tilde{t} = t - x_3/v_F$  and  $\tilde{t} = t + x_4/v_F$ . Similarly to the charge transport, the expressions  
864 in Eq. (B.3) are finite only “downstream” of the QPC on the respective edge (i.e., for  $x_3 > 0$   
865 and  $x_4 < 0$ ), because corrections to the unperturbed currents may only occur on these sides of  
866 the QPC due to the chiral propagation. Due to the imbalance of Klein factors, the first-order  
867 corrections vanish on average:

$$\langle \hat{j}_3^{(1)}(t) \rangle = \langle \hat{j}_4^{(1)}(t) \rangle = 0. \quad (\text{B.4})$$

868 We find that the second-order corrections become

$$\hat{j}_3^{(2)}(t) = -i|\Lambda|^2 \int_{-\infty}^{\tilde{t}} dt'' \left\{ e^{-ie\nu V(t''-\tilde{t})} [\hat{\psi}_R^\dagger(t'') \hat{\psi}_L(t''), \hat{\psi}_L^\dagger(\tilde{t}) \partial_t \hat{\psi}_R(\tilde{t})] \right. \\ \left. + e^{ie\nu V(t''-\tilde{t})} [\hat{\psi}_L^\dagger(t'') \hat{\psi}_R(t''), \partial_t \hat{\psi}_R^\dagger(\tilde{t}) \hat{\psi}_L(\tilde{t})] \right\}, \quad (\text{B.5a})$$

$$\hat{j}_4^{(2)}(t) = -i|\Lambda|^2 \int_{-\infty}^{\tilde{t}} dt'' \left\{ e^{-ie\nu V(t''-\tilde{t})} [\hat{\psi}_R^\dagger(t'') \hat{\psi}_L(t''), \partial_t \hat{\psi}_L^\dagger(\tilde{t}) \hat{\psi}_R(\tilde{t})] \right. \\ \left. + e^{ie\nu V(t''-\tilde{t})} [\hat{\psi}_L^\dagger(t'') \hat{\psi}_R(t''), \hat{\psi}_R^\dagger(\tilde{t}) \partial_t \hat{\psi}_L(\tilde{t})] \right\}, \quad (\text{B.5b})$$

869 where we kept only the terms with balanced Klein factors. Evaluating the averages, we find

$$\langle \hat{j}_3^{(2)} \rangle = 2i|\Lambda|^2 \int_{-\infty}^{+\infty} d\tau \cos(e\nu V \tau) G_L(\tau) \partial_\tau G_R(\tau), \quad (\text{B.6a})$$

$$\langle \hat{j}_4^{(2)} \rangle = 2i|\Lambda|^2 \int_{-\infty}^{+\infty} d\tau \cos(e\nu V \tau) G_R(\tau) \partial_\tau G_L(\tau). \quad (\text{B.6b})$$

870 These results can be also expressed in the following equivalent form:

$$\langle \hat{J}_3^{(2)} \rangle = -i|\Lambda|^2 \int_{-\infty}^{+\infty} d\tau \cos(e\nu V\tau) [G_R(\tau)\partial_\tau G_L(\tau) - G_L(\tau)\partial_\tau G_R(\tau)] + \frac{V}{2}I_T, \quad (\text{B.7a})$$

$$\langle \hat{J}_4^{(2)} \rangle = +i|\Lambda|^2 \int_{-\infty}^{+\infty} d\tau \cos(e\nu V\tau) [G_R(\tau)\partial_\tau G_L(\tau) - G_L(\tau)\partial_\tau G_R(\tau)] + \frac{V}{2}I_T, \quad (\text{B.7b})$$

871 with  $V = V_1 - V_2$ . Differently from the charge currents, these expressions are not equal and  
872 opposite, as the edge heat current is not conserved for  $V \neq 0$ . The terms  $VI_T/2$  in Eq. (B.7)  
873 are Joule heating contributions. When there is no bias between the edges,  $V = 0$ , the heat  
874 current coincides with the energy current and is then conserved. Then, Eq. (B.7) reduces to

$$\langle \hat{J}_4^{(2)} \rangle = -\langle \hat{J}_3^{(2)} \rangle = 2i|\Lambda|^2 \int_{-\infty}^{+\infty} d\tau G_R(\tau)\partial_\tau G_L(\tau) \equiv J_T, \quad (\text{B.8})$$

875 which is indeed the heat tunneling current at zero voltage bias, as defined in Eq. (37).

## 876 B.2 Zeroth order, or equilibrium, heat-current noise

877 We use the following notation to indicate the decomposition of the heat noise:

$$S_{\alpha\beta}^{JJ} = \Sigma_{\alpha\beta}^{(00)} + \Sigma_{\alpha\beta}^{(11)} + \Sigma_{\alpha\beta}^{(02)} + \Sigma_{\alpha\beta}^{(20)}, \quad (\text{B.9})$$

878 with

$$\Sigma_{\alpha\beta}^{(ij)}(t_1 - t_2) = \langle \{ \hat{J}_\alpha^{(i)}(t_1), \hat{J}_\alpha^{(j)}(t_2) \} \rangle - 2\langle \hat{J}_\alpha^{(i)}(t_1) \rangle \langle \hat{J}_\alpha^{(j)}(t_2) \rangle. \quad (\text{B.10})$$

879 We start with the evaluation of the equilibrium noise  $\Sigma_{\alpha\beta}^{(00)}$ , beginning with  $\alpha = \beta = 4$ . From  
880 the definition (B.10), we have

$$\begin{aligned} \Sigma_{44}^{(00)}(t_1 - t_2) &= \langle \hat{J}_4^{(0)}(t_1)\hat{J}_4^{(0)}(t_2) \rangle - \langle \hat{J}_4^{(0)}(t_1) \rangle \langle \hat{J}_4^{(0)}(t_2) \rangle + (t_1 \leftrightarrow t_2) \\ &= \frac{2v_F^4}{(4\pi)^2} \langle (\partial_x \hat{\phi}_L(x_0, t_1)\partial_x \hat{\phi}_L(x_0, t_2)) \rangle^2 + (t_1 \leftrightarrow t_2) = \frac{2v_F^4}{(4\pi)^2} \left( \lim_{y \rightarrow x} \partial_x \partial_y \mathcal{G}_L(x - y, \tau) \right)^2 \\ &+ (\tau \rightarrow -\tau) = \frac{2v_F^4}{(4\pi)^2} \frac{\pi^4 T_2^4}{v_F^4 (\sinh(\pi T_{1/2}(i\tau_0 - \tau))^4} + (\tau \rightarrow -\tau). \end{aligned} \quad (\text{B.11})$$

881 Here, in the second equality, we used the heat current operator definition (13b) together with  
882 Wick's theorem. In the third equality, we used the definition of the boson Green's function (20)  
883 and abbreviated  $\tau = t_1 - t_2$ . We evaluate the Fourier transform with the residue theorem as  
884 in previous sections and find

$$\Sigma_{44}^{(00)}(\omega) = \int_{-\infty}^{+\infty} d\tau e^{i\omega\tau} \Sigma_{44}^{(00)}(\tau) = \frac{\omega}{24\pi} ((2\pi T_2)^2 + \omega^2) \coth \left[ \frac{\omega}{2T_2} \right], \quad (\text{B.12})$$

885 which in the zero frequency limit reduces to

$$\Sigma_{44}^{(00)}(\omega \rightarrow 0) = \frac{\pi T_2^3}{3} = 4 \langle \hat{J}_4^{(0)}(t) \rangle T_2, \quad (\text{B.13})$$

886 upon using Eq. (B.2) for  $V = 0$ . Equation (B.13) is the equilibrium contribution that we  
887 denoted  $S_{22}^{JJ}$  in the main text. Equations (B.12)-(B.13) manifest the equilibrium fluctuation-  
888 dissipation relation for heat transport [48].

889 The remaining non-vanishing contribution to the equilibrium noise, i.e.,  $\Sigma_{33}^{(00)}(\omega)$ , is ob-  
 890 tained by substituting  $T_2 \rightarrow T_1$  in Eqs. (B.12)-(B.13). The zero frequency component thus  
 891 reads

$$\Sigma_{33}^{(00)}(0) = \frac{\pi T_1^3}{3} = 4 \langle \hat{J}_3^{(0)}(t) \rangle T_1, \quad (\text{B.14})$$

892 which gives  $S_{11}^{JJ}$  in the main text. We also have trivially from Eq. (B.10) that

$$\Sigma_{34}^{(00)}(\omega) = \Sigma_{43}^{(00)}(\omega) = 0, \quad (\text{B.15})$$

893 since the bosonic fields  $\hat{\phi}_{R/L}$  are independent at zeroth order.

### 894 B.3 First order or tunneling, heat-current noise

895 We now consider the heat-current noise for vanishing bias voltage  $V_1 = V_2 = 0$ . Using the heat  
 896 current Eq. (B.3b), we obtain

$$\begin{aligned} \Sigma_{44}^{(11)}(t_{12}) &= \langle \{ \hat{J}_4^{(1)}(t_1), \hat{J}_4^{(1)}(t_2) \} \rangle - 2 \langle \hat{J}_4^{(1)}(t_1) \rangle \langle \hat{J}_4^{(1)}(t_2) \rangle \\ &= |\Lambda|^2 \langle \hat{\psi}_R^\dagger(\bar{t}_1) \hat{\psi}_R(\bar{t}_2) \rangle \partial_{t_1} \partial_{t_2} \langle \hat{\psi}_L(\bar{t}_1) \hat{\psi}_L^\dagger(\bar{t}_2) \rangle + (t_1 \leftrightarrow t_2) \\ &\quad + |\Lambda|^2 \langle \hat{\psi}_R(\bar{t}_1) \hat{\psi}_R^\dagger(\bar{t}_2) \rangle \partial_{t_1} \partial_{t_2} \langle \hat{\psi}_L^\dagger(\bar{t}_1) \hat{\psi}_L(\bar{t}_2) \rangle + (t_1 \leftrightarrow t_2) \\ &= 2|\Lambda|^2 [G_R(\bar{t}_1 - \bar{t}_2) \partial_{t_1} \partial_{t_2} G_L(\bar{t}_1 - \bar{t}_2) + G_R(\bar{t}_2 - \bar{t}_1) \partial_{t_1} \partial_{t_2} G_L(\bar{t}_2 - \bar{t}_1)]. \end{aligned} \quad (\text{B.16})$$

897 By performing a Fourier transform, we find

$$\begin{aligned} \Sigma_{44}^{(11)}(\omega) &= 2|\Lambda|^2 \int_{-\infty}^{+\infty} dt_{12} e^{i\omega t_{12}} [G_R(t_{12}) \partial_{t_1} \partial_{t_2} G_L(t_{12}) + G_R(-t_{12}) \partial_{t_1} \partial_{t_2} G_L(-t_{12})] \\ &= -4|\Lambda|^2 \int_{-\infty}^{+\infty} d\tau \cos(\omega\tau) G_R(\tau) \partial_\tau^2 G_L(\tau). \end{aligned} \quad (\text{B.17})$$

898 In the zero-frequency limit, we thus obtain

$$\Sigma_{44}^{(11)}(0) = -4|\Lambda|^2 \int_{-\infty}^{+\infty} d\tau G_R(\tau) \partial_\tau^2 G_L(\tau) = 4|\Lambda|^2 \int_{-\infty}^{+\infty} d\tau \partial_\tau G_R(\tau) \partial_\tau G_L(\tau) \equiv S_{TT}^{JJ}, \quad (\text{B.18})$$

899 which defines the tunneling heat-current noise  $S_{TT}^{JJ}$  in Eq. (41c). With similar calculations, we  
 900 also find  $\Sigma_{33}^{(11)} = -\Sigma_{34}^{(11)} = -\Sigma_{43}^{(11)} = S_{TT}^{JJ}$ . Similar calculations for the finite bias case  $V \neq 0$ ,  
 901 give

$$\Sigma_{33}^{(11)} = -4|\Lambda|^2 \int_{-\infty}^{+\infty} d\tau \cos(\omega\tau) \cos(e\nu V\tau) G_L(\tau) \partial_\tau^2 G_R(\tau), \quad (\text{B.19a})$$

$$\Sigma_{44}^{(11)} = -4|\Lambda|^2 \int_{-\infty}^{+\infty} d\tau \cos(\omega\tau) \cos(e\nu V\tau) G_R(\tau) \partial_\tau^2 G_L(\tau), \quad (\text{B.19b})$$

$$\Sigma_{34}^{(11)} = -4|\Lambda|^2 \int_{-\infty}^{+\infty} d\tau \cos(\omega\tau) \cos(e\nu V\tau) \partial_\tau G_L(\tau) \partial_\tau G_R(\tau) = \Sigma_{43}^{(11)}. \quad (\text{B.19c})$$

902 By summing all the contributions, we find

$$\Sigma_{33}^{(11)} + \Sigma_{44}^{(11)} + \Sigma_{34}^{(11)} + \Sigma_{43}^{(11)} = V^2 S_{TT}^{II}, \quad (\text{B.20})$$

903 which corresponds to the conservation of power fluctuations for the tunneling current (i.e.,  
 904 the equality of thermal power fluctuations and electrical power fluctuations).

905 **B.4 Crossed heat-current noise terms**  $\Sigma_{\alpha\beta}^{(02)} + \Sigma_{\alpha\beta}^{(20)}$

906 **B.4.1**  $\Sigma_{44}^{(02)} + \Sigma_{44}^{(20)}$

907 We start with the contribution

$$\Sigma_{44}^{(02)}(t_1 - t_2) = \left\langle \delta \hat{J}_4^{(0)}(t_1) \delta \hat{J}_4^{(2)}(t_2) \right\rangle + \left\langle \delta \hat{J}_4^{(2)}(t_2) \delta \hat{J}_4^{(0)}(t_1) \right\rangle. \quad (\text{B.21})$$

908 Considering the term  $\langle \hat{J}_4^{(0)}(t_1) \hat{J}_4^{(2)}(t_2) \rangle$ , we have

$$\begin{aligned} \langle \hat{J}_4^{(0)}(t_1) \hat{J}_4^{(2)}(t_2) \rangle = & -\frac{i|\Lambda|^2}{4\pi} \int_{-\infty}^{\bar{t}_2} dt'' \left[ \langle (\partial_{\bar{t}_1} \hat{\phi}_L(\bar{t}_1))^2 \hat{\psi}_R^\dagger(t'') \hat{\psi}_L(t'') \partial_{\bar{t}_2} \hat{\psi}_L^\dagger(\bar{t}_2) \hat{\psi}_R(\bar{t}_2) \rangle \right. \\ & - \langle (\partial_{\bar{t}_1} \hat{\phi}_L(\bar{t}_1))^2 \partial_{\bar{t}_2} \hat{\psi}_L^\dagger(\bar{t}_2) \hat{\psi}_R(\bar{t}_2) \hat{\psi}_R^\dagger(t'') \hat{\psi}_L(t'') \rangle \\ & + \langle (\partial_{\bar{t}_1} \hat{\phi}_L(\bar{t}_1))^2 \hat{\psi}_L^\dagger(t'') \hat{\psi}_R(t'') \hat{\psi}_R^\dagger(\bar{t}_2) \partial_{\bar{t}_2} \hat{\psi}_L(\bar{t}_2) \rangle \\ & \left. - \langle (\partial_{\bar{t}_1} \hat{\phi}_L(\bar{t}_1))^2 \hat{\psi}_R^\dagger(\bar{t}_2) \partial_{\bar{t}_2} \hat{\psi}_L(\bar{t}_2) \hat{\psi}_L^\dagger(t'') \hat{\psi}_R(t'') \rangle \right]. \end{aligned} \quad (\text{B.22})$$

909 By performing the averages, and subtracting the product of the currents, we obtain

$$\begin{aligned} \langle \delta \hat{J}_4^{(0)}(t_1) \delta \hat{J}_4^{(2)}(t_2) \rangle = & \frac{i\lambda|\Lambda|^2}{2\pi} \underbrace{\int_{-\infty}^{\bar{t}_2} dt'' G_R(t'' - \bar{t}_2) \partial_{\bar{t}_2} [K(\bar{t}_1, t'', \bar{t}_2) G_L(t'' - \bar{t}_2)]}_{\mathcal{J}_1} \\ & - \frac{i\lambda|\Lambda|^2}{2\pi} \underbrace{\int_{-\infty}^{\bar{t}_2} dt'' G_R(\bar{t}_2 - t'') \partial_{\bar{t}_2} [K(\bar{t}_1, \bar{t}_2, t'') G_L(\bar{t}_2 - t'')]}_{\mathcal{J}_2}, \end{aligned} \quad (\text{B.23})$$

910 with the function

$$K(\tau_1, \tau_3, \tau_4) = \frac{\pi^2 T_2^2 \sinh^2[\pi T_2(\tau_3 - \tau_4)]}{\sinh^2[\pi T_2(i\tau_0 - (\tau_1 - \tau_3))] \sinh^2[\pi T_2(i\tau_0 - (\tau_1 - \tau_4))]} = K(\tau_1, \tau_4, \tau_3). \quad (\text{B.24})$$

911 By making a change of variable  $t'' - \bar{t}_2 = \tau$  and expanding the derivatives, the integrals  $\mathcal{J}_{1,2}$   
912 in (B.23) become

$$\mathcal{J}_1(t_{12}) = \int_{-\infty}^0 d\tau G_R(\tau) [h(t_{12}, \tau) G_L(\tau) - K_0(t_{12}, \tau) \partial_\tau G_L(\tau)], \quad (\text{B.25})$$

$$\mathcal{J}_2(t_{12}) = \int_{-\infty}^0 d\tau G_R(-\tau) [h(t_{12}, \tau) G_L(-\tau) - K_0(t_{12}, \tau) \partial_\tau G_L(-\tau)], \quad (\text{B.26})$$

913 where

$$K_0(t_{12}, \tau) = \frac{\pi^2 T_2^2 \sinh^2(\pi T_2 \tau)}{\sinh^2[\pi T_2(i\tau_0 - t_{12})] \sinh^2[\pi T_2(i\tau_0 - (t_{12} - \tau))]}, \quad (\text{B.27})$$

$$h(t_{12}, \tau) = -2\pi^2 T_2^2 \frac{\pi T_2 \coth[\pi T_2(i\tau_0 - t_{12})] - \pi T_2 \coth[\pi T_2(i\tau_0 - (t_{12} - \tau))]}{\sinh^2[\pi T_2(i\tau_0 - t_{12})]}. \quad (\text{B.28})$$

914 The other term of interest,  $\langle \hat{J}_4^{(2)}(t_2) \hat{J}_4^{(0)}(t_1) \rangle$ , can be handled in a similar way. We find:

$$\langle \hat{J}_4^{(2)}(t_2) \hat{J}_4^{(0)}(t_1) \rangle - \langle \hat{J}_4^{(2)}(t_2) \rangle \langle \hat{J}_4^{(0)}(t_1) \rangle = \frac{i\lambda|\Lambda|^2}{2\pi} [\mathcal{J}_3(t_{12}) - \mathcal{J}_4(t_{12})], \quad (\text{B.29})$$

915 with

$$\mathcal{J}_3(t_{12}) = \int_{-\infty}^0 d\tau G_R(\tau) [-h(-t_{12}, -\tau)G_L(\tau) - K_0(-t_{12}, -\tau)\partial_\tau G_L(\tau)], \quad (\text{B.30})$$

$$\mathcal{J}_4(t_{12}) = \int_{-\infty}^0 d\tau G_R(-\tau) [-h(-t_{12}, -\tau)G_L(-\tau) - K_0(-t_{12}, -\tau)\partial_\tau G_L(-\tau)]. \quad (\text{B.31})$$

916 Performing an analogous calculation for  $\Sigma_{44}^{(20)}$ , and taking a Fourier transform, we obtain

$$\begin{aligned} \Sigma_{44}^{(02)}(\omega) + \Sigma_{44}^{(20)}(\omega) &= \frac{i\lambda|\Lambda|^2}{2\pi} [\tilde{\mathcal{J}}_1(\omega) - \tilde{\mathcal{J}}_2(\omega) + \tilde{\mathcal{J}}_3(\omega) - \tilde{\mathcal{J}}_4(\omega) \\ &\quad + \tilde{\mathcal{J}}_1(-\omega) - \tilde{\mathcal{J}}_2(-\omega) + \tilde{\mathcal{J}}_3(-\omega) - \tilde{\mathcal{J}}_4(-\omega)], \end{aligned} \quad (\text{B.32})$$

917 where

$$\tilde{\mathcal{J}}_\alpha(\omega) = \int_{-\infty}^{+\infty} dt_{12} \mathcal{J}_\alpha(t_{12}) e^{i\omega t_{12}}. \quad (\text{B.33})$$

918 It is clear from the expressions of the integrals  $\mathcal{J}_\alpha(t_{12})$  that we need the Fourier transforms  
919  $\tilde{K}_0(\omega, \tau)$  and  $\tilde{h}(\omega, \tau)$ . The former is readily found by using the residue theorem and reads

$$\tilde{K}_0(\omega, \tau) = \pi i \left[ 1 + \coth\left(\frac{\omega}{2T_2}\right) \right] [i\omega(1 + e^{i\omega\tau}) + 2\pi T_2 \coth(\pi T_2 \tau)(1 - e^{i\omega\tau})]. \quad (\text{B.34})$$

920 For the latter, we use the following manipulation

$$\tilde{h}(\omega, \tau) \equiv \int_{-\infty}^{+\infty} dt_{12} h(t_{12}, \tau) e^{i\omega t_{12}} = e^{i\omega\tau} \int_{-\infty}^{+\infty} dt_{12} e^{i\omega t_{12}} h(t_{12} + \tau, \tau). \quad (\text{B.35})$$

921 The reason for this is that

$$\begin{aligned} h(t_{12} + \tau, \tau) &= 2\pi^2 T_2^2 \frac{\pi T_2 \coth[\pi T_2(i\tau_0 - t_{12})] - \pi T_2 \coth[\pi T_2(i\tau_0 - (t_{12} + \tau))]}{\sinh^2[\pi T_2(i\tau_0 - (t_{12} + \tau))]} \\ &= (\partial_y K_0(t_{12}, y))_{y=-\tau} = -\partial_\tau K_0(t_{12}, -\tau), \end{aligned} \quad (\text{B.36})$$

922 Therefore,

$$\tilde{h}(\omega, \tau) = -e^{i\omega\tau} \partial_\tau \int_{-\infty}^{+\infty} dt_{12} e^{i\omega t_{12}} K_0(t_{12}, -\tau) = -e^{i\omega\tau} \partial_\tau \tilde{K}_0(\omega, -\tau) = e^{i\omega\tau} (\partial_y \tilde{K}_0(\omega, y))_{y=-\tau}, \quad (\text{B.37})$$

923 which allows us to obtain  $\tilde{h}(\omega, \tau)$  from (B.34), yielding

$$\tilde{h}(\omega, \tau) = i\pi \left[ \coth\left(\frac{\omega}{2T_2}\right) + 1 \right] \left[ \pi T_2 \frac{2\pi T_2(1 - e^{i\tau\omega}) + i\omega \sinh(2\pi\tau T_2)}{\sinh^2(\pi\tau T_2)} - \omega^2 \right]. \quad (\text{B.38})$$

924 By combining all integrals in Eq. (B.32), we arrive at the expression

$$\begin{aligned} \Sigma_{44}^{(02)}(\omega) + \Sigma_{44}^{(20)}(\omega) &= \frac{i\lambda|\Lambda|^2}{2\pi} \int_{-\infty}^{+\infty} d\tau \{ G_R(\tau) [(\tilde{h}(\omega, \tau) - \tilde{h}(\omega, -\tau))G_L(\tau) \\ &\quad - (\tilde{K}_0(\omega, \tau) + \tilde{K}_0(\omega, -\tau))\partial_\tau G_L(\tau)] + (\omega \rightarrow -\omega) \}. \end{aligned} \quad (\text{B.39})$$

925 This formula, together with Eqs. (B.38) and (B.34), provides the expression for the finite fre-  
926 quency noise. We can also obtain an equivalent formula, which is more convenient to evaluate



927 the zero-frequency limit. By repeatedly integrating by parts, and exploiting the relation (B.37)  
928 between the functions  $\tilde{h}$  and  $\tilde{K}_0$ , we arrive at

$$\begin{aligned} \Sigma_{44}^{(02)}(\omega) + \Sigma_{44}^{(20)}(\omega) &= \frac{i\lambda|\Lambda|^2}{2\pi} \int_{-\infty}^{+\infty} d\tau \{ \partial_\tau G_R(\tau) G_L(\tau) [\tilde{K}_0(\omega, \tau) e^{-i\omega\tau} + \tilde{K}_0(\omega, -\tau) e^{i\omega\tau}] \\ &\quad + G_R(\tau) \partial_\tau G_L(\tau) [(e^{-i\omega\tau} - 1) \tilde{K}_0(\omega, \tau) + (e^{i\omega\tau} - 1) \tilde{K}_0(\omega, -\tau)] \\ &\quad - i\omega G_R(\tau) G_L(\tau) [\tilde{K}_0(\omega, \tau) e^{-i\omega\tau} - \tilde{K}_0(\omega, -\tau) e^{i\omega\tau}] + (\omega \rightarrow -\omega) \}. \end{aligned} \quad (\text{B.40})$$

929 The zero-frequency limit is therefore given by

$$\begin{aligned} \Sigma_{44}^{(02)}(0) + \Sigma_{44}^{(20)}(0) &= 2 \times \frac{i\lambda|\Lambda|^2}{2\pi} \int_{-\infty}^{+\infty} d\tau \partial_\tau G_R(\tau) [\tilde{K}_0(0, \tau) + \tilde{K}_0(0, -\tau)] G_L(\tau) \\ &= 8iT_2\lambda|\Lambda|^2 \int_{-\infty}^{+\infty} d\tau \partial_\tau G_R(\tau) [-1 + \pi T_2\tau \coth(\pi T_2\tau)] G_L(\tau). \end{aligned} \quad (\text{B.41})$$

930 Finally, we exploit the Green's function identity

$$\lambda\pi T_2 \coth(\pi T_2\tau) G_L(\tau) = -\partial_\tau G_L(\tau) \quad (\text{B.42})$$

931 and we arrive at two equivalent final expressions

$$\Sigma_{44}^{(02)}(0) + \Sigma_{44}^{(20)}(0) = 4(\lambda - 1)T_2 J_T + 8i|\Lambda|^2 T_2 \int_{-\infty}^{+\infty} d\tau \tau G_L(\tau) \partial_\tau^2 G_R(\tau) \quad (\text{B.43})$$

$$= 4\lambda T_2 J_T - 8i|\Lambda|^2 T_2 \int_{-\infty}^{+\infty} d\tau \tau \partial_\tau G_L(\tau) \partial_\tau G_R(\tau), \quad (\text{B.44})$$

932 where we recalled the expression for the heat tunneling current (B.8).

933 The remaining terms are obtained with very similar calculations and they read

$$\Sigma_{33}^{(02)}(0) + \Sigma_{33}^{(20)}(0) = -4\lambda T_1 J_T - 8i|\Lambda|^2 T_1 \int_{-\infty}^{+\infty} d\tau \tau \partial_\tau G_L(\tau) \partial_\tau G_R(\tau), \quad (\text{B.45})$$

$$\Sigma_{34}^{(02)}(0) + \Sigma_{34}^{(20)}(0) = 2\lambda(T_1 - T_2) J_T + 4i|\Lambda|^2 (T_1 + T_2) \int_{-\infty}^{+\infty} d\tau \tau \partial_\tau G_L(\tau) \partial_\tau G_R(\tau). \quad (\text{B.46})$$

934 In the presence of a finite voltage bias,  $V \neq 0$ , in addition to the temperature bias, the  
935 above results are generalized as follows:

$$\begin{aligned} \Sigma_{44}^{(02)}(0) + \Sigma_{44}^{(20)}(0) &= 4\lambda T_2 \langle \hat{j}_4^{(2)} \rangle - 4VT_2 \partial_V \langle \hat{j}_4^{(2)} \rangle \\ &\quad - 8i|\Lambda|^2 T_2 \int_{-\infty}^{+\infty} d\tau \tau \cos(e\nu V\tau) \partial_\tau G_L(\tau) \partial_\tau G_R(\tau), \end{aligned} \quad (\text{B.47})$$

$$\begin{aligned} \Sigma_{33}^{(02)}(0) + \Sigma_{33}^{(20)}(0) &= 4\lambda T_1 \langle \hat{j}_3^{(2)} \rangle - 4VT_1 \partial_V \langle \hat{j}_3^{(2)} \rangle \\ &\quad - 8i|\Lambda|^2 T_1 \int_{-\infty}^{+\infty} d\tau \tau \cos(e\nu V\tau) \partial_\tau G_L(\tau) \partial_\tau G_R(\tau), \end{aligned} \quad (\text{B.48})$$

$$\begin{aligned} \Sigma_{34}^{(02)}(0) + \Sigma_{34}^{(20)}(0) &= 2\lambda T_1 \langle \hat{j}_4^{(2)} \rangle + 2\lambda T_2 \langle \hat{j}_3^{(2)} \rangle \\ &\quad + 4i|\Lambda|^2 (T_1 + T_2) \int_{-\infty}^{+\infty} d\tau \tau \cos(e\nu V\tau) \partial_\tau G_L(\tau) \partial_\tau G_R(\tau), \end{aligned} \quad (\text{B.49})$$

936 where the expressions for the average heat currents  $\langle \hat{j}_{3,4}^{(2)} \rangle$  are given in Eq. (B.6).

## 937 B.5 Summary of heat-current noises

938 Gathering the results from all above subsections in Appendix B, we summarize the expressions  
 939 for the auto- and cross-correlated heat-current noises in Tab. 2. These results are those stated  
 in Eqs. (37) and (41) in the main text.

$S_{\alpha\beta}^{JJ}$	3	4
3	$2\frac{\pi^2 k_B^3}{3h} T_1^3 - 4\lambda k_B T_1 J_T + S_{TT}^{JJ} - 2k_B T_1 \mathcal{J}$	$-S_{TT}^{JJ} + 2\lambda k_B (T_1 - T_2) J_T + k_B (T_1 + T_2) \mathcal{J}$
4	$-S_{TT}^{JJ} + 2\lambda k_B (T_1 - T_2) J_T + k_B (T_1 + T_2) \mathcal{J}$	$2\frac{\pi^2 k_B^3}{3h} T_2^3 + 4\lambda k_B T_2 J_T + S_{TT}^{JJ} - 2k_B T_2 \mathcal{J}$

Table 2: Auto- and cross-correlation heat-current noises at zero voltage bias and zero frequency,  $S_{\alpha\beta}^{JJ}$  with  $\alpha, \beta = L, R$ . The expressions are given to  $\mathcal{O}(|\Lambda|^2)$  in the tunneling amplitude  $\Lambda$ , and we have defined the integral  $\mathcal{J} \equiv 4i|\Lambda|^2 \int_{-\infty}^{+\infty} d\tau \tau \partial_\tau G_R \partial_\tau G_L$ .

940

## 941 C Derivation of mixed noise components

### 942 C.1 General expressions

943 We decompose the mixed noise perturbatively as

$$S_{\alpha\beta}^{IJ} = M_{\alpha\beta}^{(00)} + M_{\alpha\beta}^{(11)} + M_{\alpha\beta}^{(02)} + M_{\alpha\beta}^{(20)}, \quad (\text{C.1})$$

944 where, in analogy to the charge and heat noise components, we define

$$M_{\alpha\beta}^{(ij)} = \left\langle \left\{ \delta \hat{I}_\alpha^{(i)}(t_1), \delta \hat{J}_\beta^{(j)}(t_2) \right\} \right\rangle. \quad (\text{C.2})$$

945 We readily find that the equilibrium component  $M_{\alpha\beta}^{(00)}$  vanishes, as it reduces to expectation  
 946 values of the form  $\langle \partial_{t_1} \hat{\phi}_\alpha(t_1) [\partial_{t_2} \hat{\phi}_\beta(t_2)]^2 \rangle$ , which contain an unbalanced number of bosonic  
 947 operators and thus evaluates to zero by Wick's theorem. With the same approach as for the  
 948 charge and heat noises in the above Appendixes, we obtain the ‘‘tunneling’’ terms as

$$M_{33}^{(11)} = 4e\nu|\Lambda|^2 \int_{-\infty}^{+\infty} d\tau \sin(e\nu V \tau) G_L(\tau) \partial_\tau G_R(\tau) = -M_{43}^{(11)} \equiv M_{TT} - \frac{V}{2} S_{TT}^{II}, \quad (\text{C.3})$$

$$M_{44}^{(11)} = -4e\nu|\Lambda|^2 \int_{-\infty}^{+\infty} d\tau \sin(e\nu V \tau) G_R(\tau) \partial_\tau G_L(\tau) = -M_{34}^{(11)} \equiv M_{TT} + \frac{V}{2} S_{TT}^{II}, \quad (\text{C.4})$$

949 with

$$M_{TT} \equiv 2e\nu|\Lambda|^2 \int_{-\infty}^{+\infty} d\tau \sin(e\nu V \tau) [G_L(\tau) \partial_\tau G_R(\tau) - G_R(\tau) \partial_\tau G_L(\tau)]. \quad (\text{C.5})$$

950 We note here the relations  $M_{33}^{(11)} = -M_{43}^{(11)}$  and  $M_{44}^{(11)} = -M_{34}^{(11)}$  which are a direct conse-  
 951 quence of the operator identity  $\hat{I}_3^{(1)} = -\hat{I}_4^{(1)}$ , see Eq. (A.3). These relations also show that the  
 952 ‘‘tunneling’’ mixed noise components satisfy the sum rule  $\sum_{\alpha\beta} M_{\alpha\beta}^{(11)} = 0$  for  $\alpha = 3, 4$ .

953 Next, a straightforward but long calculation of the correlations between the unperturbed  
 954 currents and their corrections induced by the tunneling lead to the following expressions for

955 the crossed terms

$$\begin{cases} M_{33}^{(20)} = -2\lambda T_1 I_T + 2T_1 \partial_V \langle \hat{J}_3^{(2)} \rangle \\ M_{33}^{(02)} = -2T_1 I_T + 2T_1 \partial_V \langle \hat{J}_3^{(2)} \rangle \end{cases} \rightarrow M_{33}^{(02+20)} = -2T_1(1+\lambda)I_T + 4T_1 \partial_V \langle \hat{J}_3^{(2)} \rangle, \quad (\text{C.6a})$$

$$\begin{cases} M_{44}^{(20)} = +2\lambda T_2 I_T - 2T_2 \partial_V \langle \hat{J}_4^{(2)} \rangle \\ M_{44}^{(02)} = +2T_2 I_T - 2T_2 \partial_V \langle \hat{J}_4^{(2)} \rangle \end{cases} \rightarrow M_{44}^{(02+20)} = +2T_2(1+\lambda)I_T - 4T_2 \partial_V \langle \hat{J}_4^{(2)} \rangle, \quad (\text{C.6b})$$

$$\begin{cases} M_{34}^{(20)} = -2\lambda T_2 I_T + 2T_2 \partial_V \langle \hat{J}_4^{(2)} \rangle \\ M_{34}^{(02)} = +2T_2 \partial_V \langle \hat{J}_4^{(2)} \rangle \end{cases} \rightarrow M_{34}^{(02+20)} = -2\lambda T_2 I_T + 2(T_1 + T_2) \partial_V \langle \hat{J}_4^{(2)} \rangle, \quad (\text{C.6c})$$

$$\begin{cases} M_{43}^{(20)} = +2\lambda T_1 I_T - 2T_1 \partial_V \langle \hat{J}_3^{(2)} \rangle \\ M_{43}^{(02)} = -2T_2 \partial_V \langle \hat{J}_3^{(2)} \rangle \end{cases} \rightarrow M_{43}^{(02+20)} = +2\lambda T_1 I_T - 2(T_1 + T_2) \partial_V \langle \hat{J}_3^{(2)} \rangle, \quad (\text{C.6d})$$

956 with the average heat currents  $\langle \hat{J}_a^{(2)} \rangle$  given in Eq. (B.6). Combining all components, we arrive  
957 at the mixed noise components

$$S_{33}^{IJ} = +M_{TT} - \frac{V}{2} S_{TT}^{II} - 2T_1(1+\lambda)I_T + 4T_1 \partial_V \langle \hat{J}_3^{(2)} \rangle, \quad (\text{C.7a})$$

$$S_{44}^{IJ} = +M_{TT} + \frac{V}{2} S_{TT}^{II} + 2T_2(1+\lambda)I_T - 4T_2 \partial_V \langle \hat{J}_4^{(2)} \rangle, \quad (\text{C.7b})$$

$$S_{34}^{IJ} = -M_{TT} - \frac{V}{2} S_{TT}^{II} - 2\lambda T_2 I_T + 2(T_1 + T_2) \partial_V \langle \hat{J}_4^{(2)} \rangle, \quad (\text{C.7c})$$

$$S_{43}^{IJ} = -M_{TT} + \frac{V}{2} S_{TT}^{II} + 2\lambda T_1 I_T - 2(T_1 + T_2) \partial_V \langle \hat{J}_3^{(2)} \rangle, \quad (\text{C.7d})$$

958 which are given in Eq. (74) in the main text.

## 959 C.2 Relation with the thermoelectric response

960 In this section, we prove Eq. (80) in the main text, namely the relation between mixed noise  
961 and the differential thermoelectric conductance.

962 To this end, consider a nonequilibrium situation with finite voltage bias ( $V \neq 0$ ), but  
963 vanishing temperature bias,  $\Delta T \rightarrow 0$ . As a result, our calculations involve only a single Green's  
964 function at temperature  $\bar{T}$ , denoted as

$$G_L(\tau) = G_R(\tau) \equiv G(\tau) = \frac{1}{2\pi a} \left( \frac{\sinh(i\pi \bar{T} \tau_0)}{\sinh[\pi \bar{T} (i\tau_0 - \tau)]} \right)^\lambda. \quad (\text{C.8})$$

965 As our next step, we combine the mixed noise components (C.3), (C.4), the average heat  
966 currents (B.6), and the charge tunneling current (A.32a) and perform an expansion at first  
967 order in  $eV/\bar{T}$ . This expansion results in

$$M_{33}^{(11)} = +4(e\nu)^2 |\Lambda|^2 \frac{V}{\bar{T}} \int_{-\infty}^{+\infty} dx x G(x/\bar{T}) G'(x/\bar{T}) \equiv +4\mathcal{L}_1 \frac{V}{\bar{T}}, \quad (\text{C.9a})$$

$$M_{44}^{(11)} = -4(e\nu)^2 |\Lambda|^2 \frac{V}{\bar{T}} \int_{-\infty}^{+\infty} dx x G(x/\bar{T}) G'(x/\bar{T}) \equiv -4\mathcal{L}_1 \frac{V}{\bar{T}}, \quad (\text{C.9b})$$

$$T_{1,2} \partial_V \langle \hat{J}_3^{(2)} \rangle = -2i(e\nu)^2 |\Lambda|^2 \frac{V}{\bar{T}} \int_{-\infty}^{+\infty} dx x^2 G(x/\bar{T}) G'(x/\bar{T}) \equiv -2\mathcal{L}_2 \frac{V}{\bar{T}}, \quad (\text{C.9c})$$

$$T_{1,2} \partial_V \langle \hat{J}_4^{(2)} \rangle = -2i(e\nu)^2 |\Lambda|^2 \frac{V}{\bar{T}} \int_{-\infty}^{+\infty} dx x^2 G(x/\bar{T}) G'(x/\bar{T}) \equiv -2\mathcal{L}_2 \frac{V}{\bar{T}}, \quad (\text{C.9d})$$

$$T_{1,2} I_T = +2i(e\nu)^2 |\Lambda|^2 \frac{V}{\bar{T}} \int_{-\infty}^{+\infty} dx x [G(x/\bar{T})]^2 \equiv +2\mathcal{L}_0 \frac{V}{\bar{T}}, \quad (\text{C.9e})$$

968 where we introduced the dimensionless variable  $x = \bar{T} \tau$  and defined the three integrals

$$\mathcal{L}_0 = i(e\nu)^2 |\Lambda|^2 \int_{-\infty}^{+\infty} dx x [G(x/\bar{T})]^2, \quad (\text{C.10a})$$

$$\mathcal{L}_1 = (e\nu)^2 |\Lambda|^2 \int_{-\infty}^{+\infty} dx x G(x/\bar{T}) G'(x/\bar{T}), \quad (\text{C.10b})$$

$$\mathcal{L}_2 = i(e\nu)^2 |\Lambda|^2 \int_{-\infty}^{+\infty} dx x^2 G(x/\bar{T}) G'(x/\bar{T}). \quad (\text{C.10c})$$

969 We define the finite-bias thermoelectric conductance as

$$\tilde{L} = \frac{\partial I_T}{\partial \Delta T} = 2i(e\nu)^2 |\Lambda|^2 \int_{-\infty}^{+\infty} d\tau \sin(e\nu V \tau) \frac{\partial}{\partial \Delta T} [G_R(\tau) G_L(\tau)]. \quad (\text{C.11})$$

970 In the limit  $\Delta T \rightarrow 0$  and  $eV/\bar{T} \ll 1$ , we get

$$\tilde{L} = \frac{2i(e\nu)^2 |\Lambda|^2 V}{\bar{T}^2} \int_{-\infty}^{+\infty} dx x^2 G(x/\bar{T}) G'(x/\bar{T}) = \frac{2\mathcal{L}_2 V}{\bar{T}^2 \bar{T}}. \quad (\text{C.12})$$

971 The integrals (C.10) can be evaluated analytically as follows (see also App. E)

$$\begin{aligned} \mathcal{L}_0 &= (e\nu)^2 \bar{T}^{2\lambda} \tau_0^{2\lambda-2} \frac{|\Lambda|^2}{v_F^2} \int_{-\infty}^{+\infty} \frac{dx}{4\pi^2} ix \left( \frac{i\pi}{\sinh[\pi(i\bar{T}\tau_0 - x)]} \right)^{2\lambda} \\ &= (e\nu)^2 \frac{\bar{T}^{2\lambda}}{8\pi} (\pi\tau_0)^{2\lambda-2} \frac{|\Lambda|^2}{v_F^2} \int_{-\infty}^{+\infty} \frac{dz}{[\cosh(z)]^{2\lambda}} = (2\pi\tau_0)^{2\lambda-2} \frac{|\Lambda|^2}{v_F^2} (e\nu)^2 \frac{\bar{T}^{2\lambda}}{4\pi} \frac{\Gamma^2(\lambda)}{\Gamma(2\lambda)}, \end{aligned} \quad (\text{C.13a})$$

$$\begin{aligned} \mathcal{L}_1 &= (e\nu)^2 \tau_0^{2\lambda-2} \frac{|\Lambda|^2}{v_F^2} \int_{-\infty}^{+\infty} \frac{dx}{4\pi^2} x \left( \frac{i\pi\bar{T}}{\sinh[\pi(i\bar{T}\tau_0 - x)]} \right)^\lambda \partial_x \left( \frac{i\pi\bar{T}}{\sinh[\pi(i\bar{T}\tau_0 - x)]} \right)^\lambda \\ &= -(e\nu)^2 \frac{\bar{T}^{2\lambda}}{4\pi} (\pi\tau_0)^{2\lambda-2} \frac{|\Lambda|^2}{v_F^2} \lambda \int_{-\infty}^{+\infty} dz \frac{z \sinh(z)}{[\cosh(z)]^{1+2\lambda}} = -\mathcal{L}_0, \end{aligned} \quad (\text{C.13b})$$

$$\begin{aligned} \mathcal{L}_2 &= (e\nu)^2 \tau_0^{2\lambda-2} \frac{|\Lambda|^2}{v_F^2} \int_{-\infty}^{+\infty} \frac{dx}{4\pi^2} ix^2 \left( \frac{i\pi}{\sinh[\pi(i\bar{T}\tau_0 - x)]} \right)^\lambda \partial_x \left( \frac{i\pi}{\sinh[\pi(i\bar{T}\tau_0 - x)]} \right)^\lambda \\ &= -(e\nu)^2 \frac{\bar{T}^{2\lambda}}{4\pi} (\pi\tau_0)^{2\lambda-2} \frac{|\Lambda|^2}{v_F^2} \lambda \int_{-\infty}^{+\infty} dz \frac{z \sinh(z)}{[\cosh(z)]^{1+2\lambda}} = -\mathcal{L}_0. \end{aligned} \quad (\text{C.13c})$$

972 In evaluating all these integrals, we performed the change of variable  $x = z/\pi + \tau_0 - i/2$  in  
973 the complex plane and deformed the contour back to the real axis, exploiting the finite cutoff  
974  $\tau_0$  [21]. Substituting the evaluated  $\mathcal{L}_i$  integrals into the mixed noise components (C.9) and  
975 then into Eq. (C.7), we find the relations

$$S_{33}^{IJ}(0) = -S_{44}^{IJ}(0) = -4\lambda \mathcal{L}_0 \frac{V}{\bar{T}}, \quad (\text{C.14a})$$

$$S_{34}^{IJ}(0) = -S_{43}^{IJ}(0) = 4(1-\lambda) \mathcal{L}_0 \frac{V}{\bar{T}}. \quad (\text{C.14b})$$

976 Similarly, the conductance in Eq. (C.12) becomes

$$\tilde{L} = -\frac{2\mathcal{L}_0 V}{\bar{T}^2 \bar{T}}, \quad (\text{C.15})$$

977 and therefore we obtain Eq. (80) in the main text.

## 978 D Scaling dimension modification by inter-channel interaction

### 979 D.1 Charge transport

980 In this Appendix, we give an example on how the addition of a local density-density interaction  
 981 at the QPC modifies the scaling dimension  $\lambda$  of the tunneling quasiparticles, from the ideal case  
 982  $\lambda = \nu$  to  $\lambda \neq \nu$ .

983 To this end, we consider adding to the free Hamiltonian  $\hat{H}_0$  in (7), not only the tunneling  
 984 term (10), but also the following local coupling between the  $R/L$  channels:

$$\hat{H}_u = \frac{2u}{4\pi} \int_{-\infty}^{+\infty} dx \delta(x) \partial_x \hat{\phi}_R(x) \partial_x \hat{\phi}_L(x). \quad (\text{D.1})$$

985 Here,  $u$  parametrizes the interaction strength and the location of the interaction coincides with  
 986 that of the QPC, here at  $x = 0$ . With this addition,  $\hat{H}_0 + \hat{H}_u$  is not diagonal in the bosons  $\hat{\phi}_{R/L}$   
 987 anymore. Still, we need to evaluate the local quasiparticle Green's functions

$$G_{R/L}(0, t) = \langle \hat{\psi}_{R/L}^\dagger(0, t) \hat{\psi}_{R/L}(0, 0) \rangle \quad (\text{D.2})$$

988 to compute observables related to the charge tunneling. To find these Green's functions when  
 989  $u \neq 0$ , we use the following approach: First, we locally diagonalize  $\hat{H}_0 + \hat{H}_u$  with the transfor-  
 990 mation

$$\begin{pmatrix} \hat{\phi}_+(0, t) \\ \hat{\phi}_-(0, t) \end{pmatrix} = \begin{pmatrix} \alpha & \beta \\ \beta & \alpha \end{pmatrix} \begin{pmatrix} \hat{\phi}_R(0, t) \\ \hat{\phi}_L(0, t) \end{pmatrix}. \quad (\text{D.3})$$

991 Here, the coefficients  $\alpha, \beta$  depend on the interaction strength  $u$  and the velocity  $v_F$  as

$$\alpha = \cosh(\theta), \quad \beta = \sinh(\theta), \quad \tanh(2\theta) = u/v_F. \quad (\text{D.4})$$

992 For  $u = 0$ , we have  $\alpha = 1 - \beta = 1$ , so that in this case  $\hat{\phi}_\pm(0, t) = \hat{\phi}_{R/L}(0, t)$  as expected.  
 993 The new modes  $\hat{\phi}_\pm(0, t)$  are the local eigenmodes at the point  $x = 0$  and the local Green's  
 994 functions at this point can be straightforwardly evaluated. We may thus write

$$\langle \hat{\psi}_R^\dagger(0, t) \hat{\psi}_R(0, 0) \rangle \times \langle \hat{\psi}_L^\dagger(0, t) \hat{\psi}_L(0, 0) \rangle = \frac{1}{(2\pi\alpha)^2} e^{\nu(\alpha^2 + \beta^2)[\mathcal{G}_+(0, t) + \mathcal{G}_-(0, t)]}, \quad (\text{D.5})$$

995 in terms of the diagonal bosonic Green's functions  $\mathcal{G}_\pm(0, t) = \langle \hat{\phi}_\pm(0, t) \hat{\phi}_\pm(0, 0) \rangle - \langle \hat{\phi}_\pm^2(0, 0) \rangle$ .

996 Our next step is to express  $\mathcal{G}_\pm(0, t)$  in terms of the known, "incoming" Green's functions,  
 997 i.e.,  $\mathcal{G}_{R/L}(x \neq 0, t)$ , which are given in terms of the original bosonic fields  $\hat{\phi}_{R/L}(t, \mp x_{1/2})$ .  
 998 These bosons are in equilibrium with their respective sources, at temperatures  $T_1$  and  $T_2$  and  
 999 at the locations  $\mp x_{1/2}$ . To this end, we solve a bosonic scattering problem with three regions:  
 1000 1) the region left of the QPC, 2) the central QPC region  $x = 0$ , and 3) the region right of the  
 1001 QPC. In brief, the matrix (D.3) constitutes the transfer matrix,  $\mathcal{T}$  for this scattering problem:

$$\mathcal{T} = \begin{pmatrix} \alpha & \beta \\ \beta & \alpha \end{pmatrix} = \frac{1}{T} \begin{pmatrix} 1 & R \\ R & 1 \end{pmatrix}, \quad (\text{D.6})$$

1002 with  $T^2 + R^2 = 1$ . Solving the scattering problem for the central region bosons,  $\hat{\phi}_\pm(0, t)$  in  
 1003 terms of the incoming modes, we find

$$\hat{\phi}_+(0, t) = \frac{R}{T} \hat{\phi}_L(x_2, t) + \frac{1}{T} \hat{\phi}_R(-x_1, t), \quad (\text{D.7a})$$

$$\hat{\phi}_-(0, t) = \frac{1}{T} \hat{\phi}_L(x_2, t) + \frac{R}{T} \hat{\phi}_R(-x_1, t), \quad (\text{D.7b})$$

1004 and since the bosons  $\hat{\phi}_{R/L}$  at the sources are uncorrelated, it follows that

$$\mathcal{G}_+(0, t) = \frac{R^2}{T^2} \mathcal{G}_L(x_2, t) + \frac{1}{T^2} \mathcal{G}_R(-x_1, t), \quad (\text{D.8a})$$

$$\mathcal{G}_-(0, t) = \frac{1}{T^2} \mathcal{G}_L(x_2, t) + \frac{R^2}{T^2} \mathcal{G}_R(-x_1, t). \quad (\text{D.8b})$$

1005 Finally, we identify  $R^2/T^2 = \beta^2$  and  $1/T^2 = \alpha^2$  and upon inserting into Eq. (D.5), we arrive  
1006 at

$$\langle \hat{\psi}_R^\dagger(0, t) \hat{\psi}_R(0, t) \rangle \times \langle \hat{\psi}_L^\dagger(0, t) \hat{\psi}_L(0, t) \rangle = \frac{1}{(2\pi\alpha)^2} e^{\nu(\alpha^2 + \beta^2)^2 [\mathcal{G}_R(-x_1, t) + \mathcal{G}_L(x_2, t)]}. \quad (\text{D.9})$$

1007 Thus, we see that  $H_u$  changes the scaling dimension from  $\nu$  to

$$\lambda \equiv \nu(\alpha^2 + \beta^2)^2 = \nu \cosh^2(2\theta) = \frac{\nu}{1 - u^2/v_F^2}. \quad (\text{D.10})$$

1008 For  $u = 0$  (i.e., without the coupling term  $\hat{H}_u$ ), we have  $\alpha = 1/T = 1$ ,  $\beta = R/T = 0$  and  $\lambda = \nu$   
1009 as expected. We emphasize that the temperatures entering the problem are the two source  
1010 contact temperatures  $T_{1/2}$ .

## 1011 D.2 Heat transport

1012 In the above calculation, we evaluated the product of  $L$  and  $R$  quasiparticle Green's functions,  
1013 which is sufficient to obtain the observables related to the charge transport, as is clear from  
1014 Eqs. (18) and (25). The situation changes when the heat transport is considered: in this case,  
1015 we deal with (for example) quantities like  $G_R(t) \partial_t G_L(t)$ , see Eq. (41). Thus, it is important to  
1016 critically analyze the behaviour of the  $L$  and  $R$  local Green's functions separately. Within the  
1017 toy model in this Appendix, we have (in terms of the ‘‘incoming’’ Green's functions)

$$\langle \hat{\psi}_R^\dagger(0, t) \hat{\psi}_R(0, t) \rangle = \frac{1}{2\pi\alpha} e^{\lambda_+ \mathcal{G}_R(t) + \lambda_- \mathcal{G}_L(t)}, \quad (\text{D.11})$$

$$\langle \hat{\psi}_L^\dagger(0, t) \hat{\psi}_L(0, t) \rangle = \frac{1}{2\pi\alpha} e^{\lambda_- \mathcal{G}_R(t) + \lambda_+ \mathcal{G}_L(t)}, \quad (\text{D.12})$$

1018 with

$$\lambda_+ = \alpha^4 + \beta^4, \quad (\text{D.13})$$

$$\lambda_- = 2\alpha^2\beta^2. \quad (\text{D.14})$$

1019 When calculating the tunneling heat noise, this renormalization gives rise to the usual expan-  
1020 sions in powers of  $\Delta T/2\bar{T}$

$$S_{TT}^{JJ} = S_0^{JJ} \left[ 1 + C_Q^{(2)} \left( \frac{\Delta T}{2\bar{T}} \right)^2 + \dots \right], \quad (\text{D.15})$$

1021 with prefactor

$$S_0^{JJ} = \frac{|\Lambda|^2}{v_F^2} \bar{T}^3 \frac{2\pi\lambda^2}{1 + 2\lambda} (2\pi\bar{T}\tau_0)^{2\lambda-2} \frac{\Gamma^2(\lambda)}{\Gamma(2\lambda)}, \quad \lambda = \lambda_+ + \lambda_-, \quad (\text{D.16})$$

1022 and coefficient

$$C_Q^{(2)} = \frac{\lambda(-4\lambda + \pi^2(\lambda + 2) - 2(\lambda + 2)\psi^{(1)}(\lambda + 1) - 2)}{2(2\lambda + 3)} + (\lambda_+ - \lambda_-)^2 \times \frac{\lambda(\pi^2(\lambda + 1) - 6) - 2\lambda(\lambda + 1)\psi^{(1)}(\lambda + 1) - 3}{\lambda^2(2\lambda + 3)}. \quad (\text{D.17})$$

1023 By comparing this result with Eq. (44a) in the main text, we see that, *at least within this*  
 1024 *toy model*, the two expressions agree only for  $\lambda_- = 0$ , which implies the ideal case  $\lambda = \nu$ .  
 1025 Otherwise, both parameters  $\lambda_{\pm}$  appear in the result. This feature stands in stark contrast with  
 1026 the charge transport properties, where the relevant parameter is always the sum  $\lambda = \lambda_+ + \lambda_-$ .  
 1027 This happens because it is the simple product of  $L$  and  $R$  Green's functions that determines  
 1028 all the relevant observables. Then, for charge transport, we can equivalently *assume* that both  
 1029 local Green's functions separately have a renormalized exponent  $\nu \rightarrow \lambda$ . The same assumption  
 1030 is required for the validity of the results concerning heat-related observables in the main text  
 1031 (beyond the ideal case  $\lambda = \nu$ , for which they are obviously valid). This does not happen in  
 1032 our toy model, but it might apply in more complicated ones, where the scaling dimension  
 1033 renormalization relies on different physical mechanisms (see the discussion below Eq. (20)  
 1034 for examples).

### 1035 D.3 Unequal scaling dimensions on the two edges

1036 Another possibility is that the two edges coupled by the tunneling Hamiltonian have inherently  
 1037 different scaling dimensions [107], which implies that the local quasiparticle Green's functions  
 1038 read

$$\langle \hat{\psi}_{R,L}^\dagger(0, \tau) \hat{\psi}_{R,L}(0, \tau) \rangle = \frac{1}{2\pi a} \left( \frac{\sinh(i\pi T_{1,2} \tau_0)}{\sinh[\pi T_{1,2}(i\tau_0 - \tau)]} \right)^{\lambda_{1,2}} \equiv G_{1,2}(\tau), \quad (\text{D.18})$$

1039 with  $\lambda_1 \neq \lambda_2$ . This property breaks the symmetry of the setup, introducing a difference be-  
 1040 tween the top and the bottom edge. The heat transport observables now read

$$J_T = -2i|\Lambda|^2 \int_{-\infty}^{+\infty} d\tau G_2(\tau) \partial_\tau G_1(\tau), \quad (\text{D.19a})$$

$$S_{TT}^{JJ} = 4|\Lambda|^2 \int_{-\infty}^{+\infty} d\tau \partial_\tau G_1(\tau) \partial_\tau G_2(\tau), \quad (\text{D.19b})$$

$$S_{33}^{JJ} = S_{11}^{JJ} + S_{TT}^{JJ} - 4\lambda_1 T_1 J_T - 8i|\Lambda|^2 T_1 \int_{-\infty}^{+\infty} d\tau \tau \partial_\tau G_1(\tau) \partial_\tau G_2(\tau), \quad (\text{D.19c})$$

$$S_{44}^{JJ} = S_{22}^{JJ} + S_{TT}^{JJ} + 4\lambda_2 T_2 J_T - 8i|\Lambda|^2 T_2 \int_{-\infty}^{+\infty} d\tau \tau \partial_\tau G_1(\tau) \partial_\tau G_2(\tau), \quad (\text{D.19d})$$

$$S_{34}^{JJ} = -S_{TT}^{JJ} + 2(\lambda_1 T_1 - \lambda_2 T_2) J_T + 4i|\Lambda|^2 (T_1 + T_2) \int_{-\infty}^{+\infty} d\tau \tau \partial_\tau G_1(\tau) \partial_\tau G_2(\tau), \quad (\text{D.19e})$$

$$S_{43}^{JJ} = S_{34}^{JJ}. \quad (\text{D.19f})$$

1041 As a consequence of the broken symmetry, we expect to find also odd coefficients in the  $\Delta T$   
 1042 power expansion, even in the presence of a symmetric bias. Indeed, using as an example the  
 1043 heat tunneling noise, we find the usual expansion

$$S_{TT}^{JJ} = S_0^{JJ} \left[ 1 + C_Q^{(1)} \left( \frac{\Delta T}{2\bar{T}} \right) + C_Q^{(2)} \left( \frac{\Delta T}{2\bar{T}} \right)^2 + C_Q^{(3)} \left( \frac{\Delta T}{2\bar{T}} \right)^3 \dots \right], \quad (\text{D.20})$$

1044 with prefactor

$$S_0^{JJ} = \frac{|\Lambda|^2}{v_F^2} 2\pi \bar{T}^3 \frac{\lambda_1 \lambda_2}{1 + 2\bar{\lambda}} (2\pi \bar{T} \tau_0)^{2\bar{\lambda} - 2} \frac{\Gamma^2(\bar{\lambda})}{\Gamma(2\bar{\lambda})}, \quad \text{where } \bar{\lambda} \equiv \frac{\lambda_1 + \lambda_2}{2}, \quad (\text{D.21})$$

1045 and coefficients

$$C_Q^{(1)} = (\lambda_1 - \lambda_2) \frac{1 + \bar{\lambda} - 2\bar{\lambda}^2}{2\bar{\lambda}(1 + \bar{\lambda})}, \quad (\text{D.22a})$$

1046

$$c_Q^{(2)} = \frac{(\pi^2(3\bar{\lambda} + 4) - 2(2\bar{\lambda} + 7))\bar{\lambda}^2 - 2(3\bar{\lambda} + 4)\bar{\lambda}^2\psi^{(1)}(\bar{\lambda}) + 8}{2\bar{\lambda}(2\bar{\lambda} + 3)} + (\lambda_1 - \lambda_2)^2 \times \frac{4 - 3(4 + \pi^2)\bar{\lambda} + 8\bar{\lambda}^2 + 6\bar{\lambda}\psi^{(1)}(\bar{\lambda})}{8\bar{\lambda}(2\bar{\lambda} + 3)}, \quad (\text{D.22b})$$

1047

$$c_Q^{(3)} = (\lambda_1 - \lambda_2) \left( \frac{12\bar{\lambda}^4 + 38\bar{\lambda}^3 - 12\bar{\lambda}^2 - 38\bar{\lambda} - 12}{12\bar{\lambda}(1 + \bar{\lambda})(2 + \bar{\lambda})} + \frac{\bar{\lambda}^2(3\bar{\lambda}^2 + \bar{\lambda} - 6)[6\psi^{(1)}(1 + \bar{\lambda}) - 3\pi^2]}{12\bar{\lambda}(1 + \bar{\lambda})(2 + \bar{\lambda})} \right) + (\lambda_1 - \lambda_2)^3 \times \frac{\pi^2(9\bar{\lambda}^2 - 9\bar{\lambda} - 6) - 4\bar{\lambda}(\bar{\lambda} - 1)(2\bar{\lambda} - 1) + 6(3\bar{\lambda}^2 - 3\bar{\lambda} + 2)\psi^{(1)}(\bar{\lambda})}{64\bar{\lambda}(\bar{\lambda} + 1)(\bar{\lambda} + 2)}. \quad (\text{D.22c})$$

1048 As expected, the odd coefficients vanish when  $\lambda_1 = \lambda_2$  and the even ones reduce to those  
1049 given in the main text.

## 1050 E Some useful integral identities

1051 Our approach to evaluating integrals over Green's functions and their derivatives is based on  
1052 the integral identity [108]

$$\int_{-\infty}^{\infty} \frac{\cosh(2bz)}{(\cosh(z))^{2a}} dz = 2 \times 4^{a-1} \mathcal{B}(a + b, a - b). \quad (\text{E.1})$$

1053 Here,

$$\mathcal{B}(z_1, z_2) = \frac{\Gamma(z_1)\Gamma(z_2)}{\Gamma(z_1 + z_2)} \quad (\text{E.2})$$

1054 is Euler's beta function and  $\Gamma(z)$  is the Gamma function. By repeated differentiation of Eq. (E.1)  
1055 with respect to  $b$ , we further obtain, for any positive integer  $m$ ,

$$\int_{-\infty}^{\infty} \frac{z^{2m} \cosh(2bz)}{(\cosh(z))^{2a}} dz = \frac{1}{2^{2m}} \frac{\partial^{2m}}{\partial b^{2m}} [2 \times 4^{a-1} \mathcal{B}(a + b, a - b)], \quad (\text{E.3})$$

$$\int_{-\infty}^{\infty} \frac{z^{2m-1} \sinh(2bz)}{(\cosh(z))^{2a}} dz = \frac{1}{2^{2m-1}} \frac{\partial^{2m-1}}{\partial b^{2m-1}} [2 \times 4^{a-1} \mathcal{B}(a + b, a - b)]. \quad (\text{E.4})$$

1056 Our strategy in this paper is to expand all integrals involving Green's functions and their deriva-  
1057 tives into terms on the form (E.1), (E.3), or (E.4) and then sum up all contributions.

## 1058 F Fourier transforms of the Green's function

1059 In the time-domain, the exponentiated bosonic (retarded) Green's function at temperature  $T_\alpha$   
1060 is given as

$$e^{\lambda \mathcal{G}_{R/L}(\tau)} = \left[ \frac{\sinh(i\pi T \tau_0)}{\sinh(\pi T_{1,2}(i\tau_0 - \tau))} \right]^\lambda, \quad (\text{F.1})$$



1061 where  $\tau_0 = a/v_F$  is the UV cutoff in the time domain. The Fourier transform of (F.1) can be  
 1062 evaluated to [21]

$$P_{1,2}(E) \equiv \int_{-\infty}^{+\infty} d\tau e^{iE\tau} e^{\lambda \mathcal{G}_{R/L}(\tau)} = (2\pi T_{1,2} \tau_0)^{\lambda-1} \frac{\tau_0}{\Gamma(\lambda)} e^{E/2T_{1,2}} \left| \Gamma\left(\frac{\lambda}{2} + i\frac{E}{2\pi T_{1,2}}\right) \right|^2. \quad (\text{F.2})$$

1063 At zero temperature, this expression reduces to

$$P_{1,2}(E)|_{T_{1,2} \rightarrow 0} = \frac{2\pi\tau_0^\lambda}{\Gamma(\lambda)} E^{\lambda-1} \Theta(E), \quad (\text{F.3})$$

1064 where  $\Theta(E)$  is the Heaviside step function. Finally, by comparing to the quasiparticle Green's  
 1065 function (19), we have the Fourier transforms

$$\int_{-\infty}^{\infty} d\tau e^{iE\tau} G_{R/L}(\tau) = \frac{1}{2\pi a} P_{1,2}(E). \quad (\text{F.4})$$

## 1066 G Scattering theory for non-interacting electrons

1067 To describe the setup in Fig. 1 in the integer quantum Hall regime, here described by setting  
 1068  $\nu = 1$ , we can alternatively use scattering theory, closely following Ref. [20]. The scattering  
 1069 matrix describing the setup reads

$$s = \begin{pmatrix} 0 & 0 & 0 & 1 \\ 0 & 0 & 1 & 0 \\ t & -r & 0 & 0 \\ r & t & 0 & 0 \end{pmatrix}, \quad (\text{G.1})$$

1070 where the element  $s_{\alpha\beta}$  is the amplitude for electron scattering from terminal  $\beta$  to  $\alpha$ . In  
 1071 Eq. (G.1), we have introduced  $t$  and  $r$  (assumed to be energy independent) as the trans-  
 1072 mission and reflection amplitude, respectively, at the QPC. It holds that  $|t|^2 + |r|^2 \equiv T + R = 1$ .  
 1073 Note that the top right corner of  $s$  describes ballistic propagation (unit entries) from terminal  
 1074 4 to 1 and 3 to 2. These entries ensures the unitarity of  $s$  as well as fully capturing that the  
 1075 ballistic edge channels propagate along the boundary of a two-dimensional electron gas. *Note*  
 1076 *that this propagation was not included in Sec. (2)*. For consistency, we shall therefore neglect  
 1077 these terms in the following.

1078 With the scattering matrix (G.1), the net charge ( $\hat{X} = \hat{I}$ ) and heat ( $\hat{X} = \hat{J}$ ) current flowing  
 1079 out of terminal  $\alpha$  reads

$$\langle \hat{X}_{\alpha, \text{out}} \rangle = \frac{1}{h} \sum_{\beta=1}^4 \int_{-\infty}^{+\infty} dE x_\alpha (\delta_{\alpha\beta} - (s_{\alpha\beta})^2) f_\beta(E), \quad (\text{G.2})$$

1080 with  $x_\alpha = -e$  for  $\hat{X} = \hat{I}$ ,  $x_\alpha = E - \mu_\alpha$  for  $\hat{X} = \hat{J}$ , and  $f_\beta(E) = \{1 + \exp[(E - \mu_\beta)/k_B T_\beta]\}^{-1}$  is the  
 1081 Fermi function in reservoir  $\beta$ . Likewise, the zero-frequency correlations  $S_{\alpha\beta}^{XX}(\omega = 0) \equiv S_{\alpha\beta}^{XX}$   
 1082 between the  $X$  current in terminal  $\alpha$  and the  $X$  current in terminal  $\beta$  read

$$S_{\alpha\beta}^{XX} = \frac{2}{h} \sum_{\gamma, \delta=1}^4 \int_{-\infty}^{+\infty} dE x_\alpha x_\beta (\delta_{\alpha\gamma} \delta_{\alpha\delta} - s_{\alpha\gamma} s_{\alpha\delta}) (\delta_{\beta\delta} \delta_{\beta\gamma} - s_{\beta\delta} s_{\beta\gamma}) \\ \times [f_\gamma(E)(1 - f_\delta(E)) + f_\delta(E)(1 - f_\gamma(E))]. \quad (\text{G.3})$$

1083 If we further assume that there are no voltage biases in the setup, it is possible to set  $\mu_\alpha = \mu_0, \forall \alpha$   
 1084 and  $\mu_0 \equiv 0$  can be taken as energy reference. In such case,  $x_\alpha$  loses the dependence on the

1085 chemical potential  $\mu_\alpha$  and we can just write a single  $x = -e$  for  $\hat{X} = \hat{I}$  and  $x = E$  for  $\hat{X} = \hat{J}$ .  
 1086 Note that this simplification arises in our setup also for  $x_3$  and  $x_4$ , because terminal 3 and 4  
 1087 are kept at the reference energy.

1088 Of key interest in this section are the auto-correlation functions in the drain contacts, i.e.  
 1089  $\alpha, \beta = 3, 4$ . By using the scattering matrix (G.1) in the correlation function (G.3), we find

$$S_{33}^{XX} = \frac{2}{h} \int_{-\infty}^{+\infty} dEx^2 \left[ RT(f_1(E) - f_2(E))^2 + Tf_1(E)(1 - f_1(E)) + Rf_2(E)(1 - f_2(E)) \right], \quad (\text{G.4})$$

$$S_{44}^{XX} = \frac{2}{h} \int_{-\infty}^{+\infty} dEx^2 \left[ RT(f_1(E) - f_2(E))^2 + Rf_1(E)(1 - f_1(E)) + Tf_2(E)(1 - f_2(E)) \right], \quad (\text{G.5})$$

$$S_{34}^{XX} = S_{43}^{XX} = -\frac{2}{h} \int_{-\infty}^{+\infty} dEx^2 \left[ RT(f_1(E) - f_2(E))^2 \right]. \quad (\text{G.6})$$

1090 We see that the correlators (G.4), (G.5), and (G.6) satisfy the conservation laws (6).

1091 Next, we define the charge and heat tunneling currents as

$$\langle \hat{X}_T \rangle \equiv \langle \hat{X}_{1,\text{out}} \rangle - \langle \hat{X}_{3,\text{in}} \rangle. \quad (\text{G.7})$$

1092 Inserting this expression into the noise definition (1) leads to the tunneling noise

$$S_{TT}^{XX} = S_{11}^{XX} + S_{33}^{XX} + 2S_{31}^{XX}, \quad (\text{G.8})$$

1093 which, via Eq. (G.3), we evaluate as

$$S_{TT}^{XX} = \frac{2}{h} \int_{-\infty}^{+\infty} dEx^2 \left[ RT(f_1(E) - f_2(E))^2 + Rf_1(E)(1 - f_1(E)) + Rf_2(E)(1 - f_2(E)) \right]. \quad (\text{G.9})$$

1094 Here, we note that the tunneling charge-current noise in the four-terminal setup we are investi-  
 1095 gating coincides with the total (thermal and shot) noise in a two-terminal setup with reservoirs  
 1096 described by Fermi functions  $f_1$  and  $f_2$  [20, 24]. Similarly, the cross correlation noise  $S_{34}^{II}$  coin-  
 1097 cides with the shot noise component (up to a sign) in the said two-terminal setup [34]. Now,  
 1098 since we assume energy independent tunneling, we can compare Eqs. (G.6) and (G.8) to relate  
 1099  $S_{34}^{XX}$  and  $S_{TT}^{XX}$  as

$$S_{TT}^{XX} = -S_{34}^{XX} + R(S_{11}^{XX} + S_{22}^{XX}). \quad (\text{G.10})$$

1100 As follows, we are interested in the weak tunneling limit. We thus assume that  $R = 1 - T \ll 1$ ,  
 1101 which we employ as taking

$$R \rightarrow D, \quad RT \rightarrow D, \quad T \rightarrow 1 \quad (\text{G.11})$$

1102 for  $D \ll 1$ , in the following subsections.

### 1103 G.1 Delta-T noise

1104 For the delta-T noise, we have  $\hat{X} = \hat{I}$  and  $x = -e$ . By inserting these specifications, to-  
 1105 gether with the weak tunneling expressions (G.11), into the tunneling noise (G.9), we set  
 1106  $\mu_1 = \mu_2 = 0$ ,  $T_{1/2} = \bar{T} \pm \Delta T/2$ , and then expand in powers of  $\Delta T/(2\bar{T})$ . We then obtain

$$S_{TT}^{II} = S_0^{II} \times \left[ 1 + \frac{\pi^2 - 6}{9} \left( \frac{\Delta T}{2\bar{T}} \right)^2 + \left( -\frac{7\pi^4}{675} + \frac{\pi^2}{9} - \frac{2}{15} \right) \left( \frac{\Delta T}{2\bar{T}} \right)^4 + \dots \right]. \quad (\text{G.12})$$

1107 Here,  $S_0^{II} = 4e^2 D k_B \bar{T} / h \equiv 4g_T(\bar{T}) k_B \bar{T}$ . Note here that  $g_T(\bar{T})$  is independent of  $\bar{T}$ . We thus  
 1108 obtain the expansion coefficients  $\mathcal{C}^{(2)}$  and  $\mathcal{C}^{(4)}$  as presented in Eqs. (31a)-(31b).

1109 We repeat the above procedure for the cross correlation noise (G.6) and find

$$S_{34}^{II} = S_{43}^{II} = -S_0^{II} \times \left[ \frac{\pi^2 - 6}{9} \left( \frac{\Delta T}{2\bar{T}} \right)^2 + \left( -\frac{7\pi^4}{675} + \frac{\pi^2}{9} - \frac{2}{15} \right) \left( \frac{\Delta T}{2\bar{T}} \right)^4 + \dots \right] \quad (\text{G.13})$$

1110 Upon identification of  $\mathcal{C}^{(2)}$  and  $\mathcal{C}^{(4)}$ , we readily see that the coefficients  $\mathcal{D}^{(2)}$  and  $\mathcal{D}^{(4)}$  [see  
 1111 Eqs. (30a)-(30b)] both vanish at  $\nu = 1$ . This result is clear also from a direct compari-  
 1112 son between the noises (G.6) and (G.9). In essence, absence of  $\mathcal{D}^{(2)}$  and  $\mathcal{D}^{(4)}$  follows be-  
 1113 cause in contrast to strongly correlated electrons, the tunneling conductance for free electrons,  
 1114  $g_T(\bar{T}) = e^2 D / h$ , does not depend on the temperature  $\bar{T}$ .

1115 In the large temperature bias limit,  $T_1 = T_{\text{hot}}$  and  $T_2 \rightarrow 0$ , the integrals (G.9) and (G.6)  
 1116 evaluate to

$$S_{TT}^{II} = \frac{4e^2 D}{h} k_B T_{\text{hot}} \ln 2, \quad (\text{G.14})$$

$$S_{34}^{II} = S_{43}^{II} = -\frac{2e^2 D}{h} k_B T_{\text{hot}} (2 \ln 2 - 1), \quad (\text{G.15})$$

1117 which we obtained in Sec. 3.3 by setting  $\lambda = \nu = 1$ .

## 1118 G.2 Heat-current noise

1119 For the heat-current noise, we have  $\hat{X} = \hat{J}$  and  $x = E$ . Just as for the delta- $T$  noise, we use  
 1120 these specifications, set  $\mu_1 = \mu_2 = 0$ , assume weak tunneling (G.11), and expand in  $\Delta T / (2\bar{T})$   
 1121 the tunneling noise (G.9) and the cross correlation noise (G.6). We then obtain

$$S_{TT}^{JJ} = S_0^{JJ} \left[ 1 + \frac{1}{15} (7\pi^2 - 15) \left( \frac{\Delta T}{2\bar{T}} \right)^2 + 2\pi^2 \left( \frac{7}{15} - \frac{31}{630} \pi^2 \right) \left( \frac{\Delta T}{2\bar{T}} \right)^4 + \dots \right], \quad (\text{G.16})$$

$$S_{34}^{JJ} = S_{43}^{JJ} = S_0^{JJ} \left[ \frac{1}{15} (60 - 7\pi^2) \left( \frac{\Delta T}{2\bar{T}} \right)^2 + 2\pi^2 \left( -\frac{7}{15} + \frac{31}{630} \pi^2 \right) \left( \frac{\Delta T}{2\bar{T}} \right)^4 + \dots \right]. \quad (\text{G.17})$$

1122 Here, we have identified the equilibrium heat tunneling conductance

$$S_0^{JJ} = \frac{2\pi^2}{3h} D k_B^3 \bar{T}^3. \quad (\text{G.18})$$

1123 By comparing  $S_{TT}^{JJ}$  and  $S_{34}^{JJ}$  term by term, we see that our scattering theory is in full agreement  
 1124 with the expansion coefficients (47a)-(47d).

1125 Let us here briefly comment why we have  $\mathcal{D}_Q^{(2)} = 3$  for the heat-current noise, in contrast  
 1126 to the delta- $T$  noise where  $\mathcal{D}^{(2)} = 0$ . If we compare the cross-correlation noise (G.6) to the  
 1127 tunneling noise (G.9), we see that they differ both by a negative sign and that the tunneling  
 1128 noise contains two contributions present even in equilibrium. For the charge-current noise,  
 1129 these parts contribute only to  $S_0^{II}$ . However for the heat-current noise, these contributions,  
 1130 when expanded in  $\Delta T / (2\bar{T})$ , produce

$$\begin{aligned} D(S_{11}^{JJ} + S_{22}^{JJ}) &= \frac{D}{h} \int_{-\infty}^{+\infty} dE E^2 [f_1(E)(1 - f_1(E)) + f_2(E)(1 - f_2(E))] = \frac{2\pi^2}{3h} D k_B^3 (T_1^3 + T_2^3) \\ &= \frac{2\pi^2}{3h} D k_B^3 \bar{T}^3 \left[ 1 + 3 \left( \frac{\Delta T}{2\bar{T}} \right)^2 \right]. \end{aligned} \quad (\text{G.19})$$

1131 We thus see that while the zero-frequency charge-current noise is linear in the temperature  
 1132  $S^{II} \sim k_B \bar{T}$ , the heat-current noise is instead cubic:  $S^{JJ} \sim (k_B \bar{T})^3$ . The reason for this is that  
 1133 for heat flow, the transported quantity depends on the energy (an  $E^2$  weight to the Fermi  
 1134 functions) but for the charge flow, the charge  $e$  does not depend on the energy. From the  
 1135 result (G.19), we thus see that already the lowest order term in (G.9) contributes a factor of  
 1136 3 to the  $\mathcal{C}^{(2)}$  coefficient. We see that this contribution is absent in the cross-correlation noise  
 1137 and is thus accounted for by the finite  $\mathcal{D}_Q^{(2)}$  coefficient.

1138 Finally, we compute the heat-current noise in the large temperature bias limit. We thus  
 1139 take  $T_1 = T_{\text{hot}}$  and  $T_2 \rightarrow 0$ , and the integrals (G.9) and (G.6) for the heat-current noise then  
 1140 evaluate to

$$S_{TT}^{JJ} = \frac{3D}{h} (k_B T_{\text{hot}})^3 \zeta(3), \quad (\text{G.20})$$

$$S_{34}^{JJ} = S_{43}^{JJ} = -\frac{3D}{h} (k_B T_{\text{hot}})^3 \left( \zeta(3) - \frac{\pi^2}{3} \right), \quad (\text{G.21})$$

1141 where  $\zeta(z)$  is the Riemann zeta-function with  $\zeta(3) \approx 1.2$ . These results were also obtained in  
 1142 the  $\nu = 1$  limit in Sec. 4.2.

## 1143 References

- 1144 [1] J. P. Pekola and B. Karimi, *Colloquium: Quantum heat transport in condensed matter*  
 1145 *systems*, Rev. Mod. Phys. **93**, 041001 (2021), doi:[10.1103/RevModPhys.93.041001](https://doi.org/10.1103/RevModPhys.93.041001).
- 1146 [2] K. von Klitzing, G. Dorda and M. Pepper, *New method for high-accuracy determination*  
 1147 *of the fine-structure constant based on quantized Hall resistance*, Phys. Rev. Lett. **45**, 494  
 1148 (1980), doi:[10.1103/PhysRevLett.45.494](https://doi.org/10.1103/PhysRevLett.45.494).
- 1149 [3] D. C. Tsui, H. L. Stormer and A. C. Gossard, *Two-dimensional magneto-*  
 1150 *transport in the extreme quantum limit*, Phys. Rev. Lett. **48**, 1559 (1982),  
 1151 doi:[10.1103/PhysRevLett.48.1559](https://doi.org/10.1103/PhysRevLett.48.1559).
- 1152 [4] S. Jezouin, F. D. Parmentier, A. Anthore, U. Gennser, A. Cavanna, Y. Jin and F. Pierre,  
 1153 *Quantum limit of heat flow across a single electronic channel*, Science **342**(6158), 601  
 1154 (2013), doi:[10.1126/science.1241912](https://doi.org/10.1126/science.1241912).
- 1155 [5] M. Banerjee, M. Heiblum, A. Rosenblatt, Y. Oreg, D. E. Feldman, A. Stern and  
 1156 V. Umansky, *Observed quantization of anyonic heat flow*, Nature **545**, 75 (2017),  
 1157 doi:[10.1038/nature22052](https://doi.org/10.1038/nature22052).
- 1158 [6] S. K. Srivastav, M. R. Sahu, K. Watanabe, T. Taniguchi, S. Banerjee and A. Das, *Uni-*  
 1159 *versal quantized thermal conductance in graphene*, Sci. Adv. **5**(7), eaaw5798 (2019),  
 1160 doi:[10.1126/sciadv.aaw5798](https://doi.org/10.1126/sciadv.aaw5798).
- 1161 [7] R. A. Melcer, B. Dutta, C. Spånslätt, J. Park, A. D. Mirlin and V. Umansky, *Absent thermal*  
 1162 *equilibration on fractional quantum Hall edges over macroscopic scale*, Nat. Commun.  
 1163 **13**(376), 1 (2022), doi:[10.1038/s41467-022-28009-0](https://doi.org/10.1038/s41467-022-28009-0).
- 1164 [8] S. K. Srivastav, R. Kumar, C. Spånslätt, K. Watanabe, T. Taniguchi, A. D. Mir-  
 1165 lin, Y. Gefen and A. Das, *Vanishing thermal equilibration for hole-conjugate frac-*  
 1166 *tional quantum Hall states in graphene*, Phys. Rev. Lett. **126**(21), 216803 (2021),  
 1167 doi:[10.1103/PhysRevLett.126.216803](https://doi.org/10.1103/PhysRevLett.126.216803).

- 1168 [9] S. K. Srivastav, R. Kumar, C. Spånslätt, K. Watanabe, T. Taniguchi, A. D. Mirlin, Y. Gefen  
1169 and A. Das, *Determination of topological edge quantum numbers of fractional quantum*  
1170 *Hall phases by thermal conductance measurements*, Nat. Commun. **13**(5185), 1 (2022),  
1171 doi:[10.1038/s41467-022-32956-z](https://doi.org/10.1038/s41467-022-32956-z).
- 1172 [10] G. Le Breton, R. Delagrangé, Y. Hong, M. Garg, K. Watanabe, T. Taniguchi, R. Ribeiro-  
1173 Palau, P. Roulleau, P. Roche and F. D. Parmentier, *Heat Equilibration of Integer and*  
1174 *Fractional Quantum Hall Edge Modes in Graphene*, Phys. Rev. Lett. **129**(11), 116803  
1175 (2022), doi:[10.1103/PhysRevLett.129.116803](https://doi.org/10.1103/PhysRevLett.129.116803).
- 1176 [11] M. Banerjee, M. Heiblum, V. Umansky, D. E. Feldman, Y. Oreg and A. Stern, *Ob-*  
1177 *servation of half-integer thermal Hall conductance*, Nature **559**(7713), 205 (2018),  
1178 doi:[10.1038/s41586-018-0184-1](https://doi.org/10.1038/s41586-018-0184-1).
- 1179 [12] B. Dutta, W. Yang, R. Melcer, H. K. Kundu, M. Heiblum, V. Umansky, Y. Oreg, A. Stern  
1180 and D. Mross, *Distinguishing between non-Abelian topological orders in a quantum Hall*  
1181 *system*, Science **375**(6577), 193 (2022), doi:[10.1126/science.abg6116](https://doi.org/10.1126/science.abg6116).
- 1182 [13] S. Manna, A. Das, M. Goldstein and Y. Gefen, *Full Classification of Transport on*  
1183 *an Equilibrated 5/2 Edge via Shot Noise*, Phys. Rev. Lett. **132**(13), 136502 (2024),  
1184 doi:[10.1103/PhysRevLett.132.136502](https://doi.org/10.1103/PhysRevLett.132.136502).
- 1185 [14] S. Manna, A. Das and M. Goldstein, *Shot noise classification of different conduc-*  
1186 *tance plateaus in a quantum point contact at the  $\nu = 2/3$  edge*, arXiv (2023),  
1187 doi:[10.48550/arXiv.2307.05175](https://doi.org/10.48550/arXiv.2307.05175), [2307.05175](https://arxiv.org/abs/2307.05175).
- 1188 [15] S. Manna, A. Das, Y. Gefen and M. Goldstein, *Diagnostics of Anoma-*  
1189 *lous Conductance Plateaus in Abelian Quantum Hall Regime*, arXiv (2023),  
1190 doi:[10.48550/arXiv.2307.05173](https://doi.org/10.48550/arXiv.2307.05173), [2307.05173](https://arxiv.org/abs/2307.05173).
- 1191 [16] J. Nakamura, S. Liang, G. C. Gardner and M. J. Manfra, *Half-Integer Conductance Plateau*  
1192 *at the  $\nu = 2/3$  Fractional Quantum Hall State in a Quantum Point Contact*, Phys. Rev.  
1193 Lett. **130**(7), 076205 (2023), doi:[10.1103/PhysRevLett.130.076205](https://doi.org/10.1103/PhysRevLett.130.076205).
- 1194 [17] M. Hashisaka, T. Ito, T. Akiho, S. Sasaki, N. Kumada, N. Shibata and K. Muraki,  
1195 *Coherent-Incoherent Crossover of Charge and Neutral Mode Transport as Evidence for*  
1196 *the Disorder-Dominated Fractional Edge Phase*, Phys. Rev. X **13**(3), 031024 (2023),  
1197 doi:[10.1103/PhysRevX.13.031024](https://doi.org/10.1103/PhysRevX.13.031024).
- 1198 [18] D. C. Glatli, C. Boudet, A. De and P. Roulleau, *A Toy Model for the 2/3 Fractional*  
1199 *Quantum Hall edge channel*, arXiv (2024), doi:[10.48550/arXiv.2407.07208](https://doi.org/10.48550/arXiv.2407.07208), [2407.](https://arxiv.org/abs/2407.07208)  
1200 [07208](https://arxiv.org/abs/2407.07208).
- 1201 [19] X. G. Wen, *Topological orders in rigid states*, Int. J. Mod. Phys. B **04**(02), 239 (1990),  
1202 doi:[10.1142/S0217979290000139](https://doi.org/10.1142/S0217979290000139).
- 1203 [20] Y. Blanter and M. Büttiker, *Shot noise in mesoscopic conductors*, Physics Reports **336**(1),  
1204 1 (2000), doi:[https://doi.org/10.1016/S0370-1573\(99\)00123-4](https://doi.org/10.1016/S0370-1573(99)00123-4).
- 1205 [21] T. Martin, *Noise in mesoscopic physics*, In H. Bouchiat, Y. Gefen, S. Guéron, G. Montam-  
1206 baux and J. Dalibard, eds., *Nanophysics: Coherence and Transport*, vol. 81 of *Les Houches*,  
1207 pp. 283–359. Elsevier, Waltham, MA, USA, doi:[10.1016/S0924-8099\(05\)80047-2](https://doi.org/10.1016/S0924-8099(05)80047-2)  
1208 (2005).

- 1209 [22] K. Kobayashi and M. Hashisaka, *Shot noise in mesoscopic systems: From sin-*  
1210 *gle particles to quantum liquids*, J. Phys. Soc. Jpn. **90**(10), 102001 (2021),  
1211 doi:[10.7566/JPSJ.90.102001](https://doi.org/10.7566/JPSJ.90.102001).
- 1212 [23] E. V. Sukhorukov and D. Loss, *Noise in multiterminal diffusive conductors: Uni-*  
1213 *versality, nonlocality, and exchange effects*, Phys. Rev. B **59**, 13054 (1999),  
1214 doi:[10.1103/PhysRevB.59.13054](https://doi.org/10.1103/PhysRevB.59.13054).
- 1215 [24] O. S. Lumbroso, L. Simine, A. Nitzan, D. Segal and O. Tal, *Electronic noise due*  
1216 *to temperature differences in atomic-scale junctions*, Nature **562**(7726), 240 (2018),  
1217 doi:[10.1038/s41586-018-0592-2](https://doi.org/10.1038/s41586-018-0592-2).
- 1218 [25] E. S. Tikhonov, D. V. Shovkun, D. Ercolani, F. Rossella, M. Rocci, L. Sorba, S. Roddaro  
1219 and V. S. Khrapai, *Local noise in a diffusive conductor*, Scientific Reports **6**(1), 30621  
1220 (2016), doi:[10.1038/srep30621](https://doi.org/10.1038/srep30621).
- 1221 [26] A. Mu and D. Segal, *Anomalous electronic shot noise in resonant tunneling junctions*,  
1222 arXiv (2019), doi:[10.48550/arXiv.1902.06312](https://doi.org/10.48550/arXiv.1902.06312), [1902.06312](https://arxiv.org/abs/1902.06312).
- 1223 [27] E. Sivre, H. Duprez, A. Anthore, A. Aassime, F. D. Parmentier, A. Cavanna, A. Ouerghi,  
1224 U. Gennser and F. Pierre, *Electronic heat flow and thermal shot noise in quantum circuits*,  
1225 Nature Communications **10**(1), 5638 (2019), doi:[10.1038/s41467-019-13566-8](https://doi.org/10.1038/s41467-019-13566-8).
- 1226 [28] E. S. Tikhonov, A. O. Denisov, S. U. Piatrusha, I. N. Khrapach, J. P. Pekola, B. Karimi,  
1227 R. N. Jabdaraghi and V. S. Khrapai, *Spatial and energy resolution of electronic states by*  
1228 *shot noise*, Phys. Rev. B **102**, 085417 (2020), doi:[10.1103/PhysRevB.102.085417](https://doi.org/10.1103/PhysRevB.102.085417).
- 1229 [29] S. Larocque, E. Pinsolle, C. Lupien and B. Reulet, *Shot noise of a*  
1230 *temperature-biased tunnel junction*, Phys. Rev. Lett. **125**, 106801 (2020),  
1231 doi:[10.1103/PhysRevLett.125.106801](https://doi.org/10.1103/PhysRevLett.125.106801).
- 1232 [30] E. Zhitlukhina, M. Belogolovskii and P. Seidel, *Electronic noise generated by a tem-*  
1233 *perature gradient across a hybrid normal metal–superconductor nanojunction*, Applied  
1234 Nanoscience **10**(12), 5121 (2020), doi:[10.1007/s13204-020-01329-7](https://doi.org/10.1007/s13204-020-01329-7).
- 1235 [31] A. Rosenblatt, S. Konyzheva, F. Lafont, N. Schiller, J. Park, K. Snizhko, M. Heiblum,  
1236 Y. Oreg and V. Umansky, *Energy relaxation in edge modes in the quantum Hall effect*,  
1237 Phys. Rev. Lett. **125**, 256803 (2020), doi:[10.1103/PhysRevLett.125.256803](https://doi.org/10.1103/PhysRevLett.125.256803).
- 1238 [32] J. Rech, T. Jonckheere, B. Grémaud and T. Martin, *Negative Delta-T Noise*  
1239 *in the Fractional Quantum Hall Effect*, Phys. Rev. Lett. **125**, 086801 (2020),  
1240 doi:[10.1103/PhysRevLett.125.086801](https://doi.org/10.1103/PhysRevLett.125.086801).
- 1241 [33] M. Hasegawa and K. Saito, *Delta-T noise in the Kondo regime*, Phys. Rev. B **103**, 045409  
1242 (2021), doi:[10.1103/PhysRevB.103.045409](https://doi.org/10.1103/PhysRevB.103.045409).
- 1243 [34] J. Eriksson, M. Acciai, L. Tesser and J. Splettstoesser, *General Bounds on Electronic*  
1244 *Shot Noise in the Absence of Currents*, Phys. Rev. Lett. **127**(13), 136801 (2021),  
1245 doi:[10.1103/PhysRevLett.127.136801](https://doi.org/10.1103/PhysRevLett.127.136801).
- 1246 [35] H. Duprez, F. Pierre, E. Sivre, A. Aassime, F. D. Parmentier, A. Cavanna,  
1247 A. Ouerghi, U. Gennser, I. Safi, C. Mora and A. Anthore, *Dynamical Coulomb*  
1248 *blockade under a temperature bias*, Phys. Rev. Research **3**, 023122 (2021),  
1249 doi:[10.1103/PhysRevResearch.3.023122](https://doi.org/10.1103/PhysRevResearch.3.023122).

- 1250 [36] A. Popoff, J. Rech, T. Jonckheere, L. Raymond, B. Grémaud, S. Malherbe and T. Mar-  
1251 tin, *Scattering theory of non-equilibrium noise and delta T current fluctuations through*  
1252 *a quantum dot*, Journal of Physics: Condensed Matter **34**(18), 185301 (2022),  
1253 doi:[10.1088/1361-648x/ac5200](https://doi.org/10.1088/1361-648x/ac5200).
- 1254 [37] N. Schiller, Y. Oreg and K. Snizhko, *Extracting the scaling dimension of quantum*  
1255 *Hall quasiparticles from current correlations*, Phys. Rev. B **105**, 165150 (2022),  
1256 doi:[10.1103/PhysRevB.105.165150](https://doi.org/10.1103/PhysRevB.105.165150).
- 1257 [38] G. Zhang, I. V. Gornyi and C. Spånslätt, *Delta-T noise for weak tunneling in one-*  
1258 *dimensional systems: Interactions versus quantum statistics*, Phys. Rev. B **105**, 195423  
1259 (2022), doi:[10.1103/PhysRevB.105.195423](https://doi.org/10.1103/PhysRevB.105.195423).
- 1260 [39] R. A. Melcer, B. Dutta, C. Spånslätt, J. Park, A. D. Mirlin and V. Umansky, *Absent thermal*  
1261 *equilibration on fractional quantum Hall edges over macroscopic scale*, Nature Commu-  
1262 nications **13**(1), 376 (2022), doi:[10.1038/s41467-022-28009-0](https://doi.org/10.1038/s41467-022-28009-0).
- 1263 [40] G. Rebora, J. Rech, D. Ferraro, T. Jonckheere, T. Martin and M. Sassetti, *Delta-T noise*  
1264 *for fractional quantum Hall states at different filling factor*, Phys. Rev. Res. **4**(4), 043191  
1265 (2022), doi:[10.1103/PhysRevResearch.4.043191](https://doi.org/10.1103/PhysRevResearch.4.043191).
- 1266 [41] M. Hein and C. Spånslätt, *Thermal conductance and noise of majorana modes along*  
1267 *interfaced  $\nu = \frac{5}{2}$  fractional quantum Hall states*, Phys. Rev. B **107**(24), 245301 (2023),  
1268 doi:[10.1103/PhysRevB.107.245301](https://doi.org/10.1103/PhysRevB.107.245301).
- 1269 [42] M. Hübner and W. Belzig, *Light emission in delta-T-driven mesoscopic conductors*, Phys.  
1270 Rev. B **107**(15), 155405 (2023), doi:[10.1103/PhysRevB.107.155405](https://doi.org/10.1103/PhysRevB.107.155405).
- 1271 [43] K. Iyer, J. Rech, T. Jonckheere, L. Raymond, B. Grémaud and T. Martin, *Colored delta-*  
1272 *T noise in fractional quantum Hall liquids*, Phys. Rev. B **108**(24), 245427 (2023),  
1273 doi:[10.1103/PhysRevB.108.245427](https://doi.org/10.1103/PhysRevB.108.245427).
- 1274 [44] T. Mohapatra and C. Benjamin, *Spin-flip scattering engendered negative  $\Delta_T$  noise*, arXiv  
1275 (2023), doi:[10.48550/arXiv.2307.14072](https://doi.org/10.48550/arXiv.2307.14072), [2307.14072](https://arxiv.org/abs/2307.14072).
- 1276 [45] A. Crépieux, T. Q. Duong and M. Lavagna, *Fano factor,  $\delta t$ -noise and cross-correlations*  
1277 *in double quantum dots*, arXiv (2023), doi:[10.48550/arXiv.2306.02146](https://doi.org/10.48550/arXiv.2306.02146), [2306.02146](https://arxiv.org/abs/2306.02146).
- 1278 [46] I. V. Krive, E. N. Bogachek, A. G. Scherbakov and U. Landman, *Heat cur-*  
1279 *rent fluctuations in quantum wires*, Phys. Rev. B **64**(23), 233304 (2001),  
1280 doi:[10.1103/PhysRevB.64.233304](https://doi.org/10.1103/PhysRevB.64.233304).
- 1281 [47] D. Sergi, *Energy transport and fluctuations in small conductors*, Phys. Rev. B **83**(3),  
1282 033401 (2011), doi:[10.1103/PhysRevB.83.033401](https://doi.org/10.1103/PhysRevB.83.033401).
- 1283 [48] D. V. Averin and J. P. Pekola, *Violation of the fluctuation-dissipation theorem in*  
1284 *time-dependent mesoscopic heat transport*, Phys. Rev. Lett. **104**(22), 220601 (2010),  
1285 doi:[10.1103/PhysRevLett.104.220601](https://doi.org/10.1103/PhysRevLett.104.220601).
- 1286 [49] F. Battista, F. Haupt and J. Splettstoesser, *Energy and power fluctuations*  
1287 *in ac-driven coherent conductors*, Phys. Rev. B **90**(8), 085418 (2014),  
1288 doi:[10.1103/PhysRevB.90.085418](https://doi.org/10.1103/PhysRevB.90.085418).
- 1289 [50] L. Vannucci, F. Ronetti, J. Rech, D. Ferraro, T. Jonckheere, T. Martin and M. Sassetti,  
1290 *Minimal excitation states for heat transport in driven quantum Hall systems*, Phys. Rev. B  
1291 **95**(24), 245415 (2017), doi:[10.1103/PhysRevB.95.245415](https://doi.org/10.1103/PhysRevB.95.245415).

- 1292 [51] N. Dashti, M. Misiorny, P. Samuelsson and J. Splettstoesser, *Probing charge- and heat-*  
1293 *current noise by frequency-dependent fluctuations in temperature and potential*, Phys.  
1294 Rev. Appl. **10**(2), 024007 (2018), doi:[10.1103/PhysRevApplied.10.024007](https://doi.org/10.1103/PhysRevApplied.10.024007).
- 1295 [52] F. Ronetti, M. Acciai, D. Ferraro, J. Rech, T. Jonckheere, T. Martin and M. Sassetti,  
1296 *Symmetry Properties of Mixed and Heat Photo-Assisted Noise in the Quantum Hall Regime*,  
1297 Entropy **21**(8), 730 (2019), doi:[10.3390/e21080730](https://doi.org/10.3390/e21080730).
- 1298 [53] F. Ronetti, L. Vannucci, D. Ferraro, T. Jonckheere, J. Rech, T. Martin and M. Sassetti,  
1299 *Hong-Ou-Mandel heat noise in the quantum Hall regime*, Phys. Rev. B **99**(20), 205406  
1300 (2019), doi:[10.1103/PhysRevB.99.205406](https://doi.org/10.1103/PhysRevB.99.205406).
- 1301 [54] A. Crépieux, *Electronic heat current fluctuations in a quantum dot*, Phys. Rev. B **103**(4),  
1302 045427 (2021), doi:[10.1103/PhysRevB.103.045427](https://doi.org/10.1103/PhysRevB.103.045427).
- 1303 [55] H. Ebisu, N. Schiller and Y. Oreg, *Fluctuations in Heat Current and Scaling Dimension*,  
1304 Phys. Rev. Lett. **128**(21), 215901 (2022), doi:[10.1103/PhysRevLett.128.215901](https://doi.org/10.1103/PhysRevLett.128.215901).
- 1305 [56] E. G. Idrisov, I. P. Levkivskiy and E. V. Sukhorukov, *Thermal drag effect in quantum Hall*  
1306 *circuits*, Phys. Rev. B **106**(12), L121405 (2022), doi:[10.1103/PhysRevB.106.L121405](https://doi.org/10.1103/PhysRevB.106.L121405).
- 1307 [57] C. Spånslätt, F. Stäbler, E. V. Sukhorukov and J. Splettstoesser, *Impact of po-*  
1308 *tential and temperature fluctuations on charge and heat transport in quantum Hall*  
1309 *edges in the heat Coulomb blockade regime*, Phys. Rev. B **110**(7), 075431 (2024),  
1310 doi:[10.1103/PhysRevB.110.075431](https://doi.org/10.1103/PhysRevB.110.075431).
- 1311 [58] A. Crépieux and F. Michelini, *Mixed, charge and heat noises in thermoelectric nanosys-*  
1312 *tems*, J. Phys.: Condens. Matter **27**(1), 015302 (2014), doi:[10.1088/0953-](https://doi.org/10.1088/0953-8984/27/1/015302)  
1313 [8984/27/1/015302](https://doi.org/10.1088/0953-8984/27/1/015302).
- 1314 [59] P. Eyméoud and A. Crépieux, *Mixed electrical-heat noise spectrum in a quantum dot*,  
1315 Phys. Rev. B **94**(20), 205416 (2016), doi:[10.1103/PhysRevB.94.205416](https://doi.org/10.1103/PhysRevB.94.205416).
- 1316 [60] P. Francesco, P. Mathieu and D. Sénéchal, *Conformal Field Theory*, Springer, New York,  
1317 NY, USA, ISBN 978-1-4612-2256-9, doi:[10.1007/978-1-4612-2256-9](https://doi.org/10.1007/978-1-4612-2256-9) (1997).
- 1318 [61] J. Nakamura, S. Liang, G. C. Gardner and M. J. Manfra, *Direct observation of anyonic*  
1319 *braiding statistics*, Nat. Phys. **16**, 931 (2020), doi:[10.1038/s41567-020-1019-1](https://doi.org/10.1038/s41567-020-1019-1).
- 1320 [62] H. Bartolomei, M. Kumar, R. Bisognin, A. Marguerite, J.-M. Berroir, E. Bocquillon,  
1321 B. Plaçais, A. Cavanna, Q. Dong, U. Gennser, Y. Jin and G. Fève, *Fractional statistics*  
1322 *in anyon collisions*, Science **368**(6487), 173 (2020), doi:[10.1126/science.aaz5601](https://doi.org/10.1126/science.aaz5601).
- 1323 [63] A. Veillon, C. Piquard, P. Glidic, Y. Sato, A. Aassime, A. Cavanna, Y. Jin, U. Gennser,  
1324 A. Anthore and F. Pierre, *Observation of the scaling dimension of fractional quantum Hall*  
1325 *anyons*, Nature (2024), doi:[10.1038/s41586-024-07727-z](https://doi.org/10.1038/s41586-024-07727-z).
- 1326 [64] N. Schiller, T. Alkalay, C. Hong, V. Umansky, M. Heiblum, Y. Oreg and K. Snizhko, *Scaling*  
1327 *tunnelling noise in the fractional quantum Hall effect tells about renormalization and*  
1328 *breakdown of chiral Luttinger liquid*, arXiv (2024), doi:[10.48550/arXiv.2403.17097](https://doi.org/10.48550/arXiv.2403.17097),  
1329 [2403.17097](https://doi.org/10.48550/arXiv.2403.17097).
- 1330 [65] A. M. Chang, *Chiral Luttinger liquids at the fractional quantum Hall edge*, Rev. Mod.  
1331 Phys. **75**, 1449 (2003), doi:[10.1103/RevModPhys.75.1449](https://doi.org/10.1103/RevModPhys.75.1449).



- 1332 [66] L. A. Cohen, N. L. Samuelson, T. Wang, T. Taniguchi, K. Watanabe, M. P. Zaletel and A. F.  
1333 Young, *Universal chiral Luttinger liquid behavior in a graphene fractional quantum Hall*  
1334 *point contact*, Science **382**(6670), 542 (2023), doi:[10.1126/science.adf9728](https://doi.org/10.1126/science.adf9728).
- 1335 [67] C. L. Kane and M. P. A. Fisher, *Nonequilibrium noise and fractional charge in the quantum*  
1336 *hall effect*, Phys. Rev. Lett. **72**, 724 (1994), doi:[10.1103/PhysRevLett.72.724](https://doi.org/10.1103/PhysRevLett.72.724).
- 1337 [68] L. Saminadayar, D. C. Glattli, Y. Jin and B. Etienne, *Observation of the  $e/3$*   
1338 *fractionally charged Laughlin quasiparticle*, Phys. Rev. Lett. **79**, 2526 (1997),  
1339 doi:[10.1103/PhysRevLett.79.2526](https://doi.org/10.1103/PhysRevLett.79.2526).
- 1340 [69] R. de Picciotto, M. Reznikov, M. Heiblum, V. Umansky, G. Bunin and D. Mahalu, *Direct*  
1341 *observation of a fractional charge*, Nature **389**(6647), 162 (1997), doi:[10.1038/38241](https://doi.org/10.1038/38241).
- 1342 [70] C. L. Kane, M. P. A. Fisher and J. Polchinski, *Randomness at the edge: Theory of*  
1343 *quantum Hall transport at filling  $\nu = 2/3$* , Phys. Rev. Lett. **72**(26), 4129 (1994),  
1344 doi:[10.1103/PhysRevLett.72.4129](https://doi.org/10.1103/PhysRevLett.72.4129).
- 1345 [71] D. Ferraro, A. Braggio, M. Merlo, N. Magnoli and M. Sasseti, *Relevance of multiple*  
1346 *quasiparticle tunneling between edge states at  $\nu = p/(2np + 1)$* , Phys. Rev. Lett. **101**,  
1347 166805 (2008), doi:[10.1103/PhysRevLett.101.166805](https://doi.org/10.1103/PhysRevLett.101.166805).
- 1348 [72] A. Bid, N. Ofek, H. Inoue, M. Heiblum, C. L. Kane, V. Umansky and D. Mahalu, *Observation*  
1349 *of neutral modes in the fractional quantum Hall regime*, Nature **466**, 585 (2010),  
1350 doi:[10.1038/nature09277](https://doi.org/10.1038/nature09277).
- 1351 [73] R. Kumar, S. K. Srivastav, C. Spånslätt, K. Watanabe, T. Taniguchi, Y. Gefen, A. D. Mirlin  
1352 and A. Das, *Observation of ballistic upstream modes at fractional quantum Hall edges of*  
1353 *graphene*, Nat. Commun. **13**(213), 1 (2022), doi:[10.1038/s41467-021-27805-4](https://doi.org/10.1038/s41467-021-27805-4).
- 1354 [74] D. Sen and A. Agarwal, *Line junction in a quantum Hall system with two filling fractions*,  
1355 Phys. Rev. B **78**(8), 085430 (2008), doi:[10.1103/PhysRevB.78.085430](https://doi.org/10.1103/PhysRevB.78.085430).
- 1356 [75] I. Protopopov, Y. Gefen and A. Mirlin, *Transport in a disordered  $\nu = 2/3$*   
1357 *fractional quantum Hall junction*, Annals of Physics **385**, 287 (2017),  
1358 doi:<https://doi.org/10.1016/j.aop.2017.07.015>.
- 1359 [76] C. Spånslätt, J. Park, Y. Gefen and A. D. Mirlin, *Topological classification of shot*  
1360 *noise on fractional quantum Hall edges*, Phys. Rev. Lett. **123**, 137701 (2019),  
1361 doi:[10.1103/PhysRevLett.123.137701](https://doi.org/10.1103/PhysRevLett.123.137701).
- 1362 [77] C. Spånslätt, J. Park, Y. Gefen and A. D. Mirlin, *Conductance plateaus and shot*  
1363 *noise in fractional quantum Hall point contacts*, Phys. Rev. B **101**, 075308 (2020),  
1364 doi:[10.1103/PhysRevB.101.075308](https://doi.org/10.1103/PhysRevB.101.075308).
- 1365 [78] T. Giamarchi and H. J. Schulz, *Anderson localization and interactions in one-dimensional*  
1366 *metals*, Phys. Rev. B **37**, 325 (1988), doi:[10.1103/PhysRevB.37.325](https://doi.org/10.1103/PhysRevB.37.325).
- 1367 [79] C. Wu, B. A. Bernevig and S.-C. Zhang, *Helical liquid and the edge of quantum spin Hall*  
1368 *systems*, Phys. Rev. Lett. **96**, 106401 (2006), doi:[10.1103/PhysRevLett.96.106401](https://doi.org/10.1103/PhysRevLett.96.106401).
- 1369 [80] X. G. Wen, *Chiral Luttinger liquid and the edge excitations in the fractional quantum Hall*  
1370 *states*, Phys. Rev. B **41**, 12838 (1990), doi:[10.1103/PhysRevB.41.12838](https://doi.org/10.1103/PhysRevB.41.12838).
- 1371 [81] X. G. Wen, *Theory of the edge states in fractional quantum Hall effects*, Int. J. Mod. Phys.  
1372 B **06**(10), 1711 (1992), doi:[10.1142/S0217979292000840](https://doi.org/10.1142/S0217979292000840).

- 1373 [82] S. Manna and A. Das, *Experimentally Motivated Order of Length Scales Affect Shot Noise*,  
1374 arXiv (2023), doi:[10.48550/arXiv.2307.08264](https://doi.org/10.48550/arXiv.2307.08264), [2307.08264](https://arxiv.org/abs/2307.08264).
- 1375 [83] J. Park, C. Spånslätt and A. D. Mirlin, *Fingerprints of Anti-Pfaffian Topological Or-*  
1376 *der in Quantum Point Contact Transport*, Phys. Rev. Lett. **132**(25), 256601 (2024),  
1377 doi:[10.1103/PhysRevLett.132.256601](https://doi.org/10.1103/PhysRevLett.132.256601).
- 1378 [84] O. Shtanko, K. Snizhko and V. Cheianov, *Nonequilibrium noise in transport across a*  
1379 *tunneling contact between  $\nu = \frac{2}{3}$  fractional quantum Hall edges*, Phys. Rev. B **89**(12),  
1380 125104 (2014), doi:[10.1103/PhysRevB.89.125104](https://doi.org/10.1103/PhysRevB.89.125104).
- 1381 [85] G. Campagnano, P. Lucignano and D. Giuliano, *Chirality and current-current cor-*  
1382 *relation in fractional quantum Hall systems*, Phys. Rev. B **93**(7), 075441 (2016),  
1383 doi:[10.1103/PhysRevB.93.075441](https://doi.org/10.1103/PhysRevB.93.075441).
- 1384 [86] L. P. Pryadko, E. Shimshoni and A. Auerbach, *Coulomb interactions and delo-*  
1385 *calization in quantum Hall constrictions*, Phys. Rev. B **61**(16), 10929 (2000),  
1386 doi:[10.1103/PhysRevB.61.10929](https://doi.org/10.1103/PhysRevB.61.10929).
- 1387 [87] B. Rosenow and B. I. Halperin, *Nonuniversal Behavior of Scattering be-*  
1388 *tween Fractional Quantum Hall Edges*, Phys. Rev. Lett. **88**, 096404 (2002),  
1389 doi:[10.1103/PhysRevLett.88.096404](https://doi.org/10.1103/PhysRevLett.88.096404).
- 1390 [88] E. Papa and A. H. MacDonald, *Interactions suppress quasiparticle tunneling at hall bar*  
1391 *constrictions*, Phys. Rev. Lett. **93**, 126801 (2004), doi:[10.1103/PhysRevLett.93.126801](https://doi.org/10.1103/PhysRevLett.93.126801).
- 1392 [89] E. Papa and A. H. MacDonald, *Edge state tunneling in a split Hall bar model*, Phys. Rev.  
1393 B **72**(4), 045324 (2005), doi:[10.1103/PhysRevB.72.045324](https://doi.org/10.1103/PhysRevB.72.045324).
- 1394 [90] A. Braggio, D. Ferraro, M. Carrega, N. Magnoli and M. Sassetti, *Environmental induced*  
1395 *renormalization effects in quantum Hall edge states due to  $1/f$  noise and dissipation*, New  
1396 Journal of Physics **14**(9), 093032 (2012), doi:[10.1088/1367-2630/14/9/093032](https://doi.org/10.1088/1367-2630/14/9/093032).
- 1397 [91] M. Carrega, D. Ferraro, A. Braggio, N. Magnoli and M. Sassetti, *Anomalous charge*  
1398 *tunneling in fractional quantum Hall edge states at a filling factor  $\nu = 5/2$* , Phys. Rev.  
1399 Lett. **107**, 146404 (2011), doi:[10.1103/PhysRevLett.107.146404](https://doi.org/10.1103/PhysRevLett.107.146404).
- 1400 [92] L. Tesser, M. Acciai, C. Spånslätt, J. Monsel and J. Splettstoesser, *Charge, spin, and heat*  
1401 *shot noises in the absence of average currents: Conditions on bounds at zero and finite*  
1402 *frequencies*, Phys. Rev. B **107**(7), 075409 (2023), doi:[10.1103/PhysRevB.107.075409](https://doi.org/10.1103/PhysRevB.107.075409).
- 1403 [93] I. P. Levkivskyi and E. V. Sukhorukov, *Shot-noise thermometry of the*  
1404 *quantum Hall edge states*, Phys. Rev. Lett. **109**(24), 246806 (2012),  
1405 doi:[10.1103/PhysRevLett.109.246806](https://doi.org/10.1103/PhysRevLett.109.246806).
- 1406 [94] L. Tesser and J. Splettstoesser, *Out-of-equilibrium fluctuation-dissipation bounds*, Phys.  
1407 Rev. Lett. **132**, 186304 (2024), doi:[10.1103/PhysRevLett.132.186304](https://doi.org/10.1103/PhysRevLett.132.186304).
- 1408 [95] C. L. Kane and M. P. A. Fisher, *Quantized thermal transport in the fractional quantum*  
1409 *Hall effect*, Phys. Rev. B **55**, 15832 (1997), doi:[10.1103/PhysRevB.55.15832](https://doi.org/10.1103/PhysRevB.55.15832).
- 1410 [96] C. Nosiglia, J. Park, B. Rosenow and Y. Gefen, *Incoherent transport on the  $\nu = 2/3$  quan-*  
1411 *tum Hall edge*, Phys. Rev. B **98**, 115408 (2018), doi:[10.1103/PhysRevB.98.115408](https://doi.org/10.1103/PhysRevB.98.115408).
- 1412 [97] H. Asasi and M. Mulligan, *Partial equilibration of anti-Pfaffian edge modes at  $\nu = 5/2$* ,  
1413 Phys. Rev. B **102**(20), 205104 (2020), doi:[10.1103/PhysRevB.102.205104](https://doi.org/10.1103/PhysRevB.102.205104).

- 1414 [98] K. Saito and A. Dhar, *Fluctuation Theorem in Quantum Heat Conduction*, Phys. Rev. Lett.  
1415 99(18), 180601 (2007), doi:[10.1103/PhysRevLett.99.180601](https://doi.org/10.1103/PhysRevLett.99.180601).
- 1416 [99] M. Sasseti and U. Weiss, *Transport of 1d interacting electrons through barriers and effective tunnelling density of states*, Europhys. Lett. 27(4), 311 (1994), doi:[10.1209/0295-5075/27/4/010](https://doi.org/10.1209/0295-5075/27/4/010).
- 1419 [100] L. Vannucci, F. Ronetti, G. Dolcetto, M. Carrega and M. Sasseti, *Interference-induced thermoelectric switching and heat rectification in quantum Hall junctions*, Phys. Rev. B  
1420 92(7), 075446 (2015), doi:[10.1103/PhysRevB.92.075446](https://doi.org/10.1103/PhysRevB.92.075446).
- 1422 [101] G. Zhang, I. Gornyi and Y. Gefen, *Landscapes of an out-of-equilibrium anyonic sea*, arXiv  
1423 (2024), doi:[10.48550/arXiv.2407.14203](https://doi.org/10.48550/arXiv.2407.14203), [2407.14203](https://arxiv.org/abs/2407.14203).
- 1424 [102] L. S. Levitov and M. Reznikov, *Counting statistics of tunneling current*, Phys. Rev. B  
1425 70(11), 115305 (2004), doi:[10.1103/PhysRevB.70.115305](https://doi.org/10.1103/PhysRevB.70.115305).
- 1426 [103] G. B. Lesovik and R. Loosen, *On the detection of finite-frequency current fluctuations*,  
1427 JETP Lett. 65(3), 295 (1997), doi:[10.1134/1.567363](https://doi.org/10.1134/1.567363).
- 1428 [104] G. Benenti, G. Casati, K. Saito and R. S. Whitney, *Fundamental aspects of steady-state conversion of heat to work at the nanoscale*, Phys. Rep. 694, 1 (2017),  
1429 doi:[10.1016/j.physrep.2017.05.008](https://doi.org/10.1016/j.physrep.2017.05.008).
- 1431 [105] A. Furusaki, *Resonant tunneling through a quantum dot weakly coupled to quantum wires or quantum Hall edge states*, Phys. Rev. B 57(12), 7141 (1998),  
1432 doi:[10.1103/PhysRevB.57.7141](https://doi.org/10.1103/PhysRevB.57.7141).
- 1434 [106] A. Cappelli, M. Huerta and G. R. Zemba, *Thermal transport in chiral conformal theories and hierarchical quantum Hall states*, Nuclear Physics B 636(3), 568 (2002),  
1435 doi:[https://doi.org/10.1016/S0550-3213\(02\)00340-1](https://doi.org/10.1016/S0550-3213(02)00340-1).
- 1437 [107] G. Yang and D. E. Feldman, *Influence of device geometry on tunneling in the  $\nu = \frac{5}{2}$  quantum Hall liquid*, Phys. Rev. B 88, 085317 (2013), doi:[10.1103/PhysRevB.88.085317](https://doi.org/10.1103/PhysRevB.88.085317).
- 1439 [108] I. S. Gradshteyn, I. M. Ryzhik, A. Jeffrey and D. Zwillinger, *Table of Integrals, Series, and Products*, p. 908, Elsevier, Academic Press, ISBN 978-0-12-373637-6,  
1440 doi:[10.1016/C2009-0-22516-5](https://doi.org/10.1016/C2009-0-22516-5) (2007).
- 1441